USGS
science for a changing world

National Water Quality Program
National Water-Quality Assessment Project

Optimal Hydrograph Separation Using a Recursive Digital Filter Constrained by Chemical Mass Balance, with Application to Selected Chesapeake Bay Watersheds

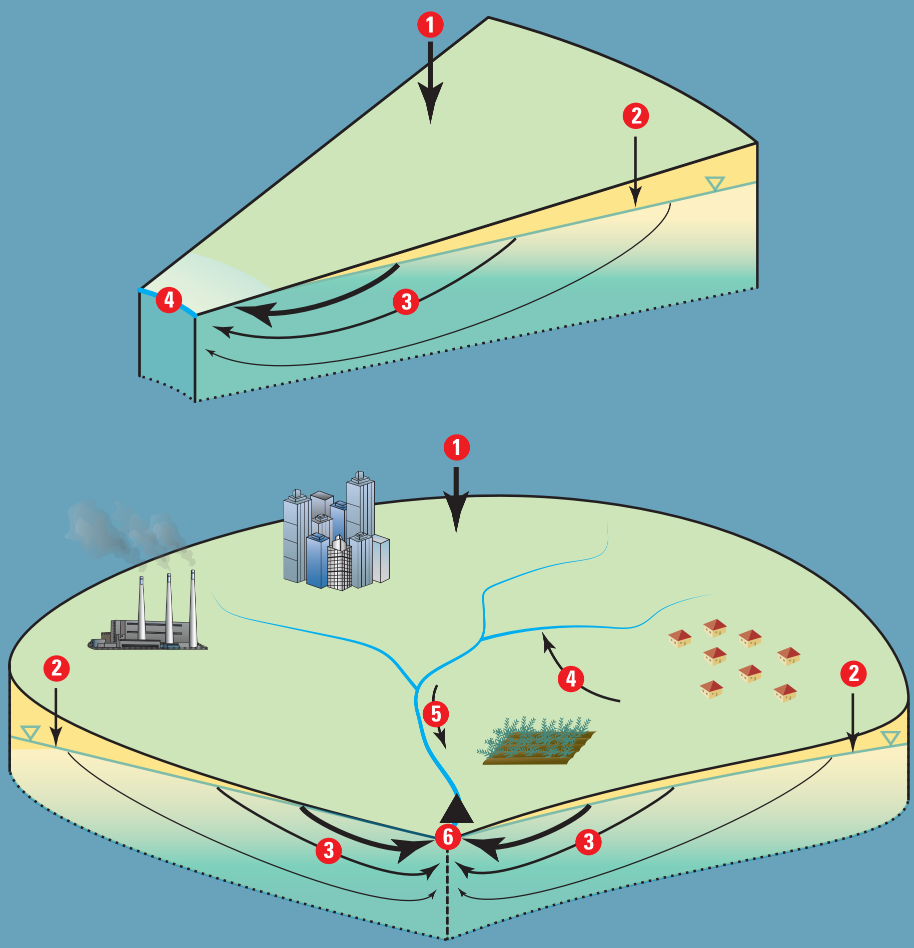

Scientific Investigations Report 2017–5034

U.S. Department of the Interior
U.S. Geological Survey

Cover. Schematic diagram of two scales of analysis for discussion of base flow and groundwater discharge: (top) the reach or contributing area scale, and (bottom) the watershed scale. Refer to figure 1 for explanation.

Optimal Hydrograph Separation Using a Recursive Digital Filter Constrained by Chemical Mass Balance, with Application to Selected Chesapeake Bay Watersheds

By Jeff P. Raffensperger, Anna C. Baker, Joel D. Blomquist, and
Jessica A. Hopple

National Water Quality Program
National Water-Quality Assessment Project

Scientific Investigations Report 2017–5034

U.S. Department of the Interior
U.S. Geological Survey

U.S. Department of the Interior
RYAN K. ZINKE, Secretary

U.S. Geological Survey
William H. Werkheiser, Acting Director

U.S. Geological Survey, Reston, Virginia: 2017

For more information on the USGS—the Federal source for science about the Earth, its natural and living resources, natural hazards, and the environment—visit https://www.usgs.gov or call 1-888-ASK-USGS

For an overview of USGS information products, including maps, imagery, and publications, visit https://store.usgs.gov

Suggested citation:
Raffensperger, J.P., Baker, A.C., Blomquist, J.D., and Hopple, J.A., 2017, Optimal hydrograph separation using a recursive digital filter constrained by chemical mass balance, with application to selected Chesapeake Bay watersheds: U.S. Geological Survey Scientific Investigations Report 2017–5034, 51 p., https://doi.org/10.3133/sir20175034.

ISSN 2328-031X (print)
ISSN 2328-0328 (online)
ISBN 978-1-4113-4135-7

Foreword

Sustaining the quality of the Nation's water resources and the health of our diverse ecosystems depends on the availability of sound water-resources data and information to develop effective, science-based policies. Effective management of water resources also brings more certainty and efficiency to important economic sectors. Taken together, these actions lead to immediate and long-term economic, social, and environmental benefits that make a difference to the lives of the almost 400 million people projected to live in the U.S. by 2050.

In 1991, Congress established the National Water-Quality Assessment (NAWQA) to address where, when, why, and how the Nation's water quality has changed, or is likely to change in the future, in response to human activities and natural factors. Since then, NAWQA has been a leading source of scientific data and knowledge used by national, regional, state, and local agencies to develop science-based policies and management strategies to improve and protect water resources used for drinking water, recreation, irrigation, energy development, and ecosystem needs (https://water.usgs.gov/nawqa/applications/). Plans for the third decade of NAWQA (2013–23) address priority water-quality issues and science needs identified by NAWQA stakeholders, such as the Advisory Committee on Water Information, and the National Research Council, and are designed to meet increasing challenges related to population growth, increasing needs for clean water, and changing land-use and weather patterns.

Quantitative estimates of groundwater contributions to streamflow are needed to address questions concerning the vulnerability and response of the Nation's water supply to natural and human-induced changes in environmental conditions. This report presents a comparison of methods for estimating groundwater contributions to streams and applies a new method that incorporates stream chemistry data to improve estimates. The method is applied to streamflow data from 225 sites in the Chesapeake Bay watershed, where groundwater contributions to streamflow may be affecting the lag times between implementation of management practices targeted to reduce nutrients and subsequent improvements in water quality. The results of this study can be used to address a number of questions regarding the role of groundwater in understanding past changes in stream-water quality and forecasting possible future changes, such as the timing and magnitude of land use and management practice effects on stream and groundwater quality. A companion data release is available online at https://doi.org/10.5066/F757194G. All NAWQA reports are available online at https://water.usgs.gov/nawqa/bib/.

We hope this publication will provide you with insights and information to meet your water resource needs and will foster increased citizen awareness and involvement in the protection and restoration of our Nation's waters. The information in this report is intended primarily for those interested or involved in resource management and protection, conservation, regulation, and policymaking at the regional and national level.

Dr. Donald W. Cline
Associate Director for Water
U.S. Geological Survey

Contents

Abstract 1
Introduction....2
    Purpose and Scope 2
    Background....2
        Base-Flow Terminology and Concepts....2
        Hydrograph Separation Methods 4
        Base Flow in the Chesapeake Bay Watershed....5
    Study Goals 5
Hydrograph-Separation Methods....5
    The Institute of Hydrology BFI Method 5
    Recursive Digital Filters....5
        Estimating the Filter Parameter Alpha 6
        Estimating the Filter Parameter Beta 6
    Optimal Hydrograph Separation....6
        Models of Base-Flow and Quickflow Specific Conductance....15
Application to Chesapeake Bay Watershed 15
    Site Selection....15
    Comparison of Hydrograph Separation Methods 15
    Results of Optimal Hydrograph Separation (OHS) 33
Limitations of Hydrograph Separation 39
Summary and Conclusions....46
Acknowledgments....47
References Cited....47

Figures

1. Schematic diagram of two scales of analysis for discussion of base flow and groundwater discharge: *A*, the reach or contributing area scale, and *B*, the watershed scale 3
2. Graph showing values of alpha and beta as functions of watershed area 24
3. Graph showing values of the base-flow index (BFI) as a function of watershed area 24
4. Graph showing values of the base-flow index (BFI) and fraction of days at base flow (determined as base flow equal to streamflow) for the ECK-CaF method versus the PART method 33
5. Graphs showing values of the base-flow index (BFI) and fraction of days at base flow (determined as base flow equal to streamflow) for the ECK-CaF method versus *A*, HYSEP-Fixed, *B*, HYSEP-LocMin, and *C*, HYSEP-Slide methods 34
6. Graph showing values of the base-flow index (BFI) and fraction of days at base flow (determined as base flow equal to streamflow) for the ECK-CaF method versus the BFI method 34
7. Graphs showing scatterplot matrix of the base-flow index (BFI) compared for all methods 35
8. Graphs showing scatterplot matrix of the fraction of days at base flow (determined as base flow equal to streamflow) compared for all methods 36
9. Hydrographs for water year 2009 showing total streamflow and base flow estimated using all methods for site 01614500, Conococheague Creek at Fairview, Maryland 37
10. Hydrographs showing base flow estimated using the ECK-CaF method for varying values of *A*, alpha, and *B*, beta for site 01614500, Conococheague Creek at Fairview, Maryland 38
11. Graphs showing optimal hydrograph separation results using the sin-cos model for base-flow specific conductance (SC) for site 02015700, Bullpasture River at Williamsville, Virginia, showing *A*, simulated compared to observed SC, *B*, the streamflow hydrograph, and *C*, time series of simulated and observed SC values and simulated base-flow SC 43
12. Graphs showing optimal hydrograph separation results using the SCfit model for base-flow specific conductance (SC) for site 01516350, Tioga River near Mansfield, Pennsylvania, showing *A*, simulated compared to observed SC, *B*, the streamflow hydrograph, and *C*, time series of simulated and observed SC values and simulated base-flow SC 44
13. Graph showing comparison of beta values estimated using the ECK-OHS and ECK-CaF methods for 67 acceptable models 45
14. Graph showing comparison of base-flow index (BFI) values estimated using the ECK-OHS and ECK-CaF methods for 67 acceptable models 45
15. Graph showing comparison of fraction of days at base flow estimated using the ECK-OHS and ECK-CaF methods for 67 acceptable models 45

Tables

1. Streamflow sites used for base-flow analysis 7
2. Long-term average base-flow index (BFI) produced by different methods 16
3. Fraction of days with base flow equal to streamflow for the period of analysis, as produced by different methods 25
4. Results of Optimal Hydrograph Separation (OHS) for accepted models 40

Conversion Factors

Multiply	By	To obtain
	Length	
inch (in.)	2.54	centimeter (cm)
inch (in.)	25.4	millimeter (mm)
foot (ft)	0.3048	meter (m)
mile (mi)	1.609	kilometer (km)
	Area	
square mile (mi^2)	2.590	square kilometer (km^2)
	Volume	
gallon (gal)	3.785	liter (L)
gallon (gal)	0.003785	cubic meter (m^3)
	Flow rate	
cubic foot per second (ft^3/s)	0.02832	cubic meter per second (m^3/s)
gallon per minute (gal/min)	0.06309	liter per second (L/s)
million gallons per day (Mgal/d)	0.04381	cubic meter per second (m^3/s)

Datums

Vertical coordinate information is referenced to the National Geodetic Vertical Datum of 1983 (NGVD 83).

Horizontal coordinate information is referenced to North American Datum of 1983 (NAD 83).

Supplemental Information

Water year refers to a continuous 12-month period selected to present data relative to hydrologic or meteorological phenomena during which a complete annual hydrologic cycle normally occurs. The water year used by the U.S. Geological Survey runs from October 1 through September 30, and is designated by the year in which it ends.

Specific conductance is given in microsiemens per centimeter at 25 degrees Celsius (µS/cm at 25 °C).

Optimal Hydrograph Separation Using a Recursive Digital Filter Constrained by Chemical Mass Balance, with Application to Selected Chesapeake Bay Watersheds

By Jeff P. Raffensperger, Anna C. Baker, Joel D. Blomquist, and Jessica A. Hopple

Abstract

Quantitative estimates of base flow are necessary to address questions concerning the vulnerability and response of the Nation's water supply to natural and human-induced change in environmental conditions. An objective of the U.S. Geological Survey National Water-Quality Assessment Project is to determine how hydrologic systems are affected by watershed characteristics, including land use, land cover, water use, climate, and natural characteristics (geology, soil type, and topography). An important component of any hydrologic system is base flow, generally described as the part of streamflow that is sustained between precipitation events, fed to stream channels by delayed (usually subsurface) pathways, and more specifically as the volumetric discharge of water, estimated at a measurement site or gage at the watershed scale, which represents groundwater that discharges directly or indirectly to stream reaches and is then routed to the measurement point.

Hydrograph separation using a recursive digital filter was applied to 225 sites in the Chesapeake Bay watershed. The recursive digital filter was chosen for the following reasons: it is based in part on the assumption that groundwater acts as a linear reservoir, and so has a physical basis; it has only two adjustable parameters (alpha, obtained directly from recession analysis, and beta, the maximum value of the base-flow index that can be modeled by the filter), which can be determined objectively and with the same physical basis of groundwater reservoir linearity, or that can be optimized by applying a chemical-mass-balance constraint. Base-flow estimates from the recursive digital filter were compared with those from five other hydrograph-separation methods with respect to two metrics: the long-term average fraction of streamflow that is base flow, or base-flow index, and the fraction of days where streamflow is entirely base flow. There was generally good correlation between the methods, with some biased slightly high and some biased slightly low compared to the recursive digital filter. There were notable differences between the days at base flow estimated by the different methods, with the recursive digital filter having a smaller range of values. This was attributed to how the different methods determine cessation of quickflow (the part of streamflow which is not base flow).

For 109 Chesapeake Bay watershed sites with available specific conductance data, the parameters of the filter were optimized using a chemical-mass-balance constraint and two different models for the time-dependence of base-flow specific conductance. Sixty-seven models were deemed acceptable and the results compared well with non-optimized results. There are a number of limitations to the optimal hydrograph-separation approach resulting from the assumptions implicit in the conceptual model, the mathematical model, and the approach taken to impose chemical mass balance (including tracer choice). These limitations may be evidenced by poor model results; conversely, poor model fit may provide an indication that two-component separation does not adequately describe the hydrologic system's runoff response.

The results of this study may be used to address a number of questions regarding the role of groundwater in understanding past changes in stream-water quality and forecasting possible future changes, such as the timing and magnitude of land-use and management practice effects on stream and groundwater quality. Ongoing and future modeling efforts may benefit from the estimates of base flow as calibration targets or as a means to filter chemical data to model base-flow loads and trends. Ultimately, base-flow estimation might provide the basis for future work aimed at improving the ability to quantify groundwater discharge, not only at the scale of a gaged watershed, but at the scale of individual reaches as well.

Introduction

An objective of the National Water-Quality Assessment (NAWQA) Project is to determine how hydrologic systems are affected by watershed characteristics, including land use, land cover, water use, climate, and natural characteristics (geology, soil type, and topography). An important component of any hydrologic system is base flow, broadly described as the part of streamflow that is sustained between precipitation events and fed to stream channels by delayed (usually subsurface) pathways (Price, 2011). Base flow is often considered synonymous with groundwater discharge, but this assumption is not always valid (Brodie and Hostetler, 2005).

In light of predicted changes in climate and human use of water, there is a growing need to study and manage groundwater and surface water as a single interconnected resource (Famiglietti, 2014; McNutt, 2014; Miller and others, 2016), although each has different characteristics, such as volume and residence time, that may impact water quality differently and require individual consideration and quantification. Base flow is generally not measured directly, but is estimated using a variety of methods. These methods have evolved over time, and application is dependent on the goal of the study and the nature of the hydrologic system, as well as the availability of data. The ability to quantify water budgets, flow paths, traveltimes, and base-flow contributions to streams, over a range of scales and environments, is an important component of improving the understanding of the status and future of the Nation's water quantity and quality.

Base-flow analysis is a valuable strategy in understanding the dynamics of the groundwater system, groundwater discharge to streams, and the transport of chemicals to streams, and is critical to effective water policy and management. Population growth is associated with increasing demands on freshwater resources for industry, agriculture, and human consumption, and water shortages are not uncommon, even in humid regions. Ensuring safe concentrations of contaminants associated with wastewater effluent requires accurate estimation of base-flow discharge, and contaminants that enter stream systems via soil or groundwater storage may be most highly concentrated during base flow.

The dynamics of base flow are an important consideration for classifying the flow regime, a primary determinant of the structure and function of stream ecosystems (Poff and others, 2010). Base-flow estimates can be an important contribution to studies of flow regime and stream ecosystem using tools such as the Ecological Limits of Hydrologic Alteration (ELOHA) framework (Poff and others, 2010) and the Hydroecological Integrity Assessment Process (HIP) (Henriksen and others, 2006). Urbanization is known to be an important stressor to the flow regime and stream ecosystem (Hamel and others, 2013), and various land-cover changes related to urbanization and implementation of Best Management Practices (BMPs) designed to mitigate adverse effects in urbanizing areas impact the groundwater system that provides base flow to streams.

Purpose and Scope

This report describes the application of several existing widely used methods for estimating base flow using hydrograph separation, and development and application of a base-flow estimation method that uses a Recursive Digital Filter (RDF) described by Eckhardt (2005) to separate a daily streamflow hydrograph into quickflow and base-flow components. The RDF method has a physical basis (assuming the groundwater system acts as a linear reservoir), and has two parameters that can be determined objectively, one using recession analysis and the other using either a backward-moving filter (Collischonn and Fan, 2013) or an optimal value constrained by chemical mass balance using specific conductance (SC) (referred to as Optimal Hydrograph Separation, or OHS). The two-parameter RDF using the backward-moving filter was applied to 225 sites in Chesapeake Bay watershed. The report describes and compares the results of the RDF, parameterized using recession analysis and the backward-moving filter, with widely used graphical methods [PART, HYSEP, and base-flow index (BFI)] in terms of the long-term average base-flow fraction, or BFI, and the fraction of days with 100 percent base flow. Hydrograph separation results are in tables as part of the report and in a Data Release (Raffensperger and others, 2017). In addition, OHS was applied to 109 sites for which SC data were available. These results are evaluated in terms of optimized parameter values and model performance.

Background

Base-Flow Terminology and Concepts

Base flow may be considered at two different scales of observation, measurement, and analysis (fig. 1). The reach scale (fig. 1*A*) includes both surface and subsurface components of a land area that drains or contributes water directly to the reach. The reach may be defined as a segment of a stream or river between two measurement points, but is more likely to be defined as a segment between two confluences, or between a confluence and an outlet to a larger surface-water body, such as a pond, lake, estuary, or ocean. Ideally, the contributing area for the reach should include all runoff (surface and groundwater) from an area that is defined topographically, and the reach itself should be a groundwater divide, although this will not always be the case. At the reach scale, the traveltime for routing along the reach itself will be relatively small compared with the traveltime from infiltration to groundwater discharge. Depending on the actual physical size of the contributing area, many relevant properties and attributes (land use/land cover, precipitation, chemical composition of the precipitation, and groundwater) may be considered spatially homogeneous; this will generally not be true at scales larger than a few square kilometers (km^2).

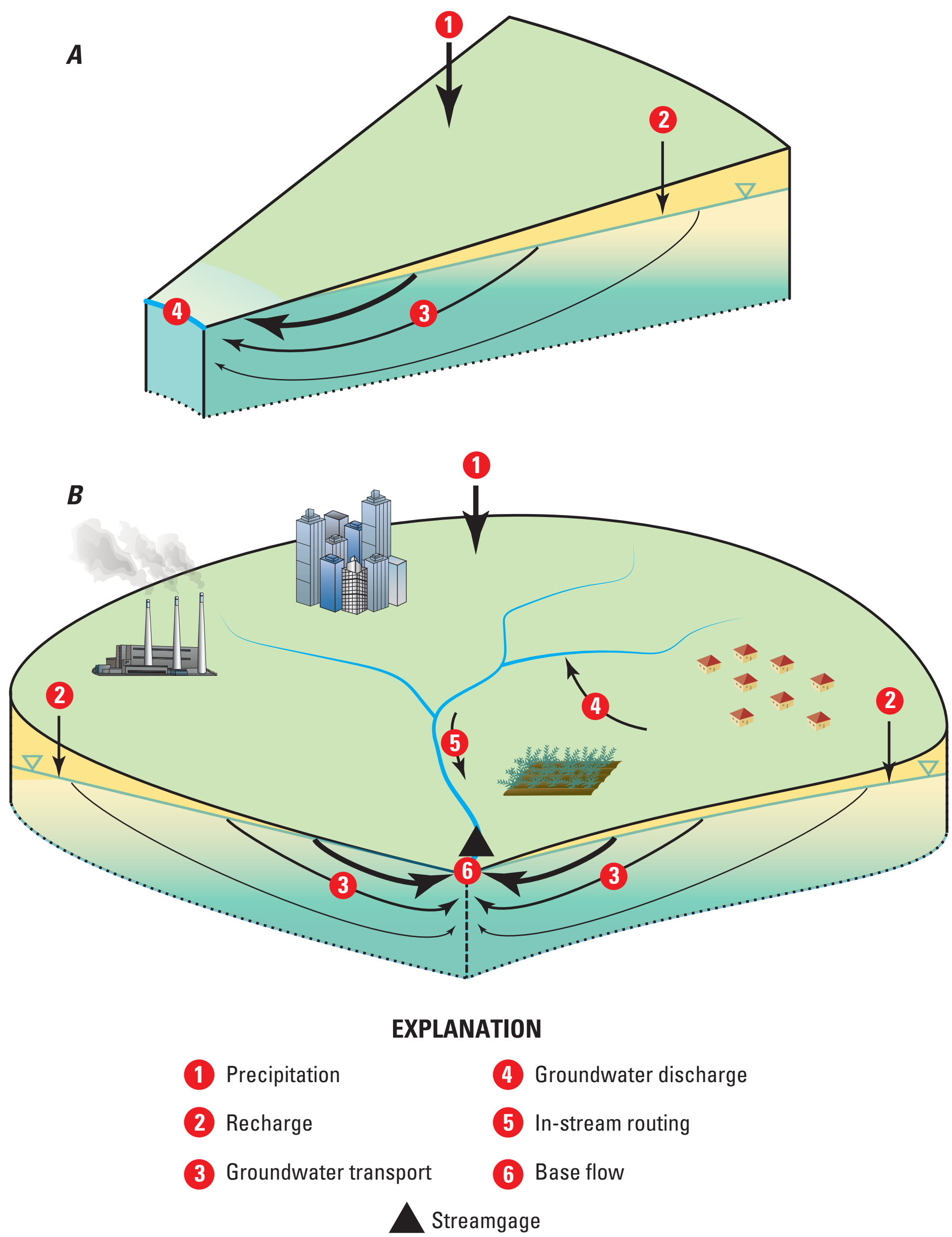

Figure 1. Schematic diagram of two scales of analysis for discussion of base flow and groundwater discharge: *A*, the reach or contributing area scale, and *B*, the watershed scale.

The watershed scale (fig. 1*B*) includes all reaches and contributing areas above an outlet or measurement point (gage). This scale will generally be larger than the reach scale, include all contributing areas from the outlet to the watershed divide, and incorporate multiple individual reaches and possibly several stream orders, including first order or headwater streams (for gaged headwater streams, the reach and watershed scales may be identical). At the watershed scale, routing within the stream network is likely to be a significant process affecting the flow of water and the transport of chemicals. In-stream chemical processes and physical mixing (including hydrodynamic dispersion within the reach and hyporheic zone exchange) become significant at this scale. Depending on the actual physical size of the watershed, many relevant properties and attributes (land use/land cover, precipitation, chemical composition of the precipitation, and groundwater) will not be spatially homogeneous.

For the purposes of this study, base flow is defined as the volumetric discharge of water, estimated at a measurement site or gage at the watershed scale, which represents groundwater that discharges directly or indirectly to stream reaches and is then routed to the measurement point. It may include other non-event flow produced by anthropogenic activities (wastewater treatment plant effluent, subsurface drainage, irrigation drainage). The term quickflow is used to describe the part of total streamflow that is not base flow. Base flow is generally not measured directly, but is estimated from observations of streamflow and (or) stream-water chemistry. There are several important distinctions between groundwater discharge and base flow. Groundwater discharge is difficult to measure, and is more likely a model output or estimate from some other analysis. Exceptions include measurement differences between closely spaced streamgages and use of seepage meters over short reaches. Base flow may include anthropogenic sources of water such as water treatment plant discharge.

Hydrograph Separation Methods

Base flow is commonly estimated using a variety of methods, most of which have the goal of separating a streamflow hydrograph into two or more flow components. Generally, two components, usually termed base flow and quickflow, are estimated. Approaches for estimating base flow can be grouped into two broad categories (Miller and others, 2015): methods that rely on streamflow data alone (including graphical methods and digital filters) and tracer- or chemical-mass-balance methods. Graphical methods initially began as manual approaches, using plots of streamflow to estimate points where base flow intersects the rising and falling limbs of the hydrograph (Blume and others, 2007; Hewlett and Hibbert, 1967). Computer programs based on graphical methods, such as PART (Rutledge, 1998) and HYSEP (Sloto and Crouse, 1996), were developed and have been widely applied to estimate base flow.

The method employed by PART designates base flow to be equal to streamflow on days that fit a requirement of antecedent recession, linearly interpolates base flow for other days, and is applied to a long period of record to obtain an estimate of the mean rate of groundwater discharge (Rutledge, 1998). Linear interpolation of daily values of streamflow is used to estimate groundwater discharge during periods of surface runoff. After a peak in streamflow, the time period when surface runoff and interflow (the combination referred to as quickflow) are significant is estimated from the following empirical relation (Linsley and others, 1982):

$$N = A^{0.2} \tag{1}$$

where N is the number of days past peak, and A is the watershed area, in square miles.

HYSEP is another computer program that can be used to separate a streamflow hydrograph into base-flow and quickflow components. The base-flow component has traditionally been associated with groundwater discharge and the quickflow component with precipitation that enters the stream via mechanisms such as direct precipitation onto the stream channel and overland runoff. HYSEP can be described conceptually as a method of interpolating between the low points of the streamflow hydrograph. HYSEP includes three algorithms for interpolation that are referred to as the fixed-interval, sliding-interval, and local-minimum methods (Sloto and Crouse, 1996).

Smoothed minima techniques have also been applied to hydrograph separation, wherein base-flow response is derived by applying simple smoothing and separation rules to the total streamflow hydrograph (Nathan and McMahon, 1990). The computer program BFI (for BFI method) (Institute of Hydrology, 1980; Wahl and Wahl, 1988, 1995) identifies and connects successive minima on a stream hydrograph, and defines base flow as the line connecting the minima. The BFI method divides the water year into N-day increments and the minimum flow for each N-day period is identified, where N is a user-specified duration in days. Minimum flows are then compared to adjacent minimum flows to determine turning points on the base-flow hydrograph. Minimum flows that are less than a fixed proportion of adjacent minimum flows are designated as turning points, and a straight line is established between turning points. The area below this line is an estimate of the volume of base flow.

Digital filters have seen increasing application in recent years (Arnold and Allen, 1999; Eckhardt, 2005; Vasconcelos and others, 2013). These methods aim to separate high frequency and low frequency signals (Nathan and McMahon, 1990). The digital filtering method proposed by Nathan and McMahon (1990) and used in subsequent studies by others originated in signal analysis and processing. Although it has no physical basis, it is objective and reproducible.

Most hydrograph separation methods (apart from tracer-based separations) lack a physical basis (Blume and others, 2007; Furey and Gupta, 2001). This is true of most graphical approaches and many filter-based approaches, although significant progress has been made in recent years (Collischonn and Fan, 2013; Eckhardt, 2005, 2012; Furey and Gupta, 2001, 2003; Li and others, 2013; Vasconcelos and others, 2013). Eckhardt (2005) proposed a generalized RDF based on the linear reservoir assumption with two adjustable parameters related to base-flow recession rate and the maximum value of the BFI, BFI_{max} (Eckhardt, 2005).

Another approach is to use chemical tracers, such as isotopes (Hooper and Shoemaker, 1986; Klaus and McDonnell, 2013; Sklash and Farvolden, 1979), SC (Miller and others, 2014; Pellerin and others, 2007; Stewart and others, 2007; Zhang and others, 2013), to construct a mass balance for the selected tracer and water. It has been suggested that tracer mass balance approaches may be more objective than methods using streamflow data alone because measured stream concentrations and measured or estimated end-member concentrations are related to physical and chemical processes in the watershed (Miller and others, 2015; Stewart and others, 2007; Zhang and others, 2013). Early application of tracer mass balance methods indicated a possible bias in graphical methods and led to research on mechanisms for delivery of groundwater and soil water to streams during precipitation events (Buttle, 1994; McDonnell, 1990; Robson and Neal, 1990; Sklash and Farvolden, 1979; Winter, 2007).

Base Flow in the Chesapeake Bay Watershed

Chesapeake Bay is the largest estuary in the United States and a vital ecological and economic resource in the Mid-Atlantic region. The Bay and its tributaries have been degraded in recent decades by excessive nitrogen and phosphorus in the water column, however, which cause harmful algal blooms and decreased water clarity, a reduction in submerged aquatic vegetation, and lower dissolved oxygen concentrations (Ator and Denver, 2015). Since the mid 1980s, the USGS has been a partner of the Chesapeake Bay Program (CBP), a multi-agency partnership working to restore the Bay ecosystem (Phillips, 2007). Significant scientific advances have been made in the understanding of the Bay and its watershed as a result.

One particular area of research has been quantifying the discharge of groundwater as base flow and the traveltime or residence time of that water in the subsurface, especially as it affects the transport of nitrate (Ator and Denver, 2015; Bachman and others, 1998; Focazio and others, 1998; Lindsey and others, 2003; Phillips and others, 1999; Phillips and Lindsey, 2003; Sanford and Pope, 2013). In one study, streamflow data collected at 276 sites in the Chesapeake Bay watershed were analyzed by Bachman and others (1998) using HYSEP (Sloto and Crouse, 1996) to estimate the total base flow. This work indicated that groundwater supplies a significant amount (about half) of water and nitrogen to streams in the watershed and is therefore an important pathway for nitrogen to reach the Chesapeake Bay. Focazio and others (1998) used a simple reservoir model, published data, and analyses of springwater to estimate residence times and apparent ages of groundwater discharge. The age of groundwater in shallow aquifers in the Chesapeake Bay watershed ranged from modern (less than 1 year) to more than 50 years, with a median age of 10 years (Phillips and Lindsey, 2003). An important implication of these findings is that there will be varying lag times between management practices implemented to reduce nutrients, and improvements in water quality.

Study Goals

The goals of the study were to evaluate existing methods of hydrograph separation, and to suggest a new or enhanced improved hydrograph-separation method based on the RDF of Eckhardt (2005) that met the following objectives: includes some physical basis related to the dynamics of the groundwater system; is consistent with chemical mass balance methods; is as objective as possible; and is reproducible and can be automated and applied to multiple sites. The methods were evaluated by applying them to selected daily streamflow records within the Chesapeake Bay watershed. A secondary goal was to provide base-flow estimates for concurrent and future investigations of base-flow quantity and quality related to land use, land cover, and management practices in the Chesapeake Bay watershed.

Hydrograph-Separation Methods

The Institute of Hydrology BFI Method

The BFI method is a widely used computerized graphical method based on determination of local minima (Combalicer and others, 2008; Gustard and others, 1992; Institute of Hydrology, 1980; Wahl and Wahl, 1988, 1995). It has been suggested that application of the BFI method could be useful in determining periods of base flow for recession analysis (David Wolock, USGS, written commun., 2014). The procedure for the standard BFI method is as follows (Wahl and Wahl, 1995):

1. The daily-mean streamflow record is divided into non-overlapping blocks of *N* days.

2. The minima for each of these blocks are calculated.

3. For each minimum, if *f* times the central value is less than outer values, the central value is an ordinate for the base-flow line. The variable *f* is referred to as the turning point test factor. This procedure is repeated until all the data have been analyzed to provide a derived set of turning points that will have different time periods between them.

4. Linear interpolation between each turning point is used to estimate daily values of base flow. (If base flow is larger than streamflow on a given day, then base flow is set equal to streamflow.)

The BFI is calculated as the total base flow divided by the total streamflow. The value for *N*, which defines the width of non-overlapping periods used in the BFI method, typically is set to a value of 5 days. However, Wahl and Wahl (1995) pointed out that the value of *N* can be optimized by computing the BFI for a range in *N* values, and then identifying the break point in the relation between the *N* and the BFI values. In this study, the break point was determined by (1) computing BFI values for a range (1–30) of *N* values, and then (2) finding the break point in the piecewise linear relation. The turning point test factor *f* is adjustable, but in this study a value of 0.9 was used.

Recursive Digital Filters

Eckhardt (2005) proposed the following RDF to estimate the base-flow component of streamflow:

$$Q_{B_j} = \frac{\left[(1-\beta)\alpha Q_{B_{j-1}} + (1-\alpha)\beta Q_j\right]}{(1-\alpha\beta)} \tag{2}$$

where α [dimensionless] and β [dimensionless] are adjustable parameters, Q [L^3/t] is streamflow, Q_B [L^3/t] is base flow, and

j is an index representing the time step (typically 1 day). Base flow at time step j is restricted to $Q_{B_j} \leq Q_j$. The parameter β is identical to the parameter BFI_{max} in Eckhardt (2005). When $\beta = 0$ or $Q_j = Q_{B_j}$,

$$Q_{B_j} = \alpha Q_{B_{j-1}} \tag{3}$$

which indicates that α is a recession constant, assuming that during dry periods without groundwater recharge base flow recedes exponentially, or that the groundwater system acts as a linear reservoir. An alternative expression of exponential base-flow recession is:

$$Q_B = Q_{B_0} e^{-ct} \tag{4}$$

where Q_B [L^3/t] is the base-flow discharge at time t after recession begins, Q_{B_0} [L^3/t] is the base-flow discharge at the beginning of the recession period, t is time measured from the beginning of the period, and c is the exponential recession constant [1/t]. The exponential recession constant c (in eq. 4) is related to α (eq. 3) as follows:

$$\alpha = e^{-c\Delta t} \tag{5}$$

or,

$$c = -\ln(\alpha/\Delta t) \tag{6}$$

where Δt is the time step. The recession constant α in the Eckhardt (2005) RDF may be estimated from streamflow data during base-flow periods, ideally when the groundwater system is not being recharged.

Estimating the Filter Parameter Alpha

The recession parameter alpha (α) may be determined using many different approaches (Cuthbert, 2014; Hall, 1968; Rutledge, 1998; Sujono and others, 2004; Tallaksen, 1995). For this study, periods of the streamflow record where base flow (estimated using the BFI method) was equal to streamflow were determined; a minimum number (3) of consecutive days of declining streamflow was used to calculate a value of α. The distribution statistics are generated, and the median value of alpha is chosen for use in the RDF.

Estimating the Filter Parameter Beta

Using a simple sensitivity analysis, Eckhardt (2005) found that alpha exerts a weaker influence on calculated base flow than beta (β). However, alpha can be determined by recession analysis whereas beta is non-measurable. Therefore, the result of the RDF depends strongly on a quantity that seemingly can only be determined by fitting. Eckhardt (2005) proposed avoiding this problem by empirically finding characteristic beta values for classes of watersheds that can be distinguished by their physical characteristics. Comparisons of the filtering method with conventional separation methods for watersheds in Pennsylvania, Maryland, Illinois, and Germany yielded the following suggested values:

- Beta = 0.80 for perennial streams with porous aquifers,
- Beta = 0.50 for ephemeral streams with porous aquifers, and
- Beta = 0.25 for perennial streams with hard rock aquifers.

Collischonn and Fan (2013) proposed a method for estimating beta based entirely on discharge records. The method is based on application of a backward-moving filter using a previously calculated recession parameter. Collischonn and Fan (2013) tested the filter using data from 15 streamflow sites in Brazil with differing physical characteristics and showed that the beta values obtained were comparable to the pre-defined values suggested by Eckhardt (2005) based on the class of aquifers encountered in each basin. The Collischonn and Fan (2013) method for estimating beta was applied in this study, as well as a new method for optimizing beta based on chemical mass balance.

Optimal Hydrograph Separation

Rimmer and Hartmann (2014) proposed an optimal hydrograph-separation approach that optimizes the value of beta for use in the Eckhardt (2005) RDF using geochemical data and a mass balance approach. The approach minimizes the value of the root-mean-square error $RMSE(\beta)$, defined as:

$$RMSE(\beta) = \left[\sum_{j=1}^{n} \left[C_{obs_j} - C_{sim_j}(\beta) \right]^2 \right]^{1/2} \tag{7}$$

where:

$$C_{sim_j} = \frac{C_B Q_{B_j}(\beta) + C_S Q_{S_j}(\beta)}{Q_j} \tag{8}$$

where C_{obs_j} is the n times measured concentration in streamflow on day j, C_{sim_j} is a modeled or simulated streamflow concentration described by separated base flow (Q_{B_j}) and quickflow (Q_{S_j}), their sum ($Q_j = Q_{B_j} + Q_{S_j}$), and their respective concentrations C_B and C_S. In this study, SC is used as the geochemical tracer for optimization. Specific conductance has been demonstrated to be effective for chemical hydrograph separation (Sanford and others, 2012; Stewart and others, 2007), and was chosen as a proxy for total solute concentration in the stream; data were available for 109 of the 225 sites analyzed in this study (table 1).

Table 1. Streamflow sites used for base-flow analysis.

[mi^2, square miles; count, number of daily streamflow values during period of analysis; SC, specific conductance]

Site number	Site name	Area (mi^2)	Beginning date	End date	Count	SC data
01409810	West Branch Wading River near Jenkins, N.J.	84.1	2/1/2006	9/30/2013	2,799	
01411300	Tuckahoe River at Head of River, N.J.	30.8	10/1/1979	6/30/2013	12,327	
01484000	Murderkill River near Felton, Del.	12.9	4/27/2007	12/31/2008	615	
01484100	Beaverdam Branch at Houston, Del.	3.02	10/1/1979	9/30/2013	12,419	
01485000	Pocomoke River near Willards, Md.	60.5	10/1/2006	9/30/2013	2,557	Yes
01485500	Nassawango Creek near Snow Hill, Md.	44.9	10/1/1979	9/30/2013	12,419	Yes
01486000	Manokin Branch near Princess Anne, Md.	4.8	10/1/1979	9/30/2013	12,419	
01486500	Beaverdam Creek near Salisbury, Md.	19.5	10/1/2000	8/29/2016	5,812	
01487000	Nanticoke River near Bridgeville, Del.	75.4	10/1/1979	9/30/2013	12,419	Yes
01488500	Marshyhope Creek near Adamsville, Del.	46.8	10/1/1979	9/30/2002	8,401	Yes
01490000	Chicamacomico River near Salem, Md.	15	10/1/2000	9/30/2013	4,748	Yes
01491000	Choptank River near Greensboro, Md.	113	10/1/1979	9/30/2013	12,419	Yes
01491500	Tuckahoe Creek near Ruthsburg, Md.	85.2	11/1/2000	4/30/2013	4,564	
01493112	Chesterville Branch near Crumpton, Md.	6.12	10/1/1996	7/31/2013	2,953	Yes
01493500	Morgan Creek near Kennedyville, Md.	12.7	10/1/2006	9/30/2013	2,557	Yes
01495000	Big Elk Creek at Elk Mills, Md.	51.6	10/1/1979	9/30/2013	12,419	
01502500	Unadilla River at Rockdale, N.Y.	520	10/1/2000	12/31/2012	4,475	
01503000	Susquehanna River at Conklin, N.Y.	2,232	10/1/1979	12/31/2012	12,146	Yes
01508803	West Branch Tioughnioga River at Homer, N.Y.	71.5	10/1/1972	9/30/1986	5,113	
01509150	Gridley Creek above East Virgil, N.Y.	10.4	10/1/1974	9/30/1981	2,557	Yes
01515000	Susquehanna River near Waverly, N.Y.	4,773	10/1/2000	12/31/2012	4,475	
01516350	Tioga River near Mansfield, Pa.	153	10/1/1976	9/30/2015	14,244	Yes
01518000	Tioga River at Tioga, Pa.	282	10/1/1938	9/30/2015	28,124	
01518500	Crooked Creek at Tioga, Pa.	122	10/1/1953	9/30/1974	7,670	
01518700	Tioga River at Tioga Junction, Pa.	446	7/1/1976	9/30/2015	14,336	Yes
01520000	Cowanesque River near Lawrenceville, Pa.	298	10/1/1951	9/30/2015	23,376	Yes
01527000	Cohocton River at Cohocton, N.Y.	52.2	10/1/1950	9/30/1981	11,323	
01527050	Switzer Creek near Cohocton, N.Y.	3.48	11/1/1978	9/30/1980	700	
01528000	Fivemile Creek near Kanona, N.Y.	66.8	10/1/1937	9/30/1994	20,819	Yes

Table 1. Streamflow sites used for base-flow analysis.—Continued

[mi^2, square miles; count, number of daily streamflow values during period of analysis; SC, specific conductance]

Site number	Site name	Area (mi^2)	Beginning date	End date	Count	SC data
01529500	Cohocton River near Campbell, N.Y.	470	10/1/1979	12/31/2012	12,146	
01531000	Chemung River at Chemung, N.Y.	2,506	10/1/1979	12/31/2012	12,146	
01531500	Susquehanna River at Towanda, Pa.	7,797	10/1/1979	9/30/2013	12,419	
01532000	Towanda Creek near Monroeton, Pa.	215	10/1/1914	9/30/2015	36,890	
01534000	Tunkhannock Creek near Tunkhannock, Pa.	383	10/1/1979	9/30/2013	12,419	Yes
01536000	Lackawanna River at Old Forge, Pa.	332	10/1/1938	9/30/2015	28,124	Yes
01536500	Susquehanna River at Wilkes-Barre, Pa.	9,960	10/1/1979	10/31/2012	12,085	
01540500	Susquehanna River at Danville, Pa.	11,220	10/1/1979	9/30/2013	12,419	Yes
01541000	West Branch Susquehanna River at Bower, Pa.	315	10/1/1913	9/30/2015	37,255	
01541500	Clearfield Creek at Dimeling, Pa.	371	10/1/1913	9/30/2015	37,255	
01542500	West Branch Susquehanna River at Karthaus, Pa.	1,462	10/1/2004	9/30/2013	3,287	Yes
01543000	Driftwood Branch Sinnemahoning Creek at Sterling Run, Pa.	272	10/1/1913	9/30/2015	37,255	
01543693	East Fork Sinnemahoning at Wharton Township, Pa.	49.2	10/1/2011	9/30/2015	1,461	
01544000	First Fork Sinnemahoning Creek near Sinnemahoning, Pa.	245	10/1/1953	9/30/2015	22,645	
01544500	Kettle Creek at Cross Fork, Pa.	136	10/1/1940	9/30/2015	27,393	Yes
01545000	Kettle Creek near Westport, Pa.	233	10/1/1954	9/30/2015	22,280	
01545600	Young Womans Creek near Renovo, Pa.	46.2	10/1/1965	9/30/2015	18,262	Yes
01546500	Spring Creek near Axemann, Pa.	87.2	10/1/1940	9/30/2015	27,393	
01547950	Beech Creek at Monument, Pa.	152	10/1/1968	9/30/2015	17,166	Yes
01548005	Bald Eagle Creek near Beech Creek Station, Pa.	562	10/1/1979	9/30/1995	5,844	
01549500	Blockhouse Creek near English Center, Pa.	37.7	10/1/1940	9/30/2015	27,393	
01549700	Pine Creek bl L Pine Creek near Waterville, Pa.	944	10/1/1979	9/30/2013	12,419	Yes
01550000	Lycoming Creek near Trout Run, Pa.	173	10/1/1914	9/30/2015	36,890	Yes
01552000	Loyalsock Creek at Loyalsockville, Pa.	435	10/1/1975	9/30/2015	14,610	
01553500	West Branch Susquehanna River at Lewisburg, Pa.	6,847	10/1/1979	9/30/2013	12,419	Yes
01553700	Chillisquaque Creek at Washingtonville, Pa.	51.3	10/1/1994	9/30/2013	6,940	
01554000	Susquehanna River at Sunbury, Pa.	18,300	10/1/1967	2/16/2015	17,306	
01555000	Penns Creek at Penns Creek, Pa.	301	10/1/1979	9/30/2013	12,419	
01555400	East Mahantango Creek at Klingerstown, Pa.	44.7	10/1/1996	9/30/2000	1,461	

Table 1. Streamflow sites used for base-flow analysis.—Continued

[mi^2, square miles; count, number of daily streamflow values during period of analysis; SC, specific conductance]

Site number	Site name	Area (mi^2)	Beginning date	End date	Count	SC data
01555500	East Mahantango Creek near Dalmatia, Pa.	162	10/1/1979	9/30/2013	12,419	
01556000	Frankstown Branch Juniata River at Williamsburg, Pa.	291	10/1/1979	9/30/2013	12,419	
01558000	Little Juniata River at Spruce Creek, Pa.	220	10/1/1979	9/30/2013	12,419	
01559795	Bobs Creek near Pavia, Pa.	16.6	10/1/1997	9/30/2000	1,096	
01562000	Raystown Branch Juniata River at Saxton, Pa.	756	10/1/1979	9/30/2013	12,419	
01564500	Aughwick Creek near Three Springs, Pa.	205	10/1/1979	9/30/2013	12,419	
01565000	Kishacoquillas Creek at Reedsville, Pa.	164	10/1/2001	9/30/2013	4,383	
01567000	Juniata River at Newport, Pa.	3354	10/1/1979	9/30/2013	12,419	Yes
01568000	Sherman Creek at Shermans Dale, Pa.	207	10/1/1979	9/30/2013	12,419	
01570000	Conodoguinet Creek near Hogestown, Pa.	470	10/1/1979	9/30/2013	12,419	Yes
01570500	Susquehanna River at Harrisburg, Pa.	24,100	10/1/1979	9/30/2013	12,419	Yes
01571000	Paxton Creek near Penbrook, Pa.	11.2	10/1/1991	9/30/1995	1,461	
01571490	Cedar Run at Eberlys Mill, Pa.	12.6	4/1/1993	9/30/1995	913	Yes
01571500	Yellow Breeches Creek near Camp Hill, Pa.	213	10/1/1979	9/30/2013	12,419	
0157155014	Swatara Creek, Site C3, at Newtown, Pa.	2.92	10/1/1996	9/30/2006	3,652	
01571820	Swatara Creek at Ravine, Pa.	43.3	10/1/1996	9/30/2006	3,652	Yes
01572000	Lower Little Swatara Creek at Pine Grove, Pa.	34.3	10/1/1981	9/30/1984	1,096	
01572025	Swatara Creek near Pine Grove, Pa.	116	10/1/1991	9/30/2015	8,766	Yes
01572950	Indiantown Run near Harper Tavern, Pa.	5.48	10/1/2002	9/30/2010	2,922	Yes
01573160	Quittapahilla Creek near Bellegrove, Pa.	74.2	10/1/1979	9/30/1994	5,479	
01573560	Swatara Creek near Hershey, Pa.	483	10/1/2007	9/30/2013	2,192	
01573695	Conewago Creek near Bellaire, Pa.	20.5	10/1/2012	9/30/2015	1,095	Yes
01573710	Conewago Creek near Falmouth, Pa.	47.5	10/1/2011	9/30/2015	1,461	Yes
01574000	West Conewago Creek near Manchester, Pa.	510	10/1/1979	9/30/2013	12,419	
01575500	Codorus Creek near York, Pa.	222	10/1/1940	9/30/1996	20,454	
01575585	Codorus Creek at Pleasureville, Pa.	267	10/1/2012	9/30/2015	1,095	
01576000	Susquehanna River at Marietta, Pa.	25,990	10/1/1979	9/30/2013	12,419	
0157608335	Little Conestoga Creek, Site 3A, near Morgantown, Pa.	1.42	10/1/1984	9/30/1991	2,556	
01576085	Little Conestoga Creek near Churchtown, Pa.	5.82	10/1/1982	9/30/1995	4,748	Yes

Table 1. Streamflow sites used for base-flow analysis.—Continued

[mi^2, square miles; count, number of daily streamflow values during period of analysis; SC, specific conductance]

Site number	Site name	Area (mi^2)	Beginning date	End date	Count	SC data
01576520	Muddy Run at Weavertown, Pa.	6.68	10/1/1992	9/30/1998	2,191	
01576521	Big Spring Run near Willow Street, Pa.	1.77	10/1/1993	9/30/2000	2,557	Yes
01576529	Unnamed tributary to Big Spring Run near Lampeter, Pa.	1.42	10/1/1993	9/30/2000	2,557	Yes
01576540	Mill Creek at Eshelman Mill Road near Lyndon, Pa.	54.2	10/1/1992	9/30/1998	2,191	Yes
01576754	Conestoga River at Conestoga, Pa.	470	10/1/1984	9/30/2013	10,592	Yes
01576787	Pequea Creek at Martic Forge, Pa.	148	2/24/1977	9/30/2013	4,259	Yes
01578310	Susquehanna River at Conowingo, Md.	27,100	10/1/1979	9/30/2013	12,419	Yes
01578475	Octoraro Creek near Richardsmere, Md.	177	12/20/2005	9/30/2013	2,842	
01580000	Deer Creek at Rocks, Md.	94.4	10/1/1979	9/30/2013	12,419	
01580520	Deer Creek near Darlington, Md.	164	1/1/2000	9/30/2013	5,022	
01581500	Bynum Run at Bel Air, Md.	8.52	10/1/1999	9/30/2015	5,844	Yes
01581649	James Run near Belcamp, Md.	9.15	10/1/2004	9/30/2015	4,017	
01581752	Plumtree Run near Bel Air, Md.	2.5	10/1/2001	9/30/2013	4,383	Yes
01582500	Gunpowder Falls at Glencoe, Md.	160	10/1/1984	9/30/2013	10,592	
01583500	Western Run at Western Run, Md.	59.8	10/1/1979	9/30/2013	12,419	
0158397967	Minebank Run near Glen Arm, Md.	2.06	10/1/2001	9/30/2015	5,113	
01586000	North Branch Patapsco River at Cedarhurst, Md.	56.6	10/1/1979	11/30/2012	12,115	
01589000	Patapsco River at Hollofield, Md.	285	10/1/2010	9/30/2015	1,826	
01589300	Gwynns Falls at Villa Nova, Md.	32.5	10/1/1996	9/30/2013	6,209	
01591000	Patuxent River near Unity, Md.	34.8	10/1/1979	9/30/2013	12,419	Yes
01593500	Little Patuxent River at Guilford, Md.	38	10/1/1979	9/30/2013	12,419	
01594000	Little Patuxent River at Savage, Md.	98.4	10/1/1975	9/30/1980	1,827	
01594440	Patuxent River near Bowie, Md.	348	10/1/1979	9/30/2013	12,419	Yes
01594526	Western Branch at Upper Marlboro, Md.	89.7	10/1/1993	9/30/2013	7,305	Yes
01594670	Hunting Creek near Huntingtown, Md.	9.38	10/1/1988	9/30/1997	3,287	Yes
01594710	Killpeck Creek at Huntersville, Md.	3.26	10/1/1985	9/30/1997	4,383	Yes
01594930	Laurel Run at Dobbin Rd near Wilson, Md.	8.23	10/1/1980	9/30/2004	8,766	Yes
01594936	North Fork Sand Run near Wilson, Md.	1.91	10/1/1980	9/30/2007	9,861	Yes
01595300	Abram Creek at Oakmont, W. Va.	42.6	10/1/1979	9/30/1982	1,096	Yes

Table 1. Streamflow sites used for base-flow analysis.—Continued

[mi^2, square miles; count, number of daily streamflow values during period of analysis; SC, specific conductance]

Site number	Site name	Area (mi^2)	Beginning date	End date	Count	SC data
01595800	North Branch Potomac River at Barnum, W. Va.	266	10/1/2003	9/30/2015	4,383	Yes
01596500	Savage River near Barton, Md.	49.1	10/1/1979	1/31/2013	12,177	Yes
01599000	Georges Creek at Franklin, Md.	72.4	10/1/1979	9/30/2013	12,419	
01601000	Wills Creek below Hyndman, Pa.	146	4/12/2002	9/30/2013	4,190	
01601500	Wills Creek near Cumberland, Md.	247	10/1/1979	9/30/2013	12,419	
01604500	Patterson Creek near Headsville, W. Va.	221	10/1/1979	9/30/2013	12,419	Yes
01605500	South Branch Potomac River at Franklin, W. Va.	179	10/1/1979	9/30/2013	12,419	
01606000	North Fork South Branch Potomac River at Cabins, W. Va.	310	10/1/1998	9/30/2013	5,479	
01606500	South Branch Potomac River near Petersburg, W. Va.	651	10/1/1967	2/16/2015	17,306	
01607500	South Fork South Branch Potomac River at Brandywine, W. Va.	103	10/1/1943	9/30/2015	26,298	
01608000	South Fork South Branch Potomac River near Moorefield, W. Va.	277	10/1/1938	9/30/2015	28,124	
01608500	South Branch Potomac River near Springfield, W. Va.	1,461	10/1/1979	9/30/2013	12,419	Yes
01609000	Town Creek near Oldtown, Md.	148	10/1/2006	9/30/2013	2,557	
01610155	Sideling Hill Creek near Bellegrove, Md.	102	4/1/1999	9/30/2013	5,297	
01610200	Lost River at McCauley near Baker, W. Va.	155	10/1/1971	9/30/1979	2,922	Yes
01610400	Waites Run near Wardensville, W. Va.	12.6	10/1/2002	9/30/2015	4,748	Yes
01611500	Cacapon River near Great Cacapon, W. Va.	675	10/1/1997	9/30/2013	5,844	Yes
01613000	Potomac River at Hancock, Md.	4,064	10/1/1932	9/30/2015	30,315	
01613030	Warm Springs Run near Berkeley Springs, W. Va.	6.76	10/1/2011	9/30/2015	1,461	
01613050	Tonoloway Creek near Needmore, Pa.	10.7	9/1/1985	9/30/2013	10,257	
01613095	Tonoloway Creek near Hancock, Md.	111	10/1/2005	9/30/2013	2,922	
01613525	Licking Creek at Pectonville, Md.	193	3/1/2005	9/30/2013	3,136	
01613900	Hogue Creek near Hayfield, Va.	15.9	10/1/1992	9/30/2012	7,305	Yes
01614000	Back Creek near Jones Springs, W. Va.	235	6/30/2004	9/30/2013	3,380	
01614500	Conococheague Creek at Fairview, Md.	494	10/1/1979	9/30/2013	12,419	Yes
01614830	Opequon Creek near Stephens City, Va.	15.2	10/1/2001	9/30/2009	2,922	Yes
01615000	Opequon Creek near Berryville, Va.	58.2	10/1/2002	9/30/2015	4,748	Yes
01616400	Mill Creek at Bunker Hill, W. Va.	18.4	10/1/2011	9/30/2015	1,461	
01616500	Opequon Creek near Martinsburg, W. Va.	273	10/1/1979	9/30/2013	12,419	Yes

Table 1. Streamflow sites used for base-flow analysis.—Continued

[mi^2, square miles; count, number of daily streamflow values during period of analysis; SC, specific conductance]

Site number	Site name	Area (mi^2)	Beginning date	End date	Count	SC data
01617800	Marsh Run at Grimes, Md.	18.9	10/1/1979	9/30/2013	12,419	
01618100	Rockymarsh Run at Scrabble, W. Va.	15.9	3/27/2008	9/30/2013	2,014	
01619000	Antietam Creek near Waynesboro, Pa.	93.5	10/1/2005	9/30/2013	2,922	
01619500	Antietam Creek near Sharpsburg, Md.	281	10/1/1979	9/30/2013	12,419	
01621050	Muddy Creek at Mount Clinton, Va.	14.3	4/13/1993	9/30/2013	7,476	Yes
01626000	South River near Waynesboro, Va.	127	10/1/1979	9/30/2013	12,419	Yes
01628500	South Fork Shenandoah River near Lynnwood, Va.	1,079	10/1/1979	9/30/2013	12,419	
01631000	South Fork Shenandoah River at Front Royal, Va.	1,634	10/1/1930	9/30/2015	31,046	Yes
01632000	North Fork Shenandoah River at Cootes Store, Va.	210	10/1/1979	9/30/2013	12,419	Yes
01632900	Smith Creek near New Market, Va.	93.6	10/1/1979	9/30/2013	12,419	Yes
01634000	North Fork Shenandoah River near Strasburg, Va.	770	10/1/1979	9/30/2013	12,419	Yes
01634500	Cedar Creek near Winchester, Va.	102	10/1/1979	4/30/2013	12,266	Yes
01636500	Shenandoah River at Millville, W. Va.	3,041	10/1/1979	9/30/2013	12,419	Yes
01637500	Catoctin Creek near Middletown, Md.	66.9	10/1/1979	9/30/2013	12,419	
01638480	Catoctin Creek at Taylorstown, Va.	89.5	10/1/1979	11/30/2012	12,115	
01639000	Monocacy River at Bridgeport, Md.	173	10/1/1979	9/30/2013	12,419	Yes
01639500	Big Pipe Creek at Bruceville, Md.	102	10/1/1979	9/30/2013	12,419	
01643000	Monocacy River at Jug Bridge near Frederick, Md.	817	10/1/1979	8/31/2013	12,389	
01643700	Goose Creek near Middleburg, Va.	122	10/1/2001	9/30/2013	4,383	Yes
01644000	Goose Creek near Leesburg, Va.	332	10/1/1968	2/16/2015	16,940	Yes
01645000	Seneca Creek at Dawsonville, Md.	101	10/1/1930	9/30/2015	31,046	
01645704	Difficult Run above Fox Lake near Fairfax, Va.	5.49	10/1/2007	9/30/2015	2,922	Yes
01645762	South Fork Little Difficult Run above mouth near Vienna, Va.	2.71	10/1/2007	9/30/2015	2,922	Yes
01646000	Difficult Run near Great Falls, Va.	57.8	10/1/1979	9/30/2013	12,419	Yes
01646305	Dead Run at Whann Avenue near McLean, Va.	2.05	10/1/2008	9/30/2015	2,556	Yes
01646500	Potomac River near Washington, D.C. Little Falls Pump Station	11,560	3/1/1930	9/30/2014	30,895	Yes
01648000	Rock Creek at Sherrill Drive, Washington, D.C.	62.2	10/1/1979	9/30/2013	12,419	
01649190	Paint Branch near College Park, Md.	13.1	10/1/2007	9/30/2015	2,922	Yes
01649500	Northeast Branch Anacostia River at Riverdale, Md.	72.8	10/1/1938	9/30/2015	28,124	Yes

Table 1. Streamflow sites used for base-flow analysis.—Continued

[mi^2, square miles; count, number of daily streamflow values during period of analysis; SC, specific conductance]

Site number	Site name	Area (mi^2)	Beginning date	End date	Count	SC data
01651000	Northwest Branch Anacostia River near Hyattsville, Md.	49.4	10/1/1979	9/30/2013	12,419	Yes
01651800	Watts Branch at Washington, D.C.	3.28	6/19/1992	9/30/2013	7,774	Yes
01653600	Piscataway Creek at Piscataway, Md.	39.5	10/1/1965	9/30/2005	14,610	
01654000	Accotink Creek near Annandale, Va.	23.9	10/1/1979	9/30/2013	12,419	Yes
01656500	Broad Run at Buckland, Va.	50.2	10/1/1980	1/6/1987	2,289	
01656903	Flatlick Branch above Frog Branch at Chantilly, Va.	4.2	10/1/2007	9/30/2014	2,557	Yes
01658000	Mattawoman Creek near Pomonkey, Md.	54.8	1/24/2001	9/30/2013	4,633	Yes
01658500	South Fork Quantico Creek near Independent Hill, Va.	7.62	10/1/1979	9/30/2013	12,419	Yes
01659000	North Branch Chopawamsic Creek near Independent Hill, Va.	5.69	10/1/2007	9/30/2011	1,461	Yes
01660920	Zekiah Swamp Run near Newtown, Md.	79.9	10/1/2006	9/30/2015	3,287	
01661050	St. Clement Creek near Clements, Md.	18.5	10/1/2006	9/30/2013	2,557	Yes
01662800	Battle Run near Laurel Mills, Va.	25.8	10/1/1997	11/30/2012	5,540	
01663500	Hazel River at Rixeyville, Va.	285	10/1/2001	9/30/2013	4,383	
01664000	Rappahannock River at Remington, Va.	619	10/1/1979	9/30/2013	12,419	
01665500	Rapidan River near Ruckersville, Va.	115	10/1/1998	2/28/2013	5,265	Yes
01666500	Robinson River near Locust Dale, Va.	179	10/1/1979	9/30/2013	12,419	Yes
01667500	Rapidan River near Culpeper, Va.	468	10/1/1979	1/31/2013	12,177	Yes
01668000	Rappahannock River near Fredericksburg, Va.	1,595	10/1/1979	9/30/2013	12,419	Yes
01669520	Dragon Swamp at Mascot, Va.	109	8/14/1981	4/30/2013	11,583	Yes
01671020	North Anna River at Hart Corner near Doswell, Va.	462	10/1/1979	9/30/2012	12,054	Yes
01671100	Little River near Doswell, Va.	107	10/1/2000	9/30/2013	4,748	Yes
01673000	Pamunkey River near Hanover, Va.	1,078	10/1/1979	9/30/2013	12,419	Yes
01673800	Po River near Spotsylvania, Va.	77.6	10/1/1979	9/30/2013	12,419	
01674000	Mattaponi River near Bowling Green, Va.	256	10/1/1979	9/30/2013	12,419	Yes
01674500	Mattaponi River near Beulahville, Va.	603	10/1/1989	9/30/2013	8,766	Yes
01677000	Ware Creek near Toano, Va.	6.29	10/1/1982	9/30/1995	4,748	
02011500	Back Creek near Mountain Grove, Va.	134	10/1/1979	9/30/2013	12,419	Yes
02012500	Jackson River at Falling Spring, Va.	410	10/1/1925	9/30/1983	21,184	Yes
02015700	Bullpasture River at Williamsville, Va.	110	10/1/1979	9/30/2013	12,419	Yes

Table 1. Streamflow sites used for base-flow analysis.—Continued

[mi², square miles; count, number of daily streamflow values during period of analysis; SC, specific conductance]

Site number	Site name	Area (mi²)	Beginning date	End date	Count	SC data
02020500	Calfpasture River above Mill Creek at Goshen, Va.	141	10/1/1998	9/30/2013	5,479	Yes
02024000	Maury River near Buena Vista, Va.	647	10/1/1979	9/30/2013	12,419	Yes
02024752	James River at Blue Ridge Parkway near Big Island, Va.	3,076	10/1/2005	9/30/2013	2,922	
02031000	Mechums River near White Hall, Va.	95.3	10/1/1979	9/30/2013	12,419	
02034000	Rivanna River at Palmyra, Va.	663	10/1/1979	9/30/2013	12,419	
02035000	James River at Cartersville, Va.	6,252	10/1/1979	9/30/2013	12,419	Yes
02037500	James River near Richmond, Va.	6,753	10/1/1979	4/30/2013	12,266	
02038850	Holiday Creek near Andersonville, Va.	8.54	10/1/1966	9/30/2015	17,897	
02039500	Appomattox River at Farmville, Va.	302	10/1/1979	9/30/2013	12,419	Yes
02041000	Deep Creek near Mannboro, Va.	158	10/1/1979	9/30/2013	12,419	Yes
02041650	Appomattox River at Matoaca, Va.	1,342	10/1/1979	9/30/2013	12,419	Yes
02042426	Upham Brook near Richmond, Va.	37.4	10/1/1990	9/30/1994	1,461	
02042500	Chickahominy River near Providence Forge, Va.	251	10/1/1979	9/30/2013	12,419	Yes
03050000	Tygart Valley River near Dailey, W. Va.	185	7/20/1988	9/30/2013	9,204	
03065000	Dry Fork at Hendricks, W. Va.	349	10/1/1995	1/31/2013	6,333	
03066000	Blackwater River at Davis, W. Va.	85.9	10/1/1979	9/30/2013	12,419	Yes
03069000	Shavers Fork at Parsons, W. Va.	213	10/1/1979	9/30/1993	5,114	
03069500	Cheat River near Parsons, W. Va.	722	10/1/1979	9/30/2013	12,419	
03070000	Cheat River at Rowlesburg, W. Va.	939	10/1/1979	9/30/1996	6,210	
03070500	Big Sandy Creek at Rockville, W. Va.	200	10/1/1979	9/30/2013	12,419	
03076600	Bear Creek at Friendsville, Md.	48.9	10/1/1979	9/30/2013	12,419	
03180500	Greenbrier River at Durbin, W. Va.	133	10/1/1979	11/15/2012	12,100	

Models of Base-Flow and Quickflow Specific Conductance

In the simplest approach, C_B and C_S are constants estimated through the optimization. However, there are a number of other possibilities that were considered in this study, leading to alternative models and parameters to be optimized in the case of C_B.

The quickflow SC (C_S) may vary with storm intensity or other factors, and might reflect transient (seasonal) or event-dependent contributions from a variety of sources other than precipitation, such as rapid delivery of riparian soil water or shallow groundwater, or runoff from agricultural or urban or other land uses, or seasonal inputs to the land surface of road salt, fertilizer, etc. These possibilities were not considered in the present study, and C_S is a constant value, estimated through optimization.

This study introduced two new approaches to mathematically model base-flow SC (C_B), each with different parameters that may be optimized. Both are seen as an improvement over specification of a constant value. In the first approach, base-flow SC is approximated as a sine/cosine function of time. This approach attempts to incorporate expected seasonality in base-flow SC. It also provides a mechanism for removing (to some extent) outliers, such as road-salt spikes, although the resultant errors (eq. 7) will impact parameter estimation and model fit. The approach is implemented using the following concentration function for C_B.

$$C_{B_j} = \overline{C}_B + C_B^{*s}\left[\sin\left(2\pi\left(t_j - t_0\right)/365.25\right)\right] + C_B^{*c}\left[\cos\left(2\pi\left(t_j - t_0\right)/365.25\right)\right] \quad (9)$$

in which the base-flow SC on day j (C_{B_j}) is a sum of sine and cosine functions of time (t_j) with an annual period, described by a mean value ($\overline{C}_B$), amplitudes (C_B^{*s}, C_B^{*c}), and a starting time (t_0). In the optimization, the following values are estimated that minimize the RMSE (eq. 7): β, $\overline{C}_B$, C_B^{*s}, t_0, C_B^{*c}, and C_S.

In the second approach, the base-flow SC is filtered or represented as a time series similar to the manual approach taken by Sanford and others (2012). Filtering would remove spurious values; the filtered data could then be modeled using the approach described above or some other approach. The advantage of filtering is that spurious values of SC do not affect the error statistics and optimization. This approach involves identifying SC values on base-flow days (according to the N-optimized BFI method), and using an algorithm to identify peaks (thought to represent base flow) in the SC record. The OHS method is programmed in MATLAB® and peaks are identified using the Signal Processing Toolbox function findpeaks. These peaks are used to generate daily interpolated base-flow SC values. In the optimization, the following values are estimated that minimize the RMSE (eq. 7): β and C_S.

Application to Chesapeake Bay Watershed

The initial application of the OHS method and comparison with other methods focuses on the Chesapeake Bay watershed. Questions regarding groundwater discharge, age, and residence time and how they impact restoration efforts have made the watershed an important area for assessment of base flow. Several efforts are underway to estimate base-flow loads, trends, and spatially and temporally varying sources of nutrients (Paul Capel, USGS, written commun., 2015; Richard Smith, USGS, oral commun., 2015).

Site Selection

Sites for analysis in the Chesapeake Bay watershed were selected on the basis of their length of record, availability of water-quality data, and their inclusion in other ongoing studies. Two hundred twenty-five sites were selected (table 1). Of these, 148 are part of the Chesapeake Nontidal Network and selected other sites with state water-quality data, and 152 had been independently selected for a statistical analysis of annual base-flow nitrogen loads and land use (Paul Capel, USGS, written commun., 2015); the two groups had 75 sites in common. Sites with watershed areas of less than 1 square mile (mi^2) were excluded. SC data were available for 109 sites.

Comparison of Hydrograph Separation Methods

The hydrograph separation methods PART (Rutledge, 1998) and HYSEP (Sloto and Crouse, 1996) were applied to streamflow data from sites within the Chesapeake Bay watershed, using the USGS groundwater toolbox (Barlow and others, 2015). The periods of analysis varied depending on availability and continuity of data (table 1). The BFI method (Institute of Hydrology, 1980; Wahl and Wahl, 1988) was programmed in MATLAB and applied to data from the sites, using an optimized value of N and $f = 0.9$. The Eckhardt (2005) RDF was programmed in MATLAB and applied to streamflow data from the sites. Alpha was determined for each site as described previously and beta was estimated using the method of Collischonn and Fan (method ECK-CaF, 2013). For reasons mentioned earlier and because ECK-CaF can be applied to all sites, the ECK-CaF method was the basis for comparison with other methods. Hydrograph separation results are in a Data Release (Raffensperger and others, 2017). OHS method results are discussed in the next section. Values of alpha, beta, and the long-term average BFI are given in table 2.

Values of alpha ranged from 0.63 to 0.99, with a mean of 0.95, and with most values larger than 0.9, especially in watersheds larger than 100 mi^2 (table 2, fig. 2). The range of values of alpha is equivalent to a range of values of the inverse recession constant, $1/c$, of approximately 2.1 to 100 days

Table 2. Long-term average base-flow index (BFI) produced by different methods.

[*N*, length of period used for BFI method, in days; *f*, BFI turning point test factor; alpha, recession constant; beta, maximum BFI, determined using the method of Collischonn and Fan (2013); ft³/s, cubic feet per second]

Site number	*N*	*f*	Alpha	Beta	Average daily streamflow (ft³/s)	BFI, by method					
						PART	HYSEP-Fixed	HYSEP-LocMin	HYSEP-Slide	BFI method	ECK-CaF
01409810	7	0.9	0.97	0.76	144	0.81	0.76	0.70	0.77	0.60	0.71
01411300	7	0.9	0.96	0.83	40	0.85	0.86	0.78	0.86	0.68	0.79
01484000	7	0.9	0.92	0.73	9	0.70	0.74	0.66	0.72	0.55	0.69
01484100	6	0.9	0.96	0.81	4	0.83	0.81	0.78	0.82	0.70	0.78
01485000	9	0.9	0.94	0.67	72	0.66	0.64	0.53	0.64	0.38	0.62
01485500	7	0.9	0.94	0.59	53	0.58	0.58	0.50	0.58	0.38	0.53
01486000	6	0.9	0.94	0.66	5	0.68	0.70	0.60	0.70	0.46	0.60
01486500	4	0.9	0.95	0.65	26	0.71	0.75	0.66	0.75	0.58	0.60
01487000	7	0.9	0.97	0.86	95	0.88	0.84	0.82	0.84	0.75	0.84
01488500	6	0.9	0.96	0.71	55	0.72	0.67	0.64	0.67	0.57	0.65
01490000	6	0.9	0.96	0.72	17	0.73	0.76	0.68	0.76	0.57	0.66
01491000	7	0.9	0.95	0.68	146	0.66	0.64	0.59	0.64	0.48	0.62
01491500	6	0.9	0.96	0.65	110	0.66	0.63	0.60	0.64	0.54	0.59
01493112	6	0.9	0.97	0.69	8	0.71	0.71	0.69	0.71	0.65	0.59
01493500	4	0.9	0.97	0.53	12	0.55	0.58	0.53	0.58	0.49	0.44
01495000	4	0.9	0.97	0.67	71	0.67	0.64	0.63	0.64	0.61	0.61
01502500	6	0.9	0.96	0.64	1,001	0.66	0.62	0.55	0.62	0.48	0.59
01503000	6	0.9	0.96	0.68	3,696	0.65	0.61	0.56	0.61	0.49	0.64
01508803	5	0.9	0.96	0.79	128	0.84	0.78	0.71	0.78	0.64	0.76
01509150	3	0.9	0.93	0.56	22	0.59	0.64	0.55	0.64	0.44	0.50
01515000	6	0.9	0.96	0.67	9,573	0.63	0.59	0.53	0.58	0.51	0.62
01516350	5	0.9	0.95	0.57	215	0.61	0.59	0.53	0.59	0.42	0.52
01518000	6	0.9	0.94	0.52	400	0.55	0.50	0.45	0.50	0.36	0.47
01518500	7	0.9	0.94	0.54	112	0.56	0.54	0.47	0.54	0.31	0.48
01518700	7	0.9	0.96	0.45	538	0.53	0.51	0.46	0.51	0.35	0.39
01520000	6	0.9	0.92	0.51	309	0.49	0.44	0.39	0.45	0.30	0.46
01527000	7	0.9	0.95	0.80	56	0.83	0.78	0.65	0.77	0.51	0.77
01527050	13	0.9	0.80	0.91	4	0.74	0.75	0.65	0.77	0.22	0.90
01528000	5	0.9	0.93	0.56	76	0.55	0.54	0.48	0.54	0.36	0.50

Table 2. Long-term average base-flow index (BFI) produced by different methods.—Continued

[*N*, length of period used for BFI method, in days; *f*, BFI turning point test factor; alpha, recession constant; beta, maximum BFI, determined using the method of Collischonn and Fan (2013); ft^3/s, cubic feet per second]

Site number	*N*	*f*	Alpha	Beta	Average daily streamflow (ft^3/s)	BFI, by method					
						PART	HYSEP-Fixed	HYSEP-LocMin	HYSEP-Slide	BFI method	ECK-CaF
01529500	6	0.9	0.96	0.63	499	0.65	0.60	0.54	0.60	0.46	0.58
01531000	6	0.9	0.97	0.50	2,776	0.52	0.51	0.47	0.51	0.41	0.44
01531500	6	0.9	0.96	0.60	11,238	0.56	0.55	0.50	0.55	0.48	0.55
01532000	6	0.9	0.93	0.55	290	0.53	0.54	0.47	0.53	0.34	0.50
01534000	6	0.9	0.95	0.61	577	0.60	0.54	0.49	0.54	0.41	0.56
01536000	7	0.9	0.95	0.68	486	0.71	0.63	0.58	0.63	0.46	0.64
01536500	7	0.9	0.97	0.59	14,554	0.56	0.57	0.53	0.57	0.48	0.54
01540500	6	0.9	0.96	0.65	16,427	0.57	0.58	0.54	0.59	0.52	0.60
01541000	6	0.9	0.95	0.56	557	0.59	0.53	0.49	0.53	0.40	0.51
01541500	6	0.9	0.95	0.60	583	0.63	0.58	0.52	0.58	0.42	0.55
01542500	8	0.9	0.97	0.66	2,283	0.69	0.63	0.58	0.62	0.46	0.61
01543000	6	0.9	0.93	0.58	454	0.57	0.51	0.45	0.51	0.36	0.53
01543693	6	0.9	0.93	0.70	82	0.69	0.63	0.54	0.64	0.40	0.65
01544000	6	0.9	0.93	0.60	406	0.58	0.52	0.45	0.52	0.36	0.54
01544500	8	0.9	0.93	0.66	229	0.67	0.65	0.53	0.64	0.36	0.61
01545000	8	0.9	0.94	0.57	376	0.62	0.62	0.52	0.63	0.34	0.52
01545600	7	0.9	0.93	0.73	74	0.75	0.69	0.57	0.69	0.43	0.69
01546500	6	0.9	0.98	0.86	96	0.90	0.86	0.82	0.86	0.77	0.83
01547950	5	0.9	0.95	0.71	263	0.78	0.74	0.63	0.74	0.54	0.67
01548005	6	0.9	0.98	0.56	855	0.70	0.69	0.62	0.69	0.53	0.50
01549500	6	0.9	0.93	0.65	59	0.65	0.60	0.51	0.59	0.39	0.60
01549700	7	0.9	0.95	0.63	1,403	0.64	0.59	0.52	0.59	0.41	0.58
01550000	6	0.9	0.94	0.64	290	0.65	0.62	0.55	0.62	0.41	0.59
01552000	6	0.9	0.95	0.58	798	0.61	0.55	0.50	0.55	0.41	0.52
01553500	11	0.9	0.96	0.65	10,972	0.61	0.57	0.53	0.57	0.40	0.60
01553700	4	0.9	0.95	0.47	77	0.50	0.48	0.44	0.48	0.38	0.40
01554000	7	0.9	0.97	0.64	28,591	0.56	0.59	0.54	0.59	0.49	0.59
01555000	7	0.9	0.97	0.68	477	0.76	0.67	0.62	0.67	0.52	0.64
01555400	4	0.9	0.92	0.62	66	0.61	0.56	0.49	0.57	0.41	0.57

Table 2. Long-term average base-flow index (BFI) produced by different methods.—Continued

[*N*, length of period used for BFI method, in days; *f*, BFI turning point test factor; alpha, recession constant; beta, maximum BFI, determined using the method of Collischonn and Fan (2013); ft^3/s, cubic feet per second]

Site number	*N*	*f*	Alpha	Beta	Average daily streamflow (ft^3/s)	BFI, by method					
						PART	HYSEP-Fixed	HYSEP-LocMin	HYSEP-Slide	BFI method	ECK-CaF
01555500	6	0.9	0.95	0.59	245	0.64	0.61	0.53	0.61	0.41	0.54
01556000	7	0.9	0.97	0.59	415	0.66	0.59	0.56	0.60	0.46	0.53
01558000	7	0.9	0.97	0.64	380	0.74	0.71	0.65	0.71	0.51	0.59
01559795	10	0.9	0.92	0.67	28	0.69	0.75	0.59	0.73	0.31	0.61
01562000	8	0.9	0.97	0.53	960	0.60	0.56	0.51	0.57	0.39	0.47
01564500	4	0.9	0.94	0.54	250	0.58	0.57	0.49	0.57	0.40	0.49
01565000	4	0.9	0.97	0.70	257	0.79	0.74	0.67	0.74	0.59	0.65
01567000	4	0.9	0.97	0.61	4,415	0.62	0.57	0.53	0.57	0.57	0.56
01568000	4	0.9	0.96	0.58	311	0.63	0.61	0.56	0.61	0.47	0.53
01570000	6	0.9	0.97	0.62	612	0.68	0.63	0.59	0.63	0.52	0.57
01570500	9	0.9	0.97	0.64	35,133	0.56	0.60	0.57	0.60	0.48	0.59
01571000	5	0.9	0.91	0.49	16	0.49	0.51	0.42	0.52	0.30	0.43
01571490	16	0.9	0.93	0.86	18	0.83	0.85	0.75	0.84	0.52	0.85
01571500	6	0.9	0.98	0.76	311	0.81	0.80	0.76	0.80	0.70	0.72
0157155014	4	0.9	0.95	0.71	5	0.78	0.77	0.66	0.77	0.56	0.67
01571820	6	0.9	0.96	0.72	88	0.75	0.70	0.63	0.69	0.54	0.67
01572000	7	0.9	0.93	0.63	72	0.62	0.57	0.50	0.57	0.36	0.58
01572025	4	0.9	0.96	0.64	224	0.69	0.65	0.58	0.65	0.52	0.59
01572950	7	0.9	0.95	0.70	12	0.77	0.77	0.67	0.77	0.47	0.65
01573160	10	0.9	0.98	0.81	99	0.86	0.83	0.81	0.83	0.67	0.78
01573560	12	0.9	0.91	0.71	904	0.60	0.55	0.50	0.54	0.36	0.66
01573695	4	0.9	0.95	0.56	28	0.57	0.60	0.54	0.60	0.47	0.50
01573710	3	0.9	0.96	0.45	61	0.47	0.45	0.42	0.45	0.39	0.40
01574000	4	0.9	0.95	0.49	667	0.50	0.46	0.43	0.46	0.39	0.44
01575500	7	0.9	0.96	0.69	223	0.69	0.67	0.63	0.67	0.51	0.65
01575585	9	0.9	0.95	0.72	406	0.67	0.61	0.56	0.61	0.49	0.67
01576000	9	0.9	0.96	0.69	38,842	0.57	0.60	0.57	0.61	0.49	0.64
0157608335	8	0.9	0.63	0.82	1	0.69	0.67	0.65	0.67	0.46	0.80
01576085	4	0.9	0.95	0.58	7	0.63	0.64	0.58	0.64	0.47	0.52

Table 2. Long-term average base-flow index (BFI) produced by different methods.—Continued

[*N*, length of period used for BFI method, in days; *f*, BFI turning point test factor; alpha, recession constant; beta, maximum BFI, determined using the method of Collischonn and Fan (2013); ft^3/s, cubic feet per second]

Site number	*N*	*f*	Alpha	Beta	Average daily streamflow (ft^3/s)	BFI, by method					
						PART	HYSEP-Fixed	HYSEP-LocMin	HYSEP-Slide	BFI method	ECK-CaF
01576520	4	0.9	0.97	0.78	9	0.81	0.80	0.78	0.80	0.73	0.73
01576521	4	0.9	0.96	0.68	3	0.69	0.68	0.65	0.68	0.60	0.62
01576529	4	0.9	0.94	0.67	2	0.69	0.66	0.63	0.67	0.56	0.61
01576540	8	0.9	0.96	0.70	81	0.71	0.67	0.66	0.67	0.55	0.65
01576754	7	0.9	0.98	0.69	687	0.70	0.66	0.64	0.66	0.57	0.65
01576787	9	0.9	0.98	0.73	199	0.74	0.73	0.71	0.72	0.65	0.68
01578310	5	0.9	0.96	0.50	40,017	0.40	0.50	0.47	0.51	0.46	0.44
01578475	9	0.9	0.97	0.62	230	0.67	0.66	0.64	0.66	0.51	0.56
01580000	5	0.9	0.98	0.77	129	0.78	0.75	0.73	0.75	0.70	0.73
01580520	4	0.9	0.98	0.75	225	0.75	0.73	0.72	0.73	0.70	0.71
01581500	4	0.9	0.96	0.38	15	0.39	0.42	0.38	0.42	0.32	0.32
01581649	4	0.9	0.95	0.41	16	0.43	0.47	0.41	0.46	0.35	0.35
01581752	2	0.9	0.94	0.46	4	0.46	0.47	0.44	0.47	0.42	0.40
01582500	4	0.9	0.98	0.76	202	0.82	0.80	0.77	0.80	0.75	0.72
01583500	4	0.9	0.97	0.79	70	0.79	0.76	0.75	0.76	0.73	0.75
0158397967	4	0.9	0.93	0.44	3	0.44	0.45	0.42	0.44	0.36	0.37
01586000	5	0.9	0.96	0.72	65	0.72	0.69	0.67	0.68	0.63	0.68
01589000	10	0.9	0.95	0.65	231	0.63	0.56	0.54	0.57	0.45	0.60
01589300	4	0.9	0.96	0.51	46	0.50	0.47	0.47	0.47	0.44	0.44
01591000	5	0.9	0.96	0.74	40	0.73	0.69	0.67	0.69	0.62	0.69
01593500	4	0.9	0.96	0.51	47	0.51	0.48	0.47	0.48	0.44	0.44
01594000	5	0.9	0.97	0.60	141	0.60	0.57	0.56	0.58	0.52	0.54
01594440	6	0.9	0.98	0.58	375	0.60	0.58	0.57	0.58	0.52	0.52
01594526	7	0.9	0.95	0.46	108	0.45	0.44	0.41	0.44	0.33	0.40
01594670	6	0.9	0.94	0.69	10	0.69	0.70	0.66	0.71	0.54	0.64
01594710	6	0.9	0.94	0.77	4	0.76	0.74	0.70	0.74	0.63	0.73
01594930	6	0.9	0.95	0.64	24	0.72	0.73	0.65	0.73	0.46	0.59
01594936	6	0.9	0.90	0.70	4	0.69	0.69	0.61	0.69	0.40	0.66
01595300	4	0.9	0.92	0.72	77	0.68	0.62	0.60	0.62	0.50	0.68

Table 2. Long-term average base-flow index (BFI) produced by different methods.—Continued

[*N*, length of period used for BFI method, in days; *f*, BFI turning point test factor; alpha, recession constant; beta, maximum BFI, determined using the method of Collischonn and Fan (2013); ft^3/s, cubic feet per second]

Site number	*N*	*f*	Alpha	Beta	Average daily streamflow (ft^3/s)	BFI, by method					
						PART	HYSEP-Fixed	HYSEP-LocMin	HYSEP-Slide	BFI method	ECK-CaF
01595800	4	0.9	0.99	0.56	493	0.75	0.73	0.69	0.71	0.63	0.48
01596500	9	0.9	0.93	0.58	78	0.59	0.57	0.49	0.57	0.30	0.53
01599000	6	0.9	0.95	0.62	89	0.68	0.64	0.56	0.64	0.44	0.58
01601000	5	0.9	0.92	0.57	233	0.56	0.56	0.46	0.55	0.35	0.52
01601500	7	0.9	0.95	0.57	355	0.62	0.54	0.50	0.55	0.39	0.52
01604500	4	0.9	0.94	0.59	181	0.68	0.64	0.51	0.64	0.44	0.55
01605500	5	0.9	0.97	0.58	189	0.66	0.63	0.56	0.63	0.48	0.52
01606000	6	0.9	0.94	0.58	433	0.59	0.53	0.49	0.53	0.36	0.53
01606500	6	0.9	0.96	0.56	796	0.61	0.57	0.52	0.56	0.44	0.50
01607500	6	0.9	0.94	0.49	105	0.51	0.50	0.42	0.50	0.31	0.43
01608000	6	0.9	0.95	0.53	238	0.56	0.49	0.44	0.49	0.36	0.47
01608500	5	0.9	0.97	0.53	1,455	0.57	0.51	0.47	0.51	0.45	0.47
01609000	4	0.9	0.95	0.50	155	0.55	0.54	0.49	0.55	0.39	0.45
01610155	4	0.9	0.91	0.49	105	0.46	0.46	0.38	0.46	0.31	0.44
01610200	6	0.9	0.92	0.47	186	0.42	0.44	0.37	0.44	0.23	0.41
01610400	4	0.9	0.94	0.67	17	0.72	0.73	0.61	0.73	0.48	0.62
01611500	5	0.9	0.97	0.51	601	0.60	0.55	0.51	0.55	0.44	0.46
01613000	6	0.9	0.97	0.56	4,178	0.56	0.52	0.48	0.52	0.45	0.50
01613030	4	0.9	0.95	0.63	7	0.66	0.68	0.60	0.70	0.54	0.56
01613050	5	0.9	0.90	0.62	14	0.59	0.66	0.50	0.67	0.34	0.57
01613095	5	0.9	0.93	0.53	116	0.51	0.50	0.43	0.50	0.32	0.48
01613525	3	0.9	0.95	0.59	217	0.63	0.61	0.54	0.61	0.49	0.54
01613900	5	0.9	0.93	0.48	16	0.52	0.59	0.47	0.59	0.33	0.42
01614000	5	0.9	0.95	0.50	201	0.53	0.53	0.47	0.53	0.35	0.44
01614500	4	0.9	0.97	0.64	628	0.69	0.63	0.59	0.63	0.56	0.59
01614830	4	0.9	0.97	0.85	8	0.87	0.86	0.83	0.86	0.77	0.82
01615000	5	0.9	0.96	0.48	53	0.52	0.49	0.45	0.49	0.38	0.42
01616400	7	0.9	0.96	0.82	16	0.83	0.82	0.78	0.83	0.67	0.79
01616500	5	0.9	0.98	0.63	262	0.68	0.63	0.61	0.63	0.58	0.59

Table 2. Long-term average base-flow index (BFI) produced by different methods.—Continued

[*N*, length of period used for BFI method, in days; *f*, BFI turning point test factor; alpha, recession constant; beta, maximum BFI, determined using the method of Collischonn and Fan (2013); ft³/s, cubic feet per second]

Site number	*N*	*f*	Alpha	Beta	Average daily streamflow (ft³/s)	BFI, by method					
						PART	HYSEP-Fixed	HYSEP-LocMin	HYSEP-Slide	BFI method	ECK-CaF
01617800	4	0.9	0.97	0.88	11	0.90	0.89	0.86	0.89	0.80	0.86
01618100	4	0.9	0.98	0.92	12	0.96	0.94	0.94	0.95	0.88	0.91
01619000	3	0.9	0.97	0.80	106	0.82	0.78	0.73	0.78	0.74	0.76
01619500	5	0.9	0.98	0.84	311	0.86	0.80	0.78	0.81	0.76	0.81
01621050	5	0.9	0.96	0.68	10	0.73	0.73	0.66	0.73	0.54	0.63
01626000	5	0.9	0.97	0.65	156	0.74	0.70	0.63	0.69	0.55	0.59
01628500	6	0.9	0.98	0.62	1,088	0.68	0.60	0.57	0.60	0.54	0.56
01631000	6	0.9	0.97	0.64	1,581	0.68	0.62	0.58	0.62	0.55	0.59
01632000	6	0.9	0.94	0.45	209	0.47	0.48	0.39	0.48	0.29	0.39
01632900	6	0.9	0.97	0.69	77	0.72	0.68	0.64	0.68	0.55	0.64
01634000	6	0.9	0.97	0.57	645	0.65	0.61	0.56	0.60	0.50	0.51
01634500	4	0.9	0.95	0.54	107	0.59	0.56	0.49	0.55	0.43	0.48
01636500	6	0.9	0.97	0.66	2,887	0.66	0.62	0.58	0.62	0.56	0.60
01637500	5	0.9	0.94	0.68	79	0.69	0.63	0.57	0.63	0.48	0.64
01638480	4	0.9	0.94	0.59	95	0.59	0.56	0.52	0.55	0.45	0.54
01639000	6	0.9	0.94	0.38	222	0.39	0.39	0.35	0.39	0.25	0.33
01639500	5	0.9	0.96	0.63	119	0.64	0.61	0.58	0.61	0.53	0.58
01643000	6	0.9	0.97	0.54	999	0.55	0.52	0.50	0.53	0.43	0.49
01643700	4	0.9	0.95	0.59	135	0.64	0.59	0.54	0.59	0.47	0.54
01644000	5	0.9	0.95	0.61	354	0.61	0.54	0.50	0.54	0.45	0.56
01645000	5	0.9	0.97	0.64	117	0.65	0.62	0.60	0.63	0.55	0.58
01645704	4	0.9	0.94	0.40	9	0.41	0.45	0.40	0.45	0.32	0.33
01645762	4	0.9	0.93	0.60	3	0.59	0.59	0.56	0.59	0.51	0.51
01646000	5	0.9	0.96	0.52	66	0.52	0.50	0.48	0.50	0.45	0.46
01646305	8	0.9	0.75	0.51	2	0.44	0.44	0.42	0.44	0.36	0.43
01646500	5	0.9	0.96	0.65	11,436	0.56	0.56	0.52	0.56	0.52	0.60
01648000	4	0.9	0.95	0.50	68	0.54	0.51	0.47	0.50	0.41	0.45
01649190	6	0.9	0.96	0.52	14	0.54	0.56	0.52	0.56	0.44	0.46
01649500	6	0.9	0.95	0.47	88	0.46	0.44	0.43	0.44	0.36	0.40

Table 2. Long-term average base-flow index (BFI) produced by different methods.—Continued

[*N*, length of period used for BFI method, in days; *f*, BFI turning point test factor; alpha, recession constant; beta, maximum BFI, determined using the method of Collischonn and Fan (2013); ft³/s, cubic feet per second]

Site number	*N*	*f*	Alpha	Beta	Average daily streamflow (ft³/s)	BFI, by method					
						PART	HYSEP-Fixed	HYSEP-LocMin	HYSEP-Slide	BFI method	ECK-CaF
01651000	4	0.9	0.95	0.44	55	0.43	0.41	0.40	0.41	0.37	0.38
01651800	5	0.9	0.93	0.40	5	0.40	0.41	0.38	0.41	0.31	0.33
01653600	6	0.9	0.91	0.60	46	0.55	0.51	0.48	0.51	0.40	0.54
01654000	3	0.9	0.95	0.29	31	0.28	0.33	0.29	0.33	0.25	0.23
01656500	4	0.9	0.94	0.59	47	0.59	0.55	0.49	0.54	0.43	0.54
01656903	6	0.9	0.92	0.40	7	0.41	0.46	0.37	0.46	0.24	0.33
01658000	6	0.9	0.88	0.49	62	0.40	0.41	0.37	0.41	0.26	0.43
01658500	5	0.9	0.93	0.45	7	0.45	0.49	0.42	0.49	0.33	0.38
01659000	6	0.9	0.88	0.53	5	0.47	0.50	0.45	0.51	0.31	0.45
01660920	4	0.9	0.95	0.36	86	0.53	0.51	0.47	0.52	0.42	0.32
01661050	4	0.9	0.92	0.56	18	0.54	0.58	0.51	0.58	0.45	0.48
01662800	4	0.9	0.94	0.65	25	0.67	0.69	0.61	0.69	0.50	0.60
01663500	6	0.9	0.96	0.68	339	0.69	0.61	0.56	0.61	0.50	0.63
01664000	6	0.9	0.96	0.64	701	0.63	0.59	0.55	0.59	0.49	0.59
01665500	6	0.9	0.96	0.68	144	0.71	0.66	0.59	0.66	0.50	0.62
01666500	6	0.9	0.97	0.65	227	0.68	0.65	0.60	0.65	0.53	0.59
01667500	6	0.9	0.96	0.63	559	0.65	0.59	0.55	0.59	0.49	0.58
01668000	6	0.9	0.96	0.58	1,716	0.55	0.51	0.49	0.51	0.45	0.53
01669520	3	0.9	0.95	0.66	122	0.74	0.73	0.61	0.73	0.62	0.61
01671020	6	0.9	0.97	0.41	372	0.50	0.49	0.45	0.49	0.39	0.34
01671100	5	0.9	0.93	0.61	80	0.58	0.59	0.51	0.58	0.44	0.54
01673000	5	0.9	0.97	0.50	961	0.51	0.49	0.46	0.49	0.44	0.44
01673800	5	0.9	0.93	0.49	73	0.47	0.46	0.42	0.46	0.35	0.42
01674000	5	0.9	0.94	0.60	224	0.56	0.53	0.49	0.52	0.43	0.54
01674500	5	0.9	0.95	0.72	520	0.67	0.69	0.59	0.68	0.55	0.67
01677000	5	0.9	0.95	0.68	6	0.71	0.73	0.66	0.73	0.57	0.63
02011500	5	0.9	0.95	0.47	181	0.54	0.54	0.46	0.54	0.37	0.41
02012500	6	0.9	0.97	0.56	490	0.64	0.58	0.54	0.58	0.46	0.50
02015700	4	0.9	0.97	0.57	158	0.65	0.62	0.56	0.61	0.50	0.51

Table 2. Long-term average base-flow index (BFI) produced by different methods.—Continued

[*N*, length of period used for BFI method, in days; *f*, BFI turning point test factor; alpha, recession constant; beta, maximum BFI, determined using the method of Collischonn and Fan (2013); ft^3/s, cubic feet per second]

Site number	*N*	*f*	Alpha	Beta	Average daily streamflow (ft^3/s)	BFI, by method					
						PART	HYSEP-Fixed	HYSEP-LocMin	HYSEP-Slide	BFI method	ECK-CaF
02020500	6	0.9	0.93	0.52	160	0.53	0.51	0.42	0.51	0.31	0.46
02024000	6	0.9	0.97	0.57	710	0.62	0.56	0.53	0.57	0.45	0.51
02024752	9	0.9	0.98	0.54	3,374	0.60	0.57	0.53	0.56	0.43	0.48
02031000	5	0.9	0.96	0.65	106	0.68	0.63	0.58	0.63	0.52	0.60
02034000	5	0.9	0.97	0.57	700	0.58	0.54	0.52	0.55	0.48	0.51
02035000	6	0.9	0.96	0.66	6,981	0.59	0.57	0.54	0.57	0.52	0.61
02037500	6	0.9	0.97	0.65	7,171	0.60	0.57	0.55	0.57	0.53	0.59
02038850	4	0.9	0.96	0.61	8	0.63	0.65	0.59	0.65	0.54	0.54
02039500	5	0.9	0.97	0.55	282	0.58	0.54	0.52	0.54	0.49	0.49
02041000	5	0.9	0.95	0.52	141	0.52	0.52	0.47	0.52	0.41	0.45
02041650	4	0.9	0.96	0.50	1,182	0.52	0.51	0.46	0.50	0.46	0.44
02042426	2	0.9	0.93	0.26	39	0.25	0.25	0.22	0.25	0.22	0.21
02042500	6	0.9	0.93	0.69	271	0.66	0.64	0.52	0.64	0.46	0.65
03050000	5	0.9	0.92	0.52	378	0.46	0.49	0.44	0.49	0.31	0.46
03065000	5	0.9	0.93	0.56	849	0.51	0.48	0.44	0.48	0.37	0.50
03066000	6	0.9	0.93	0.58	219	0.56	0.55	0.50	0.55	0.36	0.53
03069000	5	0.9	0.94	0.55	570	0.53	0.55	0.50	0.55	0.40	0.50
03069500	5	0.9	0.94	0.53	1,858	0.47	0.48	0.44	0.48	0.37	0.48
03070000	4	0.9	0.94	0.53	2,550	0.47	0.48	0.43	0.48	0.40	0.48
03070500	5	0.9	0.93	0.56	423	0.54	0.55	0.49	0.55	0.37	0.51
03076600	6	0.9	0.95	0.58	94	0.65	0.61	0.53	0.61	0.39	0.53
03180500	5	0.9	0.93	0.58	279	0.56	0.56	0.49	0.56	0.38	0.52

(eq. 6). Values of beta ranged from 0.26 to 0.92, with a mean of 0.61 (fig. 2, table 2). The range in beta generally decreased with increasing watershed area. Values of the BFI determined by all six methods displayed a similar pattern, with a range from 0.21 to 0.96 (fig. 3).

The long-term average ratio of base flow to streamflow, or BFI, provides an important measure of a watershed's response to precipitation and the dynamics of the groundwater system. In many cases, the BFI is the sought-after end result of hydrograph separation and may be used to help assess the water budget for a watershed. It is often used as a surrogate for groundwater recharge. For example, the major assumptions of PART are that base flow is equivalent to groundwater discharge and that effective recharge is approximately equal to groundwater discharge (Risser and others, 2005; Sanford and others, 2012). The time series produced by hydrograph separation may also be used to determine the fraction of days when base flow reaches some value (for example, 90 or 100 percent of streamflow), which may be useful in filtering chemical analyses or evaluating seasonality of other aspects of groundwater discharge. For this study, a value of 100 percent (base flow equal to streamflow) was used to assess the fraction of base-flow days (table 3).

Values of the BFI and fraction of base-flow days were compared for all methods with the ECK-CaF method. There is generally a reasonable correlation between the BFI values estimated using ECK-CaF and those estimated using PART, HYSEP, and BFI, although PART (fig. 4), HYSEP-Fixed (fig. 5*A*), and HYSEP-Slide (fig. 5*C*) predict higher BFI values, and the BFI method (fig. 6) predicts lower values than the ECK-CaF method. Values from HYSEP-LocMin (fig. 5*B*) are generally similar to those from ECK-CaF. The scatterplot matrix for BFI (fig. 7) from all methods indicates that the BFI method consistently predicts lower BFI values compared to the other methods, whereas the three different HYSEP BFI results are generally comparable. Larger differences are seen between the fraction of base-flow days predicted by each method. The ECK-CaF method predicts the smallest range of values (0.03–0.18), and the PART method predicts the largest range (0.08–0.65) (fig. 8).

One cause of differences in the BFI and fraction of days at base flow between the ECK-CaF method and the other methods relates to how each method quantifies base-flow recession. The ECK-CaF method models base-flow recession response assuming a linear groundwater reservoir and uses a backward filter to approximate base-flow recession during events so that base-flow recession during events is consistent with streamflow recession (alpha) between events. The other methods have no physical basis and make no assumptions regarding base-flow recession. As a result, base flow does not recede smoothly and continuously using the other methods, especially during events (rises and falls) in the streamflow hydrograph, and may display artifacts such as sudden slope breaks or plateaus (fig. 9).

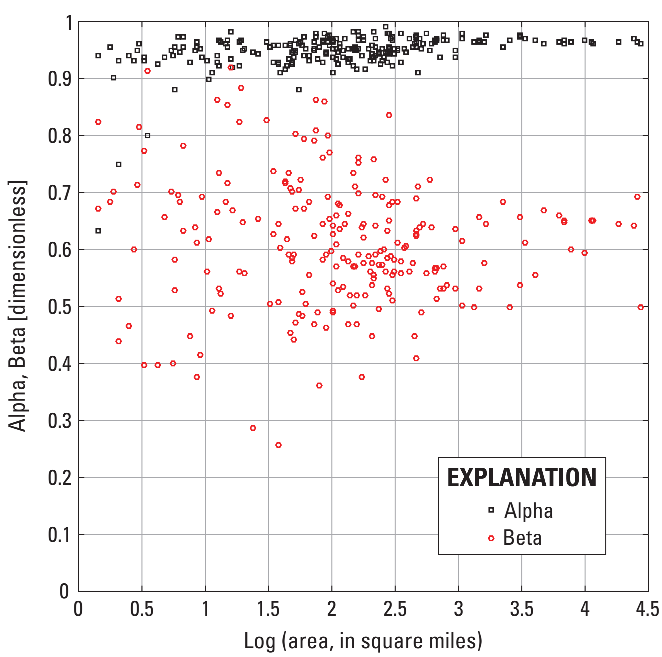

Figure 2. Values of alpha and beta as functions of watershed area.

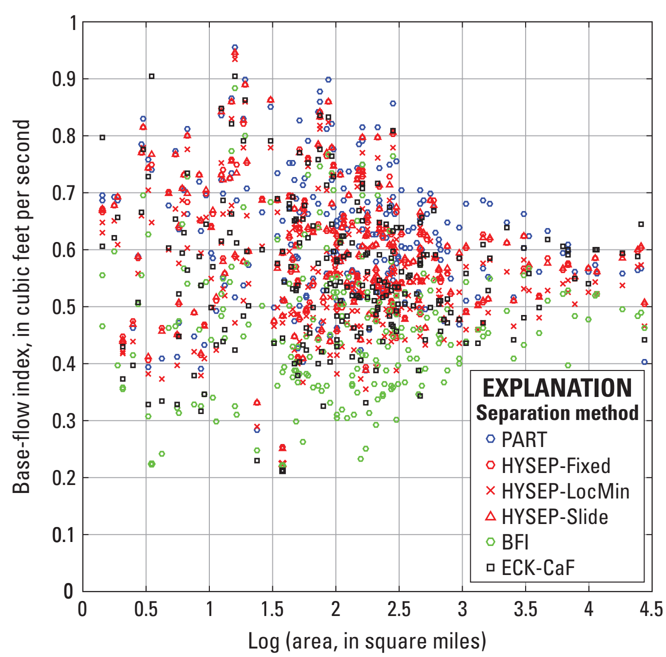

Figure 3. Values of the base-flow index (BFI) as a function of watershed area.

Table 3. Fraction of days with base flow equal to streamflow for the period of analysis, as produced by different methods.

[Count, number of daily values during period of analysis; ft^3/s, cubic feet per second]

Site number	Period of analysis		Count	Average daily streamflow (ft^3/s)	Fraction of days at base flow, by method					
	Beginning date	End date			PART	HYSEP-Fixed	HYSEP-LocMin	HYSEP-Slide	BFI	ECK-CaF
01409810	2/1/2006	9/30/2013	2,799	144	0.44	0.22	0.20	0.14	0.12	0.12
01411300	10/1/1979	6/30/2013	12,327	40	0.63	0.43	0.32	0.29	0.15	0.12
01484000	4/27/2007	12/31/2008	615	9	0.52	0.38	0.36	0.28	0.19	0.11
01484100	10/1/1979	9/30/2013	12,419	4	0.56	0.39	0.34	0.31	0.18	0.08
01485000	10/1/2006	9/30/2013	2,557	72	0.54	0.25	0.22	0.15	0.19	0.08
01485500	10/1/1979	9/30/2013	12,419	53	0.47	0.24	0.20	0.15	0.14	0.12
01486000	10/1/1979	9/30/2013	12,419	5	0.48	0.31	0.24	0.20	0.19	0.09
01486500	10/1/2000	8/29/2016	5,812	26	0.56	0.44	0.36	0.32	0.21	0.06
01487000	10/1/1979	9/30/2013	12,419	95	0.51	0.26	0.23	0.19	0.15	0.12
01488500	10/1/1979	9/30/2002	8,401	55	0.56	0.29	0.26	0.22	0.17	0.08
01490000	10/1/2000	9/30/2013	4,748	17	0.60	0.43	0.33	0.29	0.16	0.10
01491000	10/1/1979	9/30/2013	12,419	146	0.47	0.23	0.19	0.15	0.12	0.11
01491500	11/1/2000	4/30/2013	4,564	110	0.46	0.24	0.21	0.17	0.14	0.09
01493112	10/1/1996	7/31/2013	2,953	8	0.52	0.42	0.36	0.33	0.19	0.04
01493500	10/1/2006	9/30/2013	2,557	12	0.44	0.38	0.31	0.27	0.20	0.05
01495000	10/1/1979	9/30/2013	12,419	71	0.45	0.26	0.24	0.21	0.23	0.09
01502500	10/1/2000	12/31/2012	4,475	1,001	0.37	0.15	0.15	0.10	0.13	0.12
01503000	10/1/1979	12/31/2012	12,146	3,696	0.31	0.12	0.14	0.08	0.14	0.12
01508803	10/1/1972	9/30/1986	5,113	128	0.50	0.24	0.20	0.15	0.16	0.11
01509150	10/1/1974	9/30/1981	2,557	22	0.56	0.39	0.31	0.24	0.24	0.10
01515000	10/1/2000	12/31/2012	4,475	9,573	0.29	0.09	0.10	0.06	0.15	0.14
01516350	10/1/1976	9/30/2015	14,244	215	0.49	0.23	0.21	0.15	0.16	0.10
01518000	10/1/1938	9/30/2015	28,124	400	0.39	0.22	0.22	0.17	0.16	0.08
01518500	10/1/1953	9/30/1974	7,670	112	0.46	0.25	0.22	0.17	0.14	0.10
01518700	7/1/1976	9/30/2015	14,336	538	0.36	0.21	0.22	0.16	0.15	0.06
01520000	10/1/1951	9/30/2015	23,376	309	0.35	0.22	0.21	0.17	0.15	0.09
01527000	10/1/1950	9/30/1981	11,323	56	0.50	0.26	0.20	0.16	0.13	0.14
01527050	11/1/1978	9/30/1980	700	4	0.44	0.32	0.25	0.21	0.19	0.07
01528000	10/1/1937	9/30/1994	20,819	76	0.45	0.24	0.22	0.16	0.17	0.11

Table 3. Fraction of days with base flow equal to streamflow for the period of analysis, as produced by different methods.—Continued

[Count, number of daily values during period of analysis; ft^3/s, cubic feet per second]

Site number	Period of analysis		Count	Average daily streamflow (ft^3/s)	Fraction of days at base flow, by method					
	Beginning date	End date			PART	HYSEP-Fixed	HYSEP-LocMin	HYSEP-Slide	BFI	ECK-CaF
01529500	10/1/1979	12/31/2012	12,146	499	0.39	0.16	0.16	0.10	0.14	0.11
01531000	10/1/1979	12/31/2012	12,146	2,776	0.33	0.12	0.16	0.08	0.15	0.09
01531500	10/1/1979	9/30/2013	12,419	11,238	0.24	0.10	0.12	0.06	0.16	0.11
01532000	10/1/1914	9/30/2015	36,890	290	0.47	0.23	0.21	0.15	0.15	0.12
01534000	10/1/1979	9/30/2013	12,419	577	0.38	0.16	0.16	0.10	0.14	0.12
01536000	10/1/1938	9/30/2015	28,124	486	0.34	0.16	0.15	0.10	0.11	0.12
01536500	10/1/1979	10/31/2012	12,085	14,554	0.24	0.10	0.13	0.06	0.15	0.11
01540500	10/1/1979	9/30/2013	12,419	16,427	0.24	0.10	0.13	0.06	0.16	0.12
01541000	10/1/1913	9/30/2015	37,255	557	0.36	0.16	0.17	0.11	0.13	0.12
01541500	10/1/1913	9/30/2015	37,255	583	0.37	0.16	0.17	0.11	0.13	0.12
01542500	10/1/2004	9/30/2013	3,287	2,283	0.31	0.11	0.13	0.07	0.12	0.12
01543000	10/1/1913	9/30/2015	37,255	454	0.38	0.17	0.16	0.11	0.14	0.14
01543693	10/1/2011	9/30/2015	1,461	82	0.50	0.23	0.19	0.12	0.14	0.16
01544000	10/1/1953	9/30/2015	22,645	406	0.35	0.18	0.17	0.13	0.13	0.11
01544500	10/1/1940	9/30/2015	27,393	229	0.50	0.23	0.19	0.13	0.14	0.13
01545000	10/1/1954	9/30/2015	22,280	376	0.44	0.23	0.20	0.14	0.11	0.10
01545600	10/1/1965	9/30/2015	18,262	74	0.52	0.23	0.18	0.13	0.14	0.14
01546500	10/1/1940	9/30/2015	27,393	96	0.52	0.28	0.25	0.20	0.19	0.10
01547950	10/1/1968	9/30/2015	17,166	263	0.53	0.22	0.19	0.12	0.16	0.14
01548005	10/1/1979	9/30/1995	5,844	855	0.40	0.17	0.20	0.11	0.14	0.08
01549500	10/1/1940	9/30/2015	27,393	59	0.50	0.23	0.20	0.15	0.15	0.13
01549700	10/1/1979	9/30/2013	12,419	1,403	0.43	0.15	0.15	0.09	0.14	0.13
01550000	10/1/1914	9/30/2015	36,890	290	0.50	0.23	0.20	0.14	0.15	0.13
01552000	10/1/1975	9/30/2015	14,610	798	0.41	0.15	0.15	0.09	0.13	0.12
01553500	10/1/1979	9/30/2013	12,419	10,972	0.30	0.10	0.12	0.06	0.10	0.13
01553700	10/1/1994	9/30/2013	6,940	77	0.45	0.26	0.24	0.20	0.18	0.08
01554000	10/1/1967	2/16/2015	17,306	28,591	0.20	0.10	0.11	0.06	0.13	0.12
01555000	10/1/1979	9/30/2013	12,419	477	0.44	0.16	0.16	0.10	0.15	0.10
01555400	10/1/1996	9/30/2000	1,461	66	0.48	0.23	0.18	0.14	0.18	0.12

Table 3. Fraction of days with base flow equal to streamflow for the period of analysis, as produced by different methods.—Continued

[Count, number of daily values during period of analysis; ft³/s, cubic feet per second]

Site number	Period of analysis		Count	Average daily streamflow (ft³/s)	Fraction of days at base flow, by method					
	Beginning date	End date			PART	HYSEP-Fixed	HYSEP-LocMin	HYSEP-Slide	BFI	ECK-CaF
01555500	10/1/1979	9/30/2013	12,419	245	0.50	0.22	0.20	0.13	0.13	0.11
01556000	10/1/1979	9/30/2013	12,419	415	0.37	0.16	0.18	0.10	0.13	0.09
01558000	10/1/1979	9/30/2013	12,419	380	0.48	0.23	0.22	0.14	0.14	0.10
01559795	10/1/1997	9/30/2000	1,096	28	0.56	0.38	0.30	0.23	0.19	0.12
01562000	10/1/1979	9/30/2013	12,419	960	0.39	0.16	0.19	0.10	0.13	0.09
01564500	10/1/1979	9/30/2013	12,419	250	0.48	0.23	0.21	0.14	0.18	0.12
01565000	10/1/2001	9/30/2013	4,383	257	0.54	0.23	0.21	0.13	0.22	0.12
01567000	10/1/1979	9/30/2013	12,419	4,415	0.25	0.10	0.12	0.07	0.20	0.09
01568000	10/1/1979	9/30/2013	12,419	311	0.48	0.23	0.21	0.15	0.19	0.10
01570000	10/1/1979	9/30/2013	12,419	612	0.41	0.15	0.17	0.10	0.15	0.11
01570500	10/1/1979	9/30/2013	12,419	35,133	0.21	0.10	0.13	0.06	0.12	0.11
01571000	10/1/1991	9/30/1995	1,461	16	0.52	0.34	0.27	0.19	0.18	0.13
01571490	4/1/1993	9/30/1995	913	18	0.65	0.41	0.35	0.30	0.15	0.14
01571500	10/1/1979	9/30/2013	12,419	311	0.47	0.23	0.22	0.15	0.18	0.09
0157155014	10/1/1996	9/30/2006	3,652	5	0.57	0.34	0.26	0.21	0.18	0.13
01571820	10/1/1996	9/30/2006	3,652	88	0.50	0.25	0.22	0.17	0.15	0.10
01572000	10/1/1981	9/30/1984	1,096	72	0.50	0.25	0.21	0.17	0.14	0.13
01572025	10/1/1991	9/30/2015	8,766	224	0.51	0.22	0.20	0.13	0.19	0.12
01572950	10/1/2002	9/30/2010	2,922	12	0.64	0.38	0.34	0.23	0.13	0.13
01573160	10/1/1979	9/30/1994	5,479	99	0.39	0.28	0.27	0.23	0.12	0.08
01573560	10/1/2007	9/30/2013	2,192	904	0.36	0.15	0.15	0.09	0.10	0.09
01573695	10/1/2012	9/30/2015	1,095	28	0.53	0.38	0.32	0.27	0.20	0.11
01573710	10/1/2011	9/30/2015	1,461	61	0.44	0.24	0.22	0.17	0.22	0.11
01574000	10/1/1979	9/30/2013	12,419	667	0.37	0.15	0.17	0.10	0.18	0.11
01575500	10/1/1940	9/30/1996	20,454	223	0.36	0.22	0.20	0.17	0.10	0.11
01575585	10/1/2012	9/30/2015	1,095	406	0.35	0.15	0.16	0.11	0.10	0.11
01576000	10/1/1979	9/30/2013	12,419	38,842	0.19	0.09	0.12	0.06	0.11	0.12
0157608335	10/1/1984	9/30/1991	2,556	1	0.23	0.17	0.14	0.14	0.17	0.06
01576085	10/1/1982	9/30/1995	4,748	7	0.57	0.37	0.31	0.26	0.21	0.09

Table 3. Fraction of days with base flow equal to streamflow for the period of analysis, as produced by different methods.—Continued

[Count, number of daily values during period of analysis; ft³/s, cubic feet per second]

Site number	Period of analysis		Count	Average daily streamflow (ft³/s)	Fraction of days at base flow, by method					
	Beginning date	End date			PART	HYSEP-Fixed	HYSEP-LocMin	HYSEP-Slide	BFI	ECK-CaF
01576520	10/1/1992	9/30/1998	2,191	9	0.65	0.45	0.39	0.35	0.27	0.08
01576521	10/1/1993	9/30/2000	2,557	3	0.52	0.36	0.32	0.29	0.26	0.09
01576529	10/1/1993	9/30/2000	2,557	2	0.35	0.24	0.20	0.19	0.28	0.09
01576540	10/1/1992	9/30/1998	2,191	81	0.46	0.25	0.21	0.18	0.11	0.08
01576754	10/1/1984	9/30/2013	10,592	687	0.37	0.15	0.15	0.10	0.12	0.12
01576787	2/24/1977	9/30/2013	4,259	199	0.47	0.24	0.24	0.17	0.14	0.09
01578310	10/1/1979	9/30/2013	12,419	40,017	0.08	0.09	0.10	0.09	0.11	0.06
01578475	12/20/2005	9/30/2013	2,842	230	0.38	0.22	0.23	0.16	0.11	0.07
01580000	10/1/1979	9/30/2013	12,419	129	0.46	0.24	0.23	0.18	0.21	0.10
01580520	1/1/2000	9/30/2013	5,022	225	0.45	0.22	0.23	0.16	0.25	0.11
01581500	10/1/1999	9/30/2015	5,844	15	0.50	0.36	0.30	0.24	0.18	0.10
01581649	10/1/2004	9/30/2015	4,017	16	0.44	0.35	0.28	0.23	0.15	0.07
01581752	10/1/2001	9/30/2013	4,383	4	0.48	0.35	0.30	0.27	0.38	0.10
01582500	10/1/1984	9/30/2013	10,592	202	0.45	0.24	0.23	0.17	0.26	0.07
01583500	10/1/1979	9/30/2013	12,419	70	0.49	0.27	0.25	0.21	0.26	0.10
0158397967	10/1/2001	9/30/2015	5,113	3	0.33	0.27	0.24	0.22	0.24	0.11
01586000	10/1/1979	11/30/2012	12,115	65	0.46	0.26	0.23	0.20	0.17	0.10
01589000	10/1/2010	9/30/2015	1,826	231	0.34	0.16	0.15	0.12	0.12	0.09
01589300	10/1/1996	9/30/2013	6,209	46	0.48	0.29	0.27	0.24	0.21	0.09
01591000	10/1/1979	9/30/2013	12,419	40	0.50	0.28	0.25	0.21	0.18	0.10
01593500	10/1/1979	9/30/2013	12,419	47	0.44	0.26	0.24	0.21	0.19	0.11
01594000	10/1/1975	9/30/1980	1,827	141	0.44	0.25	0.24	0.18	0.18	0.09
01594440	10/1/1979	9/30/2013	12,419	375	0.28	0.16	0.17	0.12	0.16	0.07
01594526	10/1/1993	9/30/2013	7,305	108	0.42	0.23	0.22	0.16	0.12	0.13
01594670	10/1/1988	9/30/1997	3,287	10	0.45	0.34	0.27	0.23	0.13	0.17
01594710	10/1/1985	9/30/1997	4,383	4	0.51	0.36	0.29	0.27	0.16	0.14
01594930	10/1/1980	9/30/2004	8,766	24	0.56	0.37	0.30	0.23	0.14	0.14
01594936	10/1/1980	9/30/2007	9,861	4	0.40	0.27	0.21	0.15	0.13	0.16
01595300	10/1/1979	9/30/1982	1,096	77	0.45	0.24	0.21	0.17	0.19	0.18

Table 3. Fraction of days with base flow equal to streamflow for the period of analysis, as produced by different methods.—Continued

[Count, number of daily values during period of analysis; ft³/s, cubic feet per second]

Site number	Period of analysis		Count	Average daily streamflow (ft³/s)	Fraction of days at base flow, by method					
	Beginning date	End date			PART	HYSEP-Fixed	HYSEP-LocMin	HYSEP-Slide	BFI	ECK-CaF
01595800	10/1/2003	9/30/2015	4,383	493	0.41	0.25	0.29	0.20	0.28	0.03
01596500	10/1/1979	1/31/2013	12,177	78	0.48	0.23	0.21	0.14	0.13	0.14
01599000	10/1/1979	9/30/2013	12,419	89	0.51	0.24	0.22	0.16	0.15	0.11
01601000	4/12/2002	9/30/2013	4,190	233	0.47	0.22	0.19	0.12	0.17	0.15
01601500	10/1/1979	9/30/2013	12,419	355	0.43	0.17	0.17	0.11	0.14	0.11
01604500	10/1/1979	9/30/2013	12,419	181	0.54	0.23	0.20	0.13	0.20	0.14
01605500	10/1/1979	9/30/2013	12,419	189	0.53	0.24	0.22	0.15	0.18	0.09
01606000	10/1/1998	9/30/2013	5,479	433	0.42	0.16	0.17	0.10	0.13	0.15
01606500	10/1/1967	2/16/2015	17,306	796	0.42	0.16	0.16	0.10	0.15	0.11
01607500	10/1/1943	9/30/2015	26,298	105	0.51	0.25	0.22	0.16	0.15	0.10
01608000	10/1/1938	9/30/2015	28,124	238	0.47	0.19	0.18	0.12	0.15	0.11
01608500	10/1/1979	9/30/2013	12,419	1,455	0.37	0.12	0.14	0.07	0.17	0.11
01609000	10/1/2006	9/30/2013	2,557	155	0.48	0.23	0.22	0.13	0.18	0.13
01610155	4/1/1999	9/30/2013	5,297	105	0.41	0.19	0.17	0.10	0.18	0.17
01610200	10/1/1971	9/30/1979	2,922	186	0.44	0.23	0.22	0.15	0.12	0.11
01610400	10/1/2002	9/30/2015	4,748	17	0.64	0.40	0.32	0.25	0.20	0.12
01611500	10/1/1997	9/30/2013	5,844	601	0.44	0.16	0.18	0.10	0.17	0.11
01613000	10/1/1932	9/30/2015	30,315	4,178	0.28	0.10	0.12	0.07	0.14	0.11
01613030	10/1/2011	9/30/2015	1,461	7	0.54	0.41	0.33	0.28	0.22	0.10
01613050	9/1/1985	9/30/2013	10,257	14	0.41	0.28	0.21	0.15	0.17	0.14
01613095	10/1/2005	9/30/2013	2,922	116	0.46	0.22	0.20	0.13	0.16	0.16
01613525	3/1/2005	9/30/2013	3,136	217	0.50	0.24	0.23	0.15	0.24	0.12
01613900	10/1/1992	9/30/2012	7,305	16	0.50	0.35	0.29	0.22	0.16	0.09
01614000	6/30/2004	9/30/2013	3,380	201	0.48	0.22	0.21	0.13	0.16	0.12
01614500	10/1/1979	9/30/2013	12,419	628	0.42	0.16	0.17	0.10	0.21	0.11
01614830	10/1/2001	9/30/2009	2,922	8	0.62	0.44	0.38	0.33	0.25	0.09
01615000	10/1/2002	9/30/2015	4,748	53	0.44	0.24	0.22	0.17	0.14	0.09
01616400	10/1/2011	9/30/2015	1,461	16	0.63	0.43	0.36	0.33	0.14	0.12
01616500	10/1/1979	9/30/2013	12,419	262	0.40	0.17	0.17	0.11	0.19	0.08

Table 3. Fraction of days with base flow equal to streamflow for the period of analysis, as produced by different methods.—Continued

[Count, number of daily values during period of analysis; ft³/s, cubic feet per second]

Site number	Period of analysis		Count	Average daily streamflow (ft³/s)	Fraction of days at base flow, by method					
	Beginning date	End date			PART	HYSEP-Fixed	HYSEP-LocMin	HYSEP-Slide	BFI	ECK-CaF
01617800	10/1/1979	9/30/2013	12,419	11	0.59	0.44	0.38	0.34	0.23	0.13
01618100	3/27/2008	9/30/2013	2,014	12	0.64	0.51	0.47	0.43	0.33	0.10
01619000	10/1/2005	9/30/2013	2,922	106	0.52	0.25	0.23	0.17	0.34	0.10
01619500	10/1/1979	9/30/2013	12,419	311	0.40	0.16	0.15	0.10	0.23	0.11
01621050	4/13/1993	9/30/2013	7,476	10	0.58	0.38	0.31	0.26	0.16	0.09
01626000	10/1/1979	9/30/2013	12,419	156	0.55	0.26	0.24	0.18	0.20	0.09
01628500	10/1/1979	9/30/2013	12,419	1,088	0.37	0.12	0.15	0.07	0.17	0.09
01631000	10/1/1930	9/30/2015	31,046	1,581	0.29	0.12	0.13	0.08	0.14	0.09
01632000	10/1/1979	9/30/2013	12,419	209	0.53	0.23	0.20	0.13	0.17	0.13
01632900	10/1/1979	9/30/2013	12,419	77	0.55	0.28	0.25	0.20	0.15	0.09
01634000	10/1/1979	9/30/2013	12,419	645	0.39	0.15	0.16	0.09	0.14	0.09
01634500	10/1/1979	4/30/2013	12,266	107	0.48	0.24	0.21	0.16	0.18	0.10
01636500	10/1/1979	9/30/2013	12,419	2,887	0.32	0.12	0.13	0.07	0.15	0.10
01637500	10/1/1979	9/30/2013	12,419	79	0.48	0.22	0.20	0.15	0.15	0.16
01638480	10/1/1979	11/30/2012	12,115	95	0.46	0.22	0.21	0.15	0.18	0.13
01639000	10/1/1979	9/30/2013	12,419	222	0.42	0.22	0.21	0.14	0.13	0.12
01639500	10/1/1979	9/30/2013	12,419	119	0.46	0.24	0.22	0.17	0.15	0.10
01643000	10/1/1979	8/31/2013	12,389	999	0.37	0.15	0.16	0.10	0.14	0.11
01643700	10/1/2001	9/30/2013	4,383	135	0.46	0.21	0.19	0.13	0.18	0.15
01644000	10/1/1968	2/16/2015	16,940	354	0.38	0.16	0.16	0.11	0.15	0.15
01645000	10/1/1930	9/30/2015	31,046	117	0.45	0.25	0.24	0.19	0.17	0.09
01645704	10/1/2007	9/30/2015	2,922	9	0.42	0.34	0.29	0.23	0.17	0.10
01645762	10/1/2007	9/30/2015	2,922	3	0.41	0.31	0.27	0.25	0.25	0.08
01646000	10/1/1979	9/30/2013	12,419	66	0.43	0.25	0.23	0.19	0.16	0.12
01646305	10/1/2008	9/30/2015	2,556	2	0.28	0.25	0.23	0.22	0.14	0.08
01646500	3/1/1930	9/30/2014	30,895	11,436	0.22	0.10	0.11	0.06	0.15	0.12
01648000	10/1/1979	9/30/2013	12,419	68	0.44	0.24	0.23	0.18	0.17	0.12
01649190	10/1/2007	9/30/2015	2,922	14	0.53	0.37	0.32	0.26	0.15	0.11
01649500	10/1/1938	9/30/2015	28,124	88	0.43	0.26	0.24	0.20	0.13	0.10

Table 3. Fraction of days with base flow equal to streamflow for the period of analysis, as produced by different methods.—Continued

[Count, number of daily values during period of analysis; ft³/s, cubic feet per second]

Site number	Period of analysis		Count	Average daily streamflow (ft³/s)	Fraction of days at base flow, by method					
	Beginning date	End date			PART	HYSEP-Fixed	HYSEP-LocMin	HYSEP-Slide	BFI	ECK-CaF
01651000	10/1/1979	9/30/2013	12,419	55	0.39	0.26	0.24	0.21	0.18	0.11
01651800	6/19/1992	9/30/2013	7,774	5	0.36	0.32	0.28	0.26	0.17	0.11
01653600	10/1/1965	9/30/2005	14,610	46	0.37	0.21	0.18	0.15	0.12	0.17
01654000	10/1/1979	9/30/2013	12,419	31	0.46	0.36	0.32	0.25	0.21	0.13
01656500	10/1/1980	1/6/1987	2,289	47	0.45	0.26	0.21	0.17	0.17	0.12
01656903	10/1/2007	9/30/2014	2,557	7	0.38	0.29	0.21	0.18	0.12	0.13
01658000	1/24/2001	9/30/2013	4,633	62	0.29	0.17	0.14	0.11	0.09	0.15
01658500	10/1/1979	9/30/2013	12,419	7	0.36	0.28	0.22	0.17	0.16	0.10
01659000	10/1/2007	9/30/2011	1,461	5	0.32	0.25	0.21	0.16	0.15	0.09
01660920	10/1/2006	9/30/2015	3,287	86	0.33	0.18	0.15	0.11	0.15	0.09
01661050	10/1/2006	9/30/2013	2,557	18	0.43	0.34	0.28	0.23	0.17	0.12
01662800	10/1/1997	11/30/2012	5,540	25	0.55	0.37	0.29	0.24	0.18	0.13
01663500	10/1/2001	9/30/2013	4,383	339	0.40	0.15	0.13	0.10	0.13	0.16
01664000	10/1/1979	9/30/2013	12,419	701	0.39	0.15	0.15	0.09	0.14	0.15
01665500	10/1/1998	2/28/2013	5,265	144	0.53	0.22	0.18	0.13	0.14	0.14
01666500	10/1/1979	9/30/2013	12,419	227	0.50	0.22	0.19	0.13	0.14	0.12
01667500	10/1/1979	1/31/2013	12,177	559	0.41	0.15	0.15	0.09	0.14	0.13
01668000	10/1/1979	9/30/2013	12,419	1,716	0.31	0.12	0.12	0.08	0.14	0.12
01669520	8/14/1981	4/30/2013	11,583	122	0.44	0.21	0.16	0.11	0.24	0.15
01671020	10/1/1979	9/30/2012	12,054	372	0.29	0.17	0.19	0.13	0.15	0.05
01671100	10/1/2000	9/30/2013	4,748	80	0.44	0.22	0.18	0.12	0.17	0.15
01673000	10/1/1979	9/30/2013	12,419	961	0.26	0.12	0.14	0.08	0.15	0.09
01673800	10/1/1979	9/30/2013	12,419	73	0.41	0.21	0.18	0.14	0.15	0.13
01674000	10/1/1979	9/30/2013	12,419	224	0.36	0.15	0.15	0.10	0.16	0.17
01674500	10/1/1989	9/30/2013	8,766	520	0.36	0.15	0.14	0.09	0.16	0.18
01677000	10/1/1982	9/30/1995	4,748	6	0.43	0.36	0.27	0.22	0.15	0.14
02011500	10/1/1979	9/30/2013	12,419	181	0.43	0.26	0.24	0.18	0.17	0.08
02012500	10/1/1925	9/30/1983	21,184	490	0.42	0.17	0.18	0.12	0.15	0.09
02015700	10/1/1979	9/30/2013	12,419	158	0.51	0.25	0.23	0.18	0.21	0.09

Table 3. Fraction of days with base flow equal to streamflow for the period of analysis, as produced by different methods.—Continued

[Count, number of daily values during period of analysis; ft³/s, cubic feet per second]

Site number	Period of analysis		Count	Average daily streamflow (ft^3/s)	Fraction of days at base flow, by method					
	Beginning date	End date			PART	HYSEP-Fixed	HYSEP-LocMin	HYSEP-Slide	BFI	ECK-CaF
02020500	10/1/1998	9/30/2013	5,479	160	0.53	0.22	0.20	0.12	0.15	0.12
02024000	10/1/1979	9/30/2013	12,419	710	0.42	0.15	0.18	0.09	0.15	0.11
02024752	10/1/2005	9/30/2013	2,922	3,374	0.32	0.11	0.15	0.07	0.11	0.07
02031000	10/1/1979	9/30/2013	12,419	106	0.49	0.24	0.21	0.16	0.16	0.11
02034000	10/1/1979	9/30/2013	12,419	700	0.33	0.15	0.15	0.10	0.14	0.10
02035000	10/1/1979	9/30/2013	12,419	6,981	0.20	0.09	0.09	0.06	0.12	0.11
02037500	10/1/1979	4/30/2013	12,266	7,171	0.23	0.10	0.10	0.07	0.13	0.11
02038850	10/1/1966	9/30/2015	17,897	8	0.54	0.38	0.31	0.26	0.21	0.08
02039500	10/1/1979	9/30/2013	12,419	282	0.37	0.16	0.16	0.11	0.16	0.09
02041000	10/1/1979	9/30/2013	12,419	141	0.46	0.22	0.18	0.13	0.16	0.13
02041650	10/1/1979	9/30/2013	12,419	1,182	0.22	0.12	0.14	0.09	0.17	0.08
02042426	10/1/1990	9/30/1994	1,461	39	0.35	0.22	0.21	0.15	0.27	0.14
02042500	10/1/1979	9/30/2013	12,419	271	0.32	0.15	0.13	0.08	0.13	0.17
03050000	7/20/1988	9/30/2013	9,204	378	0.40	0.20	0.19	0.13	0.14	0.17
03065000	10/1/1995	1/31/2013	6,333	849	0.35	0.15	0.16	0.10	0.14	0.18
03066000	10/1/1979	9/30/2013	12,419	219	0.41	0.21	0.21	0.14	0.12	0.17
03069000	10/1/1979	9/30/1993	5,114	570	0.41	0.21	0.20	0.13	0.14	0.15
03069500	10/1/1979	9/30/2013	12,419	1,858	0.33	0.15	0.16	0.10	0.13	0.17
03070000	10/1/1979	9/30/1996	6,210	2,550	0.33	0.15	0.15	0.10	0.16	0.16
03070500	10/1/1979	9/30/2013	12,419	423	0.44	0.21	0.19	0.12	0.14	0.17
03076600	10/1/1979	9/30/2013	12,419	94	0.49	0.22	0.22	0.14	0.13	0.13
03180500	10/1/1979	11/15/2012	12,100	279	0.44	0.21	0.19	0.12	0.15	0.16

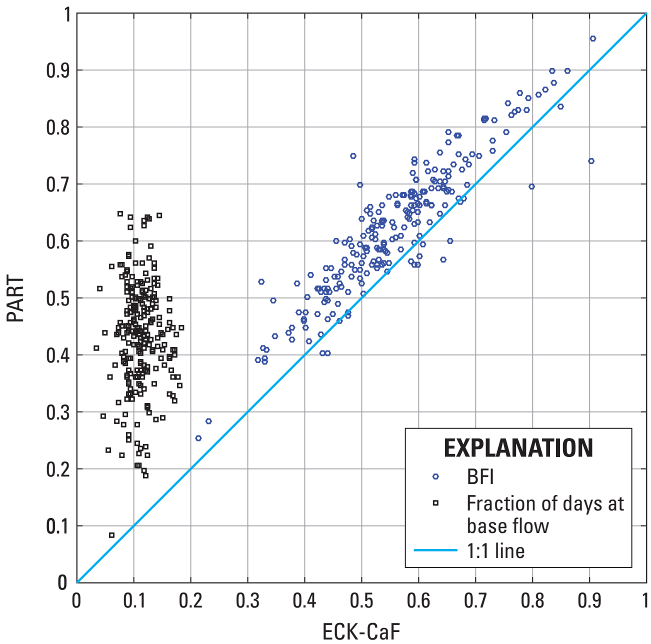

Figure 4. Values of the base-flow index (BFI) and fraction of days at base flow (determined as base flow equal to streamflow) for the ECK-CaF method versus the PART method.

Differences in the BFI and fraction of days at base flow are also related to how each separation method determines the timing of return to base flow, or cessation of quickflow, following a peak in streamflow. The method used by PART involves two steps: (1) locating periods of negligible quickflow and designating that groundwater discharge (base flow) equals streamflow during these periods, and (2) interpolating groundwater discharge between these periods. The decision that quickflow is negligible is based on antecedent recession, using the empirical relation of eq. (1). For a given day, the antecedent recession requirement is met if recession has been continuous for *N* days or more preceding the day. Therefore, the return to base flow (and the fraction of days at base flow) is a function of watershed area and time between streamflow peaks. PART characteristically displays peaks in base flow on the falling limb of the streamflow hydrograph that are not likely attributable to physical processes (fig. 9).

HYSEP (Sloto and Crouse, 1996) also uses eq. (1) as the basis for hydrograph-separation algorithms referred to as fixed interval, sliding interval, and local minimum. The fixed-interval algorithm assigns the lowest discharge in each 2*N*' (the odd integer nearest 2*N*) interval to all days in that interval starting with the first day of the period of record. The discharge at that point is assigned to all days in the interval and is considered base flow. The sliding-interval algorithm is similar but uses moving (or sliding) overlapping 2*N*' intervals. The local-minimum method checks each day to determine if it is the lowest discharge in one-half the interval minus 1 day before and after the day being considered. If it is, then it is a local minimum and is connected by straight lines to adjacent local minimums; the base-flow values for each day between local minimums are estimated by linear interpolation. As with the PART method, discontinuities and steps are observed in the estimated base-flow hydrograph that are not likely attributable to physical processes (fig. 9).

The BFI method (Institute of Hydrology, 1980; Wahl and Wahl, 1988) is similar to the HYSEP fixed-interval algorithm, using non-overlapping blocks of *N* days, where *N* is either assigned a value (typically 5) or determined using another approach, such as the optimization described earlier. Once the minima for each block are determined, ordinates (termed turning points) for the base-flow line are selected on the basis of a comparison of a fraction (f) of the central value and the surrounding values. Linear interpolation between each turning point is used to estimate daily values of base flow. This method is also prone to discontinuous base-flow time series (fig. 9), and involves two adjustable parameters (N, f) that do not have a physical basis.

The ECK-CaF method does not presume or estimate *a priori* the timing of quickflow cessation, but allows the algorithm (eq. 2) to determine periods where streamflow is entirely base flow (where recession is occurring at a rate represented by α, with base flow restricted by $Q_{B_j} \leq Q_j$), dependent on the value of β. The magnitude, length, and closeness of event runoff peaks affect the pattern of base flow and quickflow (fig. 9).

A simple graphical analysis was conducted to examine the relative sensitivity of base-flow estimates to values of alpha and beta for the ECK-CaF method. Alpha and beta were varied over the range observed for the majority of the 225 sites (fig. 2), with alpha varying from 0.95 to 0.99, and beta varying from 0.25 to 0.95. This was done for all sites for the period(s) of analysis, but the results were similar across sites and time. BFI values and the fraction of days at base flow are shown in figure 10 for Conococheague Creek (USGS site 01614500) for water year 2009. Both BFI and the fraction of days at base flow were more sensitive to beta than alpha over the range of values examined. This is due in part to the larger relative range in values of beta analyzed for sensitivity, and also serves to highlight the need to find the best possible value of (or optimize) beta.

Results of Optimal Hydrograph Separation (OHS)

The OHS (method ECK-OHS) was performed using streamflow and SC data for 109 of the 225 Chesapeake Bay watershed sites with available SC data. Quickflow SC (C_S) was assumed to be constant and two models for base-flow SC (C_B) were used. One model used a sine-cosine function (model sin-cos) and the other used a peak-fitting algorithm (model SCfit). The parameters that were optimized (including C_S and model parameters for C_B) were described earlier. Not all models provided satisfactory results. A subset of models were selected that met the following criteria: beta was considered “optimized” because it didn’t reach imposed optimization

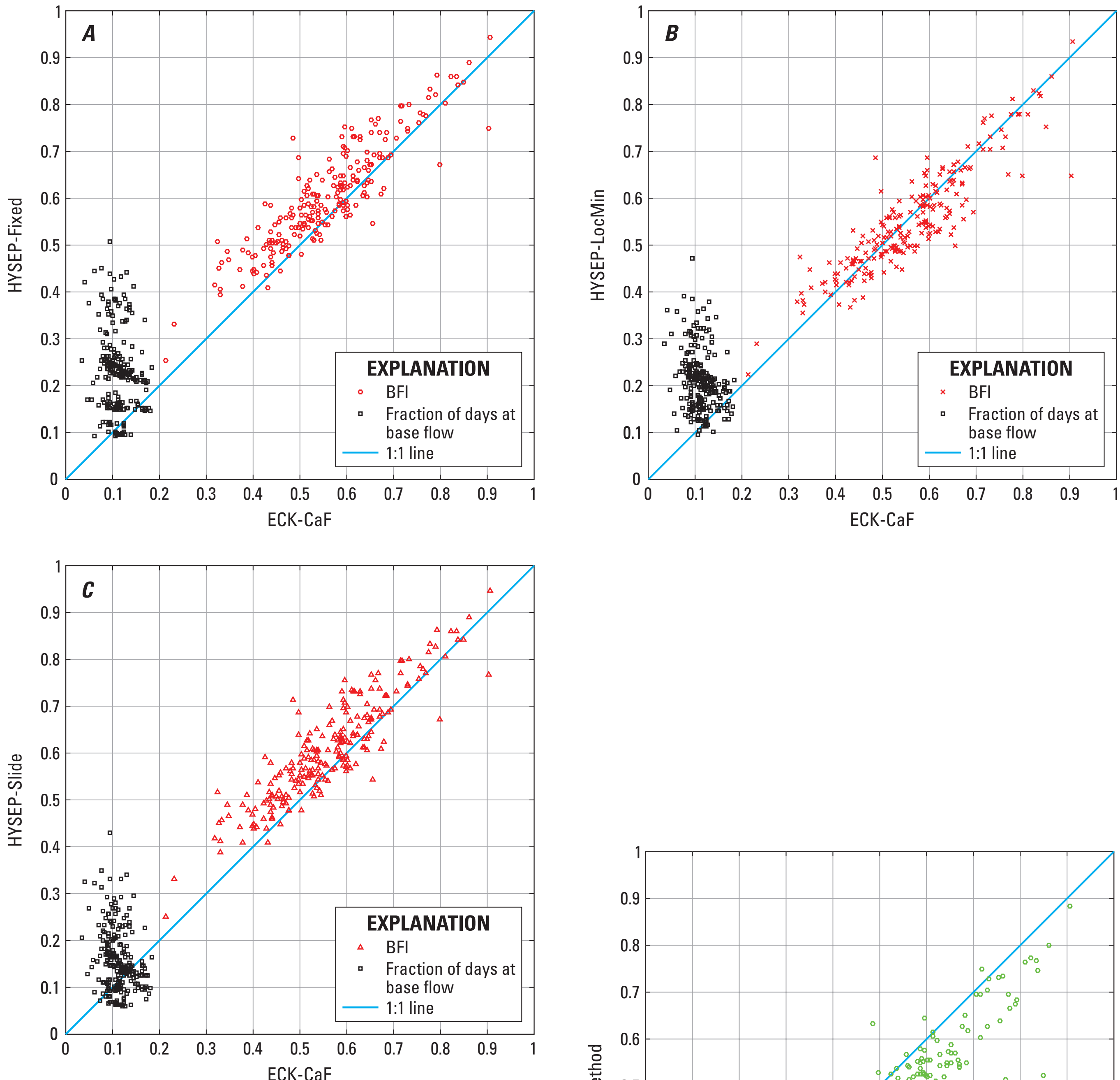

Figure 5. Values of the base-flow index (BFI) and fraction of days at base flow (determined as base flow equal to streamflow) for the ECK-CaF method versus *A*, HYSEP-Fixed, *B*, HYSEP-LocMin, and *C*, HYSEP-Slide methods.

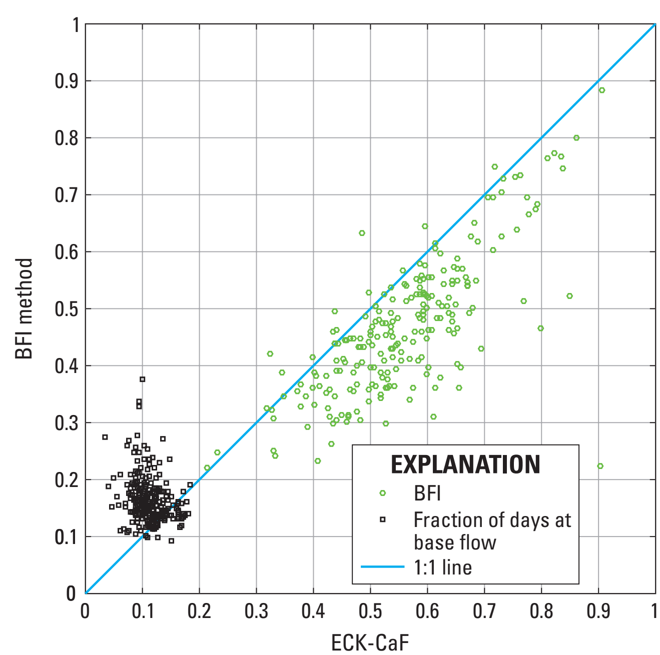

Figure 6. Values of the base-flow index (BFI) and fraction of days at base flow (determined as base flow equal to streamflow) for the ECK-CaF method versus the BFI method.

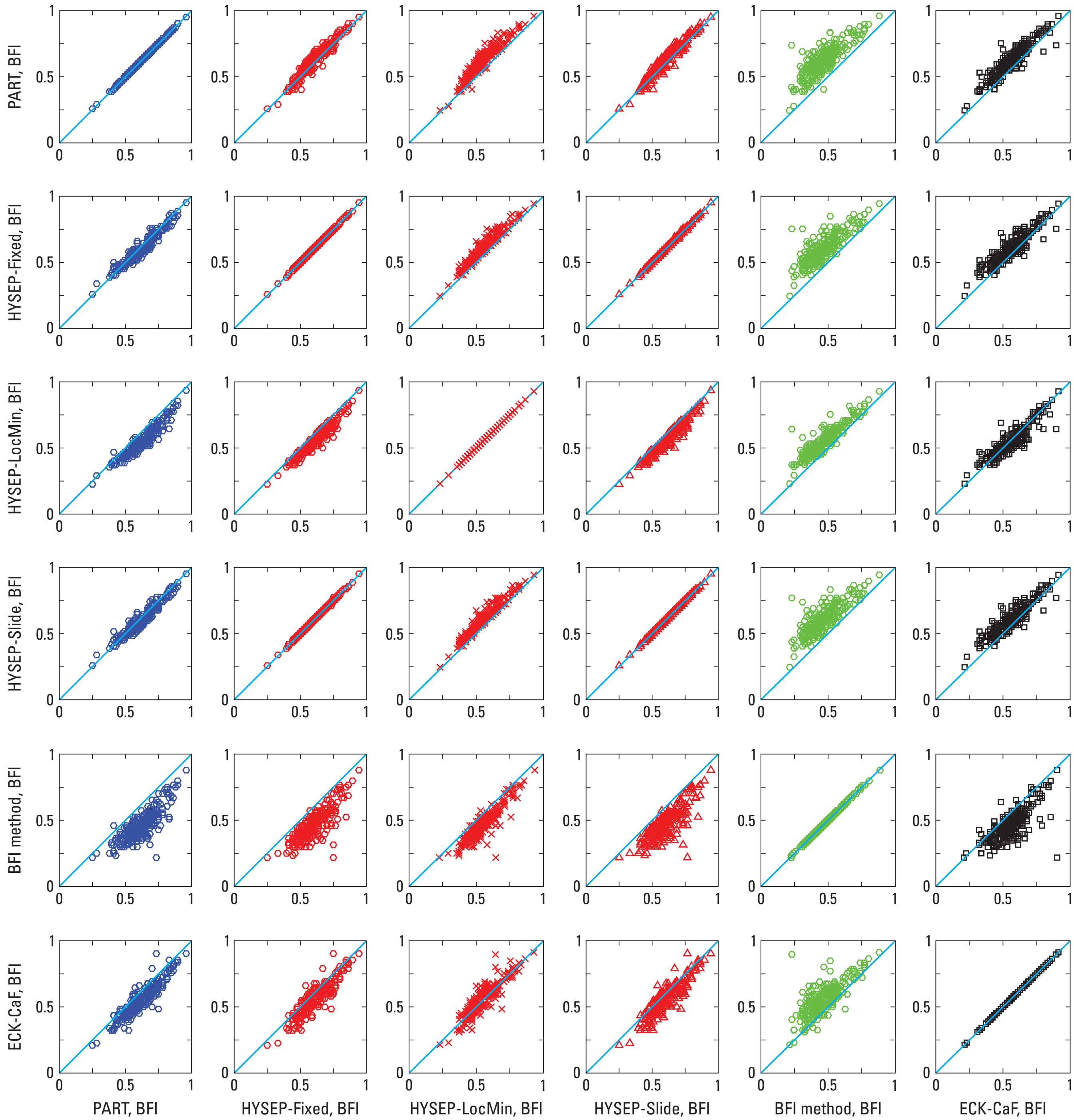

Figure 7. Scatterplot matrix of the base-flow index (BFI) compared for all methods.

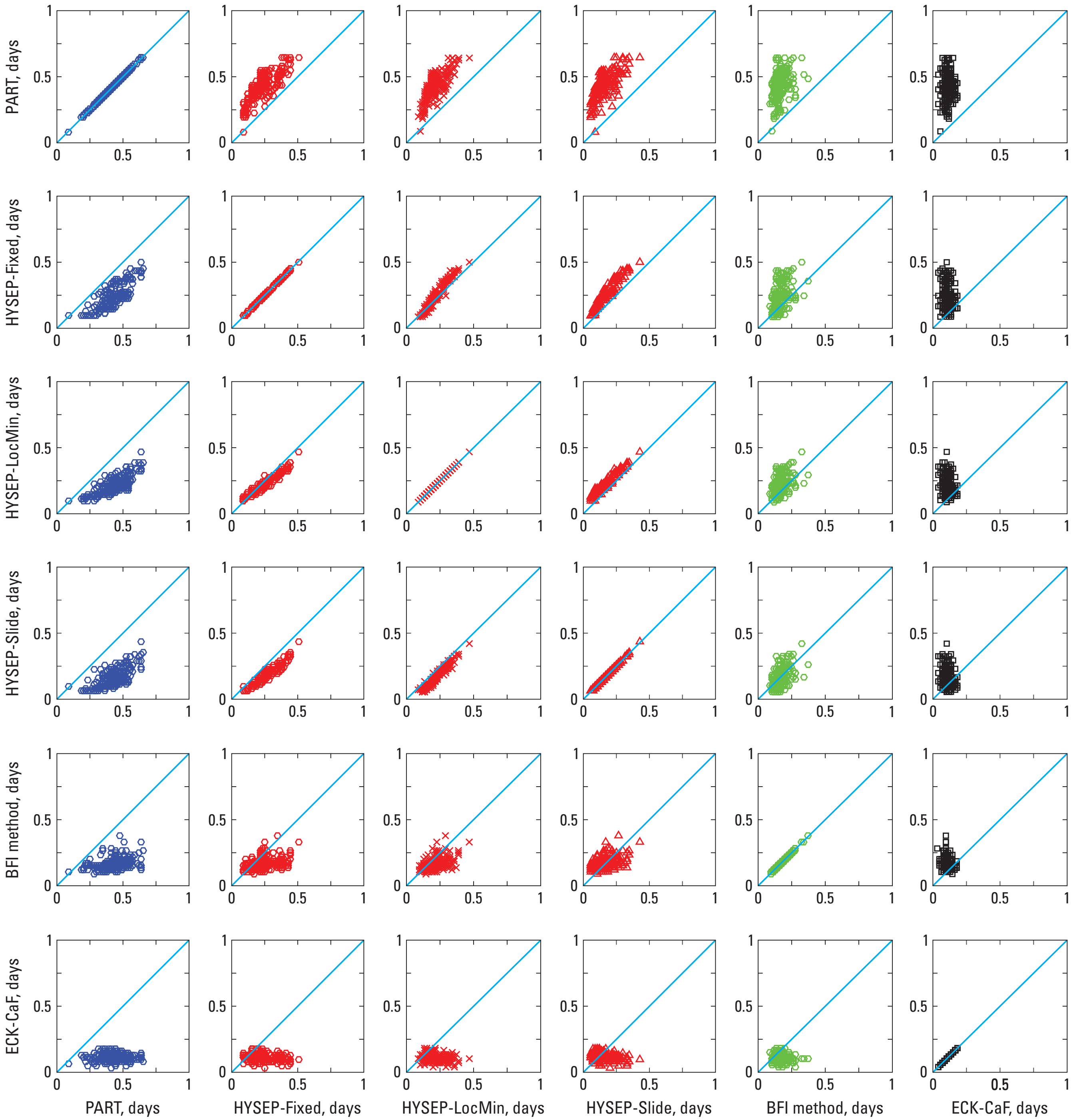

Figure 8. Scatterplot matrix of the fraction of days at base flow (determined as base flow equal to streamflow) compared for all methods.

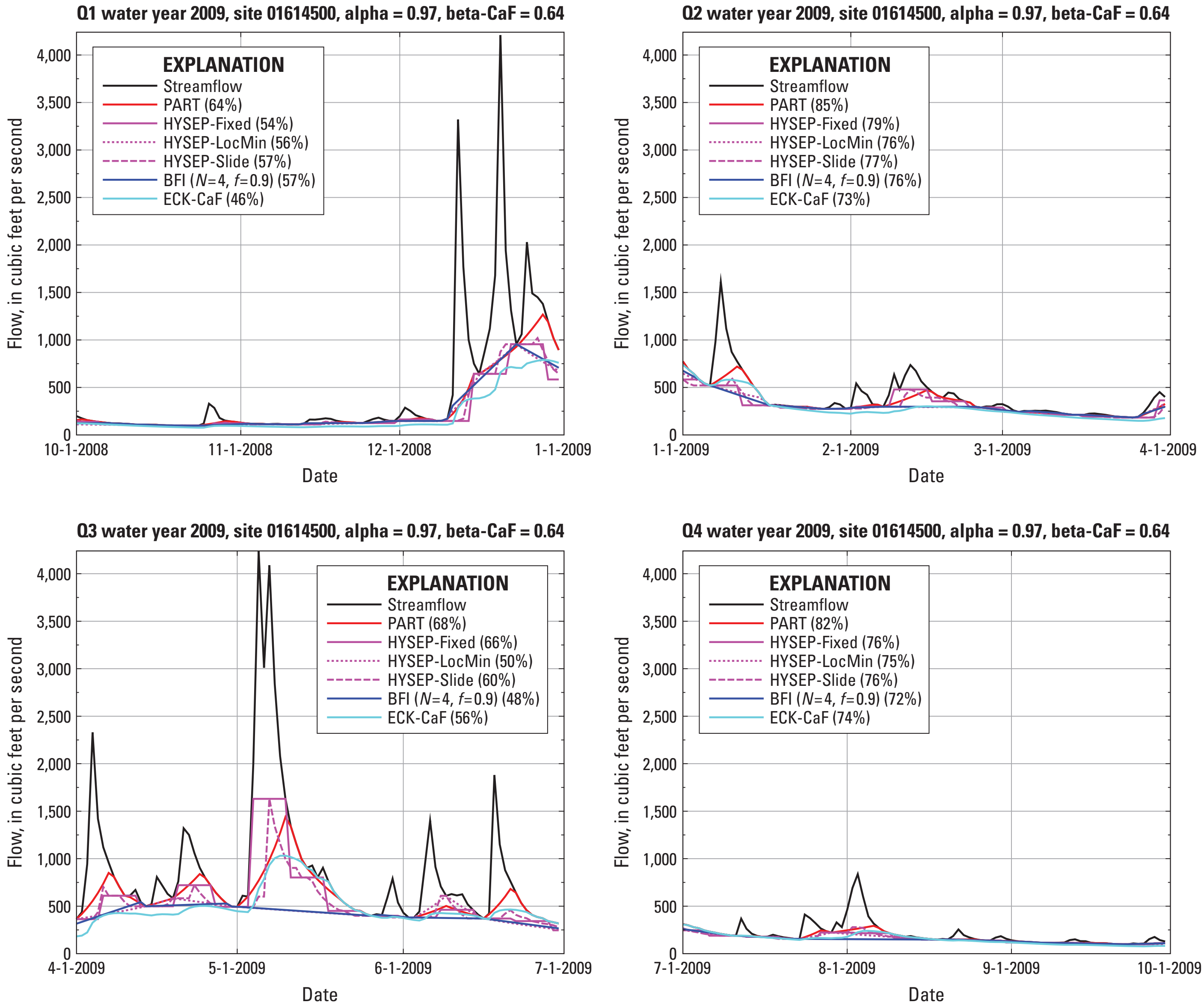

Figure 9. Hydrographs for water year 2009 showing total streamflow and base flow estimated using all methods for site 01614500, Conococheague Creek at Fairview, Maryland. (%, percent; *N*, length of period used for the base-flow index (BFI) method, in days; *f*, BFI turning point test factor)

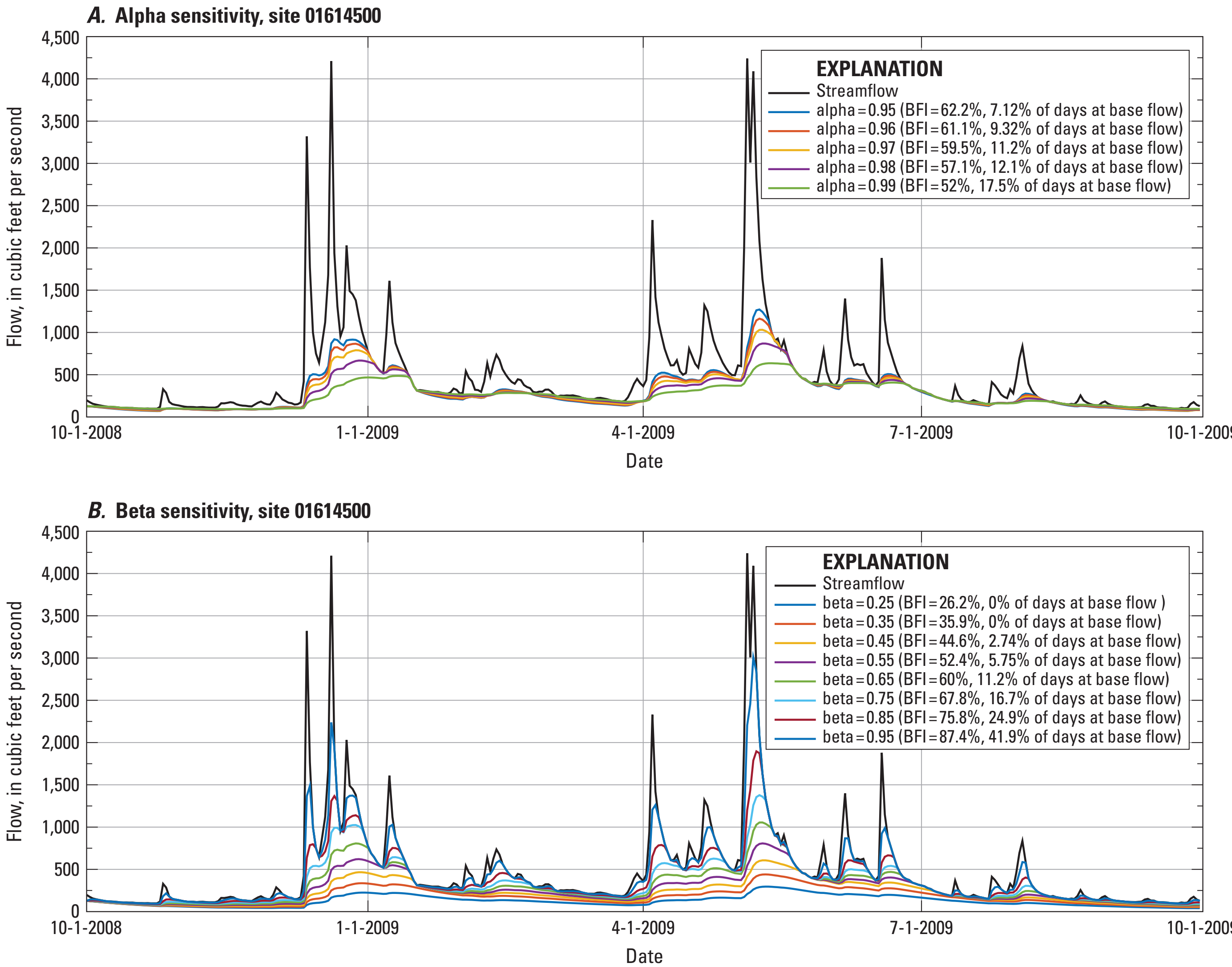

Figure 10. Hydrographs showing base flow estimated using the ECK-CaF method for varying values of *A*, alpha, and *B*, beta for site 01614500, Conococheague Creek at Fairview, Maryland. (BFI, base-flow index; %, percent)

limits (0.20 and 0.99); and the Nash-Sutcliffe efficiency was larger than 0.30. The Nash-Sutcliffe efficiency is calculated as:

$$E(\beta) = 1 - \frac{\sum_{j=1}^{n}\left[C_{obs_j} - C_{sim_j}(\beta)\right]^2}{\sum_{j=1}^{n}\left[C_{obs_j} - \overline{C}_{obs}\right]^2} \tag{10}$$

where $\overline{C}_{obs}$ = the mean observed concentration and the other terms have been defined previously. Values of the Nash-Sutcliffe efficiency equal to 1 indicate a perfect fit between observed and predicted values, and efficiencies equal to or less than 0 indicate that the model is predicting no better than the average of the observed data. Finally, where both models for C_B provided models that met these criteria, a choice between the two was made on the basis of the Nash-Sutcliffe efficiency and closeness of beta to the value determined using the Collischonn and Fan (2013) method. Sixty-seven models were considered acceptable, of which 52 used model SCfit and 15 used model sin-cos (table 4). Examples demonstrating model fit are shown in figures 11 and 12.

Values of beta estimated using the ECK-CaF and ECK-OHS methods are compared for the 67 acceptable models in figure 13. The mean values are very similar (0.610 and 0.608 for ECK-CaF and ECK-OHS, respectively). However, the range of values is larger for values of beta determined using ECK-OHS (0.20 to 0.99) than for values determined using ECK-CaF (0.40 to 0.86), and there is not a strong 1:1 relation (fig. 13). Similarly, the range of values for BFI from ECK-OHS (0.20 to 0.93) is larger than the range of values from ECK-CaF (0.33 to 0.85; fig. 14). The mean BFI values are identical (0.56), within precision limits.

For the fraction of days at base flow, it was shown previously that the range for the ECK-CaF method was smaller than for the other methods (fig. 8). Imposing chemical mass balance to optimize beta (ECK-OHS) increased the range of beta values and the fraction of days at base flow (fig. 15). The range in fraction of days at base flow for ECK-OHS is similar to the range for the PART, HYSEP, and BFI methods (fig. 8), although ECK-OHS does produce several values that are smaller than the other methods.

Application of the Eckhardt (2005) RDF to estimate base flow from streamflow data requires estimation of the parameters alpha and beta. Alpha is a recession constant that may be estimated from streamflow during recession periods. Beta may be estimated using the backward-running filter of Collischonn and Fan (2013) without the requirement of additional data, or it may be estimated using a mass-balance constraint if chemical tracer data are available. The results of this study indicate that ECK-OHS produces values of beta (for watersheds demonstrating acceptable model fit) that are similar on average to values produced by ECK-CaF, but have a larger range. Where ECK-OHS-derived beta values are smaller than ECK-CaF-derived values, the SC data indicate a larger component of flow characterized by C_S. This may indicate larger contributions of relatively new water from intermediate flow paths between rapid direct runoff and deeper groundwater discharge. Larger beta values indicate larger base-flow contributions, with stream SC during events more closely resembling base-flow SC (C_B). In either case, other factors (such as groundwater reservoir nonlinearity) may be responsible for the differences in beta produced by the two methods.

Limitations of Hydrograph Separation

There are a number of limitations to the OHS approach resulting from the assumptions implicit in the conceptual model, the RDF method, and the approach taken to impose chemical mass balance (including tracer choice). Conceptually, base flow is considered one of two and only two components of runoff. This may be insufficient to characterize systems with more complex or diverse hydrologic compartments or components (such as interflow or subsurface stormflow, movement of soil moisture, macropore flow) or with human modification (including diversions, dams, point sources and sinks, artificial drainage, and others) (Bazemore and others, 1994; Cartwright and others, 2014; Freeze, 1974; Klaus and McDonnell, 2013; Sanford and others, 2012; Vasconcelos and others, 2013). In some of these cases, multiple components may need definition, possibly using multiple tracers in an end-member mixing analysis (Genereux and others, 1993; Hooper and others, 1990; Kronholm and Capel, 2015).

The RDF invokes a linearity assumption for the groundwater reservoir, so that discharge of groundwater is proportional to volume in storage. This assumption may not be valid in regions where groundwater storage varies substantially, seasonally or annually, or where aquifer properties vary with storage (Aksoy and Wittenberg, 2011; Halford and Mayer, 2000; Hall, 1968). The linear reservoir assumption may also be violated when base flow (estimated at a gage) is not synonymous or synchronous with groundwater discharge. Channel expansion and contraction, routing, hyporheic zone water exchange, and other geomorphic and scale effects may apparently alter the simplistic linear groundwater reservoir model (Mutzner and others, 2013).

Tracer-mass-balance methods generally rely upon the assumption that end-member tracer concentrations are nonreactive, temporally constant, spatially homogeneous, and unique to each end member. A number of different tracers have been used that vary in their reactivity, adherence to constancy assumptions, and ease and cost of analysis. SC may in some cases meet these requirements (Stewart and others, 2007) and is widely available, but may not be suitable in all watersheds. For the Chesapeake Bay watershed sites considered in this study, other sources of salt (road salt, fertilizer) were especially problematic. Finally, even when considered time varying, as is the case in this study for C_B, the models for time variance may be subjective or require additional data or parameter information. The impact of all these limitations may be evidenced by poor OHS model results; conversely, poor model fit may provide an indication that two-component separation does not adequately describe the hydrologic system's runoff response.

Table 4. Results of Optimal Hydrograph Separation (OHS) for accepted models.

[SC, specific conductance; SCfit, peak-fitting base-flow SC model; sin-cos, sin-cos base-flow SC model; OHS beta, optimized value of beta using optimal hydrograph separation; ECK-CaF beta, beta determined using the method of Collischonn and Fan (2013); CS, quickflow SC; CBmn, mean base-flow SC; CBamp, amplitude of the sine term for the base-flow SC; CBamp2, amplitude of the cosine term for the base-flow SC; sday, starting time for the sin-cos base-flow SC model; RMSE, root-mean-square error; E, Nash-Sutcliffe efficiency; --, no value]

Site number	Model	Alpha	OHS beta	ECK-CaF beta	CS	CBmn	CBamp	CBamp2	sday	RMSE	E
01487000	SCfit	0.97	0.83	0.86	96.95	--	--	--	--	394	0.58
01490000	SCfit	0.96	0.84	0.72	79.30	--	--	--	--	80	0.79
01493112	SCfit	0.97	0.91	0.69	96.33	--	--	--	--	419	0.60
01503000	sin-cos	0.96	0.41	0.68	132.98	185.12	122.99	48.62	39,620	421	0.61
01509150	SCfit	0.93	0.24	0.56	138.59	--	--	--	--	383	0.60
01516350	SCfit	0.95	0.68	0.57	134.52	--	--	--	--	5,418	0.73
01518700	SCfit	0.96	0.64	0.45	159.44	--	--	--	--	3,823	0.42
01528000	sin-cos	0.93	0.95	0.56	86.38	288.56	75.19	35.67	18,113	510	0.60
01534000	SCfit	0.95	0.20	0.61	128.92	--	--	--	--	325	0.32
01536000	SCfit	0.95	0.42	0.68	254.10	--	--	--	--	4,424	0.69
01540500	SCfit	0.96	0.39	0.65	159.58	--	--	--	--	1,385	0.61
01542500	SCfit	0.97	0.37	0.66	278.40	--	--	--	--	2,803	0.58
01547950	SCfit	0.95	0.53	0.71	134.69	--	--	--	--	3,098	0.61
01549700	SCfit	0.95	0.21	0.63	85.27	--	--	--	--	781	0.31
01553500	sin-cos	0.96	0.31	0.65	137.77	303.77	10.88	80.06	27,689	543	0.70
01567000	SCfit	0.97	0.65	0.61	160.97	--	--	--	--	1,125	0.69
01570000	sin-cos	0.97	0.41	0.62	263.64	506.01	25.68	30.86	33,901	632	0.66
01570500	SCfit	0.97	0.44	0.64	163.17	--	--	--	--	1,938	0.44
01571490	SCfit	0.93	0.79	0.86	473.89	--	--	--	--	1,324	0.32
01571820	SCfit	0.96	0.62	0.72	143.41	--	--	--	--	1,823	0.62
01572025	sin-cos	0.96	0.23	0.64	94.43	186.00	15.51	10.61	35,179	80	0.76
01573710	SCfit	0.96	0.89	0.45	227.27	--	--	--	--	1,026	0.35
01576754	sin-cos	0.98	0.40	0.69	379.88	675.60	38.58	58.58	29,558	1,123	0.39
01576787	sin-cos	0.98	0.71	0.73	227.11	375.58	10.00	10.00	26,718	972	0.37
01594526	SCfit	0.95	0.98	0.46	7.00	--	--	--	--	5,053	0.48
01594930	SCfit	0.95	0.40	0.64	319.88	--	--	--	--	9,178	0.54
01594936	SCfit	0.90	0.43	0.70	194.82	--	--	--	--	10,269	0.52
01595300	SCfit	0.92	0.24	0.72	225.80	--	--	--	--	761	0.62

Table 4. Results of Optimal Hydrograph Separation (OHS) for accepted models.—Continued

[SC, specific conductance; SCfit, peak-fitting base-flow SC model; sin-cos, sin-cos base-flow SC model; OHS beta, optimized value of beta using optimal hydrograph separation; ECK-CaF beta, beta determined using the method of Collischonn and Fan (2013); CS, quickflow SC; CBmn, mean base-flow SC; CBamp, amplitude of the sine term for the base-flow SC; CBamp2, amplitude of the cosine term for the base-flow SC; sday, starting time for the sin-cos base-flow SC model; RMSE, root-mean-square error; E, Nash-Sutcliffe efficiency; --, no value]

Site number	Model	Alpha	OHS beta	ECK-CaF beta	CS	CBmn	CBamp	CBamp2	sday	RMSE	E
01595800	SCfit	0.99	0.99	0.56	327.66	--	--	--	--	576	0.90
01608500	SCfit	0.97	0.60	0.53	168.72	--	--	--	--	1,568	0.59
01610400	SCfit	0.94	0.52	0.67	31.41	--	--	--	--	307	0.72
01611500	SCfit	0.97	0.63	0.51	121.00	--	--	--	--	1,152	0.45
01613900	SCfit	0.93	0.96	0.48	89.00	--	--	--	--	666	0.74
01614500	sin-cos	0.97	0.36	0.64	248.58	441.36	42.66	52.34	27,995	862	0.69
01614830	SCfit	0.97	0.90	0.85	465.00	--	--	--	--	669	0.59
01615000	SCfit	0.96	0.46	0.48	552.77	--	--	--	--	3,000	0.43
01616500	SCfit	0.98	0.57	0.63	546.85	--	--	--	--	6,175	0.65
01621050	SCfit	0.96	0.81	0.68	366.73	--	--	--	--	1,216	0.48
01626000	SCfit	0.97	0.77	0.65	83.60	--	--	--	--	984	0.67
01631000	sin-cos	0.97	0.71	0.64	212.34	323.29	13.49	52.23	27,673	1,378	0.40
01632000	SCfit	0.94	0.56	0.45	82.88	--	--	--	--	607	0.71
01632900	SCfit	0.97	0.73	0.69	375.32	--	--	--	--	1,844	0.45
01634000	sin-cos	0.97	0.59	0.57	256.60	388.98	17.90	62.53	27,676	1,703	0.42
01634500	SCfit	0.95	0.93	0.54	99.77	--	--	--	--	674	0.63
01636500	SCfit	0.97	0.56	0.66	362.19	--	--	--	--	2,677	0.46
01643700	SCfit	0.95	0.58	0.59	152.89	--	--	--	--	1,004	0.62
01644000	SCfit	0.95	0.97	0.61	45.00	--	--	--	--	715	0.47
01645704	SCfit	0.94	0.97	0.40	67.01	--	--	--	--	16,641	0.40
01651000	SCfit	0.95	0.94	0.44	169.17	--	--	--	--	25,217	0.30
01658000	SCfit	0.88	0.94	0.49	60.32	--	--	--	--	2,224	0.32
01659000	sin-cos	0.88	0.73	0.53	0.39	108.45	60.43	30.06	37,921	335	0.31
01661050	SCfit	0.92	0.49	0.56	111.38	--	--	--	--	248	0.36
01665500	SCfit	0.96	0.66	0.68	55.49	--	--	--	--	153	0.52
01666500	SCfit	0.97	0.44	0.65	56.31	--	--	--	--	175	0.63
01667500	SCfit	0.96	0.42	0.63	67.21	--	--	--	--	454	0.60
01669520	SCfit	0.95	0.47	0.66	62.84	--	--	--	--	270	0.82

Table 4. Results of Optimal Hydrograph Separation (OHS) for accepted models.—Continued

[SC, specific conductance; SCfit, peak-fitting base-flow SC model; sin-cos, sin-cos base-flow SC model; OHS beta, optimized value of beta using optimal hydrograph separation; ECK-CaF beta, beta determined using the method of Collischonn and Fan (2013); CS, quickflow SC; CBmn, mean base-flow SC; CBamp, amplitude of the sine term for the base-flow SC; CBamp2, amplitude of the cosine term for the base-flow SC; sday, starting time for the sin-cos base-flow SC model; RMSE, root-mean-square error; E, Nash-Sutcliffe efficiency; --, no value]

Site number	Model	Alpha	OHS beta	ECK-CaF beta	CS	CBmn	CBamp	CBamp2	sday	RMSE	E
01671100	SCfit	0.93	0.25	0.61	121.99	--	--	--	--	1,860	0.50
01674000	sin-cos	0.94	0.43	0.60	58.05	89.77	28.61	23.42	37,825	486	0.43
02011500	SCfit	0.95	0.93	0.47	91.55	--	--	--	--	193	0.85
02012500	SCfit	0.97	0.43	0.56	120.53	--	--	--	--	1,256	0.41
02015700	sin-cos	0.97	0.97	0.57	102.41	155.28	31.63	14.59	37,802	269	0.83
02020500	SCfit	0.93	0.43	0.52	60.59	--	--	--	--	588	0.57
02024000	SCfit	0.97	0.69	0.57	162.69	--	--	--	--	1,273	0.63
02039500	sin-cos	0.97	0.24	0.55	110.81	86.98	81.84	28.81	37,740	684	0.34
02041000	SCfit	0.95	0.73	0.52	87.99	--	--	--	--	430	0.64
02042500	SCfit	0.93	0.53	0.69	104.18	--	--	--	--	1,013	0.34
03066000	sin-cos	0.93	0.72	0.58	67.36	71.84	27.36	13.35	39,950	179	0.39

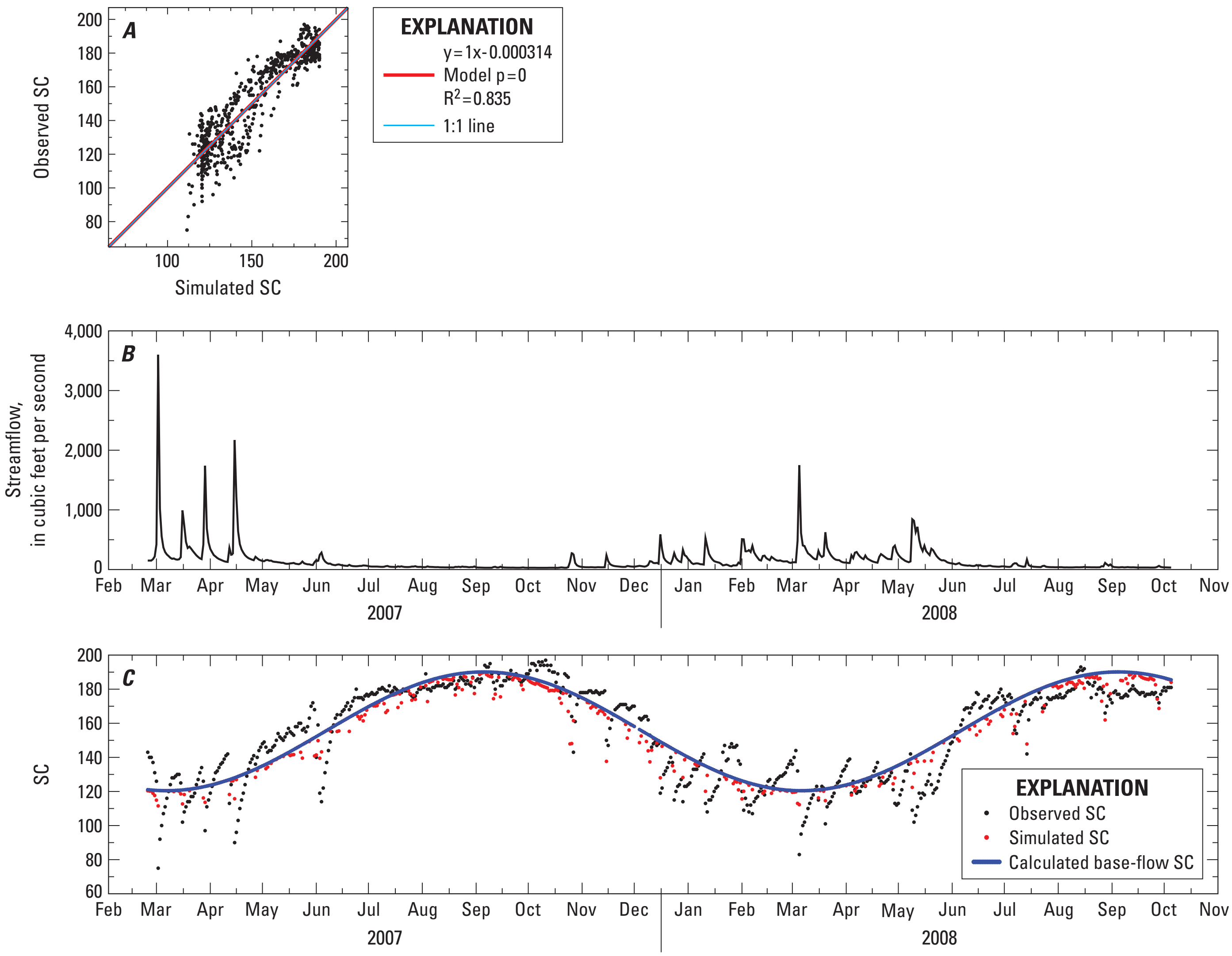

Figure 11. Optimal hydrograph separation results using the sin-cos model for base-flow specific conductance (SC) for site 02015700, Bullpasture River at Williamsville, Virginia, showing *A*, simulated compared to observed SC, *B*, the streamflow hydrograph, and *C*, time series of simulated and observed SC values and simulated base-flow SC.

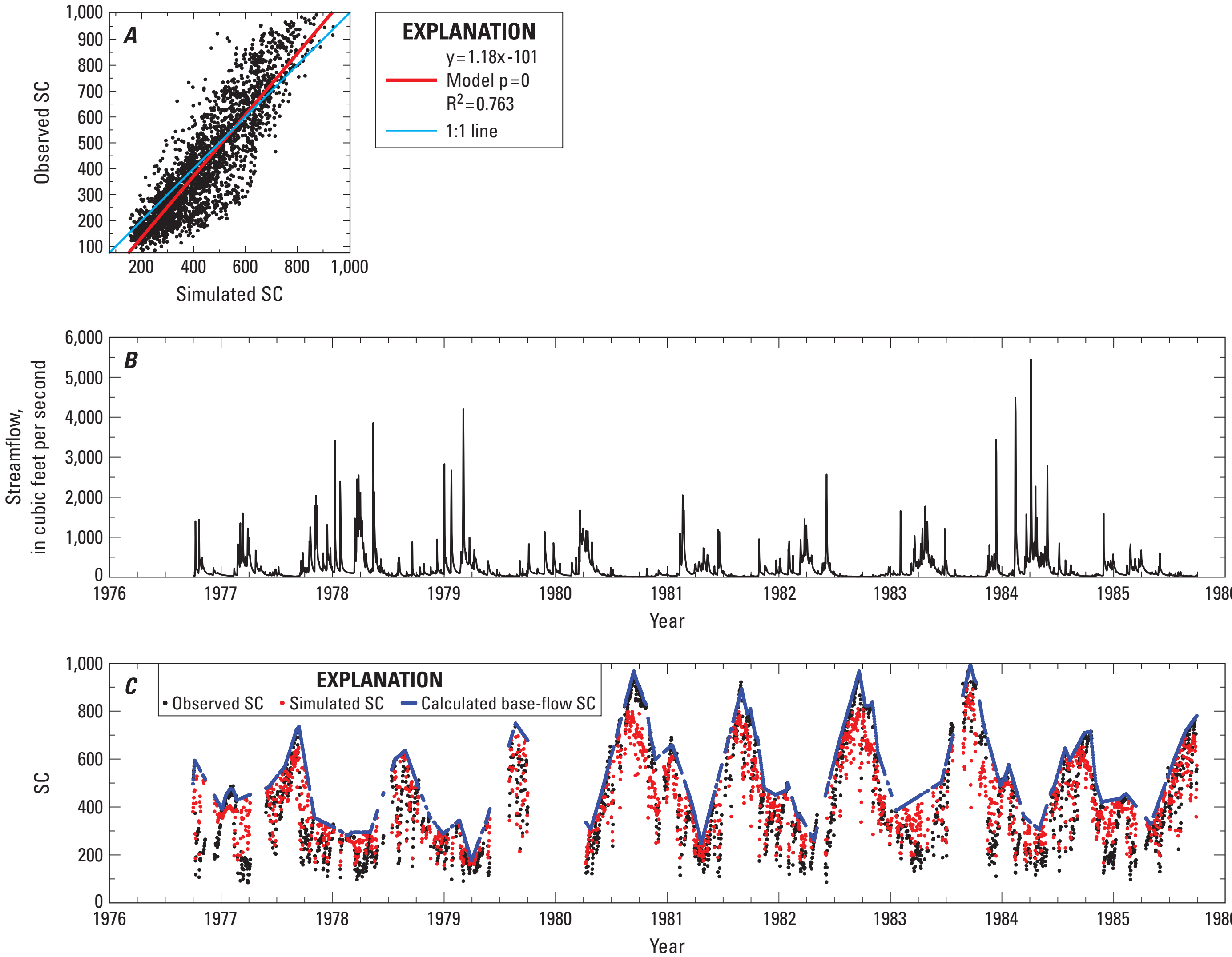

Figure 12. Optimal hydrograph separation results using the SCfit model for base-flow specific conductance (SC) for site 01516350, Tioga River near Mansfield, Pennsylvania, showing *A*, simulated compared to observed SC, *B*, the streamflow hydrograph, and *C*, time series of simulated and observed SC values and simulated base-flow SC.

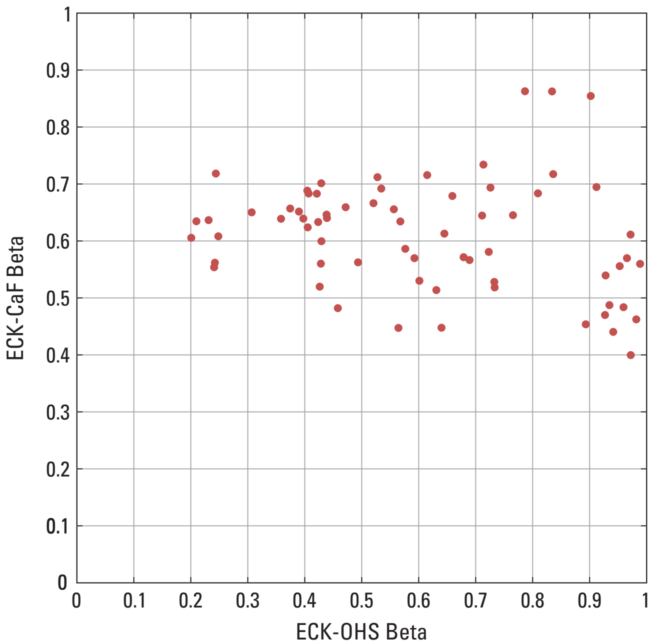

Figure 13. Comparison of beta values estimated using the ECK-OHS and ECK-CaF methods for 67 acceptable models.

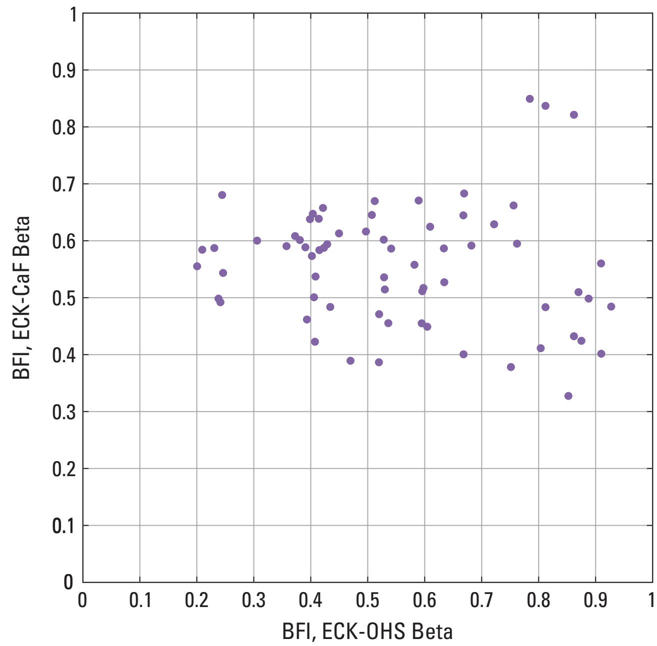

Figure 14. Comparison of base-flow index (BFI) values estimated using the ECK-OHS and ECK-CaF methods for 67 acceptable models.

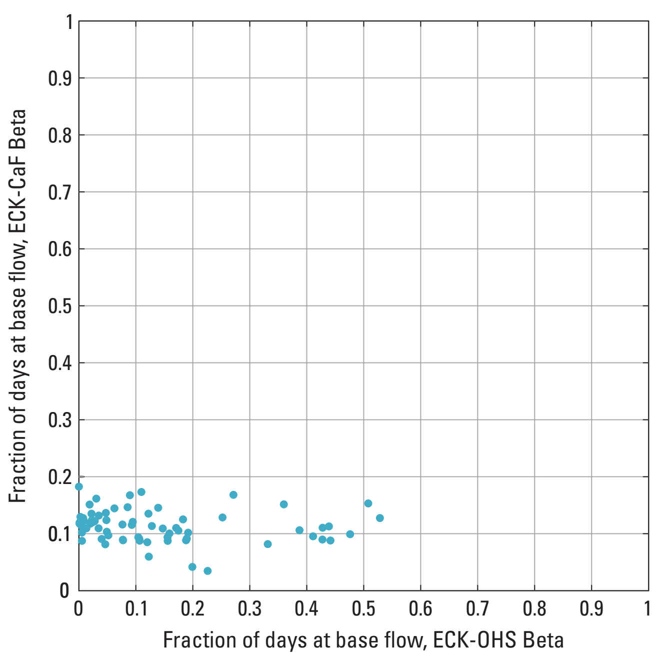

Figure 15. Comparison of fraction of days at base flow estimated using the ECK-OHS and ECK-CaF methods for 67 acceptable models.

Summary and Conclusions

An important component of a hydrologic system is base flow, broadly described as the part of streamflow that is sustained between precipitation events and fed to stream channels by delayed (usually subsurface) pathways. Base flow is generally not measured directly, but is estimated using a variety of methods, most commonly hydrograph separation. The ability to quantify water budgets, flow paths, traveltimes, and base-flow contributions to streams, over a range of scales and environments, is critical to improving the understanding of the status and future of the Nation's water quality.

A study was undertaken to evaluate the existing methods of hydrograph separation, and to suggest a new or enhanced hydrograph-separation method that met the following goals and objectives: includes some physical basis related to the dynamics of the groundwater system; is consistent with chemical mass balance methods; is as objective as possible, and is reproducible and can be automated and applied to multiple sites. Widely used graphical and filtering methods PART, HYSEP, and Base-Flow Index (BFI) were evaluated, along with a recursive digital filter (RDF). The RDF was appealing for the following reasons: it is based in part on the assumption that groundwater acts as a linear reservoir, and so has a physical basis; it has only two adjustable parameters, which can be determined objectively and theoretically with the same physical basis of groundwater reservoir linearity, or which can be optimized by applying a chemical mass balance constraint.

Substantial work has been done to evaluate the effectiveness of chemical tracers as a means of elucidating sources and flow paths for water in streams. These studies have shown differences in the results of hydrograph separation using graphical and chemical-tracer-based methods. Often these comparisons demonstrate bias in one method or the other, and indicate that tracer-based methods, or chemical mass balance constraints, provide important information beyond routine application of standard separation methods. All separation methods have assumptions that may limit the value of their application, and that must be understood in order to determine their benefit.

The RDF used in this study has two adjustable parameters: a base-flow recession constant alpha (α), quantified in this study using recession analysis, and beta (β), a measure of the maximum base-flow fraction or BFI. The latter was determined using a backward-running filter (method ECK-CaF). All methods (PART, HYSEP, BFI, and ECK-CaF) were applied to data from 225 selected streamgages in the Chesapeake Bay watershed. Results from the PART, HYSEP, and BFI methods were compared to the ECK-CaF method with respect to two general metrics: the long-term average fraction of streamflow that is base flow (BFI), and the fraction of days where streamflow is entirely base flow. There was generally good correlation between the methods, with some biased slightly high and some biased slightly low compared to ECK-CaF. There were differences among the fraction of days at base flow for the different methods, with ECK-CaF having a smaller range of values. This was attributed to how the different methods determine the cessation of quickflow.

Optimal hydrograph separation (method ECK-OHS), which uses the RDF with beta optimized using chemical mass balance constrained by specific conductance (SC), was performed using streamflow and SC data for 109 of the 225 Chesapeake Bay watershed sites with available SC data. Quickflow SC (C_S) was assumed to be constant and two new models for base-flow SC (C_B) were used. One model used a sine-cosine function (model sin-cos) and the other used a peak-fitting algorithm (model SCfit). Sixty-seven models were deemed acceptable and the results were compared with the ECK-CaF results. Imposing chemical mass balance to optimize beta (ECK-OHS) increased the range of beta values, BFI values, and fraction of days at base flow. The ECK-CaF method is widely applicable and meets the goals of the study by incorporating a physical basis and allowing for objective parameter estimation. ECK-OHS is a refinement of the ECK-CaF method that incorporates important chemical tracer information through a mass-balance constraint and provides additional insight into the applicability of the two-component model for hydrograph separation.

Hydrograph separation may have many objectives, not the least of which is providing insight into runoff-generation mechanisms and processes. Those processes are usually complex and hydrograph-separation methods all must make some simplifying assumptions. It has been noted that time-source (event and pre-event water) and geographic-source (for example, direct or surface runoff, direct precipitation onto the channel, groundwater discharge) components can be determined using tracers but that runoff mechanism-source components typically can not and must be inferred in other ways. Most graphical and filtering hydrograph-separation methods may be considered as quantifying geographic-source components (direct runoff and channel precipitation as quickflow and groundwater as base flow), although it is not clear that the methods identify these exact components. Often, the practical goal is to determine the timing, magnitude, and duration of quickflow or direct runoff. Chemical mass balance methods may be used to greater advantage to identify the groundwater component of runoff, especially when combined with a physical model for the dynamics of the groundwater system.

The results of this study may be used to address a number of questions regarding the role of groundwater in understanding past changes in stream-water quality and forecasting possible future changes, such as the timing and magnitude of the effects of land use and management practices on stream-water and groundwater quality. Ongoing and future modeling efforts in the Chesapeake Bay watershed and other watersheds may benefit from the estimates of base flow as calibration targets or as a means to filter chemical data to model base-flow loads and trends. Ultimately, base-flow estimation might provide the basis for future work aimed at improving the ability to quantify groundwater discharge, not only at the scale of a gaged watershed, but at the scale of individual reaches.

Acknowledgments

This work was supported by the U.S. Geological Survey (USGS) National Water-Quality Assessment Project, Integrated Watershed Studies (IWS) Team. The work benefitted from many discussions with Paul Capel and the other members of the IWS Team. We thank our USGS colleagues Matt Miller and Paul Juckem for their reviews. Their suggestions greatly improved the report. In addition, we thank Valerie Gaine (USGS) for editorial and publishing assistance and Timothy Auer (USGS) for his work on the illustrations.

References Cited

Aksoy, Hafzullah, and Wittenberg, Hartmut, 2011, Nonlinear baseflow recession analysis in watersheds with intermittent streamflow: Hydrological Sciences Journal, v. 56, no. 2, p. 226–237, doi:10.1080/02626667.2011.553614, accessed May 19, 2014, at http://dx.doi.org/10.1080/02626667.2011.553614.

Arnold, J.G., and Allen, P.M., 1999, Automated methods for estimating baseflow and ground water recharge from streamflow records: Journal of the American Water Resources Association, v. 35, no. 2, p. 411–424, doi:10.1111/j.1752-1688.1999.tb03599.x, accessed March 15, 2017, at http://dx.doi.org/10.1111/j.1752-1688.1999.tb03599.x.

Ator, S.W., and Denver, J.M., 2015, Understanding nutrients in the Chesapeake Bay watershed and implications for management and restoration—The Eastern Shore: U.S. Geological Survey Circular 1406, 72 p., accessed April 3, 2015, at http://dx.doi.org/10.3133/cir1406.

Bachman, L.J., Lindsey, B.D., Brakebill, J.W., and Powars, D.S., 1998, Ground-water discharge and base-flow nitrate loads of nontidal streams, and their relation to a hydrogeomorphic classification of the Chesapeake Bay watershed, Middle Atlantic Coast: U.S. Geological Survey Water-Resources Investigations Report 98–4059, 71 p., accessed March 15, 2017, at https://pubs.er.usgs.gov/publication/wri984059.

Barlow, P.M., Cunningham, W.L., Zhai, Tong, and Gray, Mark, 2015, U.S. Geological Survey groundwater toolbox, a graphical and mapping interface for analysis of hydrologic data (version 1.0)—User guide for estimation of base flow, runoff, and groundwater recharge from streamflow data: U.S. Geological Survey Techniques and Methods 3-B10, 27 p., accessed January 28, 2015, at http://dx.doi.org/10.3133/tm3B10.

Bazemore, D.E., Eshleman, K.N., and Hollenbeck, K.J., 1994, The role of soil water in stormflow generation in a forested headwater catchment: synthesis of natural tracer and hydrometric evidence: Journal of Hydrology, v. 162, nos. 1–2, p. 47–75, accessed March 15, 2017, at http://dx.doi.org/10.1016/0022-1694(94)90004-3.

Blume, Theresa, Zehe, Erwin, and Bronstert, Axel, 2007, Rainfall—runoff response, event-based runoff coefficients and hydrograph separation: Hydrological Sciences Journal, v. 52, no. 5, p. 843–862, doi:10.1623/hysj.52.5.843, accessed September 6, 2016, at http://dx.doi.org/10.1623/hysj.52.5.843.

Brodie, R.S., and Hostetler, S., 2005, A review of techniques for analysing baseflow from stream hydrographs, *in* Proceedings of the NZHS-IAH-NZSSS 2005 conference: Auckland, New Zealand, November 28–December 2, 2005.

Buttle, J.M., 1994, Isotope hydrograph separations and rapid delivery of pre-event water from drainage basins: Progress in Physical Geography, v. 18, no. 1, p. 16–41, doi:10.1177/030913339401800102, accessed March 16, 2017, at https://doi.org/10.1177/030913339401800102.

Cartwright, I., Gilfedder, B., and Hofmann, H., 2014, Contrasts between estimates of baseflow help discern multiple sources of water contributing to rivers: Hydrology and Earth System Sciences, v. 18, no. 1, p. 15–30, doi:10.5194/hess-18-15-2014, accessed March 13, 2014, at http://www.hydrol-earth-syst-sci.net/18/15/2014/.

Collischonn, Walter, and Fan, F.M., 2013, Defining parameters for Eckhardt's digital baseflow filter: Hydrological Processes, v. 27, no. 18, p. 2,614–2,622, doi:10.1002/hyp.9391, accessed March 15, 2017, http://dx.doi.org/10.1002/hyp.9391.

Combalicer, E.A., Lee, S.H., Ahn, S., Kim, D.Y., and Im, S., 2008, Comparing groundwater recharge and base flow in the Bukmoongol small-forested watershed, Korea: Journal of Earth System Science, v. 117, no. 5, p. 553–566, doi:10.1007/s12040-008-0052-8, accessed March 16, 2017, at http://dx.doi.org/10.1007/s12040-008-0052-8.

Cuthbert, M.O., 2014, Straight thinking about groundwater recession: Water Resources Research, v. 50, no. 3, p. 2,407–2,424, doi:10.1002/2013wr014060, accessed July 7, 2014, at http://dx.doi.org/10.1002/2013WR014060.

Eckhardt, K., 2005, How to construct recursive digital filters for baseflow separation: Hydrological Processes, v. 19, no. 2, p. 507–515, doi:10.1002/hyp.5675, accessed January 14, 2014, at http://dx.doi.org/10.1002/hyp.5675.

Eckhardt, K., 2012, Technical Note: Analytical sensitivity analysis of a two parameter recursive digital baseflow separation filter: Hydrology and Earth System Sciences, v. 16, no. 2, p. 451–455, doi:10.5194/hessd-8-9469-2011, accessed March 10, 2017, at http://www.hydrol-earth-syst-sci.net/16/451/2012/.

Famiglietti, J. S., 2014, The global groundwater crisis: Nature Climate Change, v. 4, no. 11, p. 945–948, doi:10.1038/nclimate2425, accessed March 15, 2017, at http://dx.doi.org/10.1038/nclimate2425.

Focazio, M.J., Plummer, L.N., Böhlke, J.K., Busenberg, Eurybiades, Bachman, L.J., and Powars, D.S., 1998, Preliminary estimates of residence times and apparent ages of ground water in the Chesapeake Bay watershed, and water-quality data from a survey of springs: U.S. Geological Survey Water-Resources Investigations Report 97–4225, 75 p., accessed September 27, 2016, at https://pubs.usgs.gov/wri/wri97-4225/.

Freeze, R.A., 1974, Streamflow generation: Reviews of Geophysics and Space Physics, v. 12, no. 4, p. 627–647, doi:10.1029/RG012i004p00627, accessed March 16, 2017, at http://dx.doi.org/10.1029/RG012i004p00627.

Furey, P.R., and Gupta, V.K., 2001, A physically based filter for separating base flow from streamflow time series: Water Resources Research, v. 37, no. 11, p. 2,709–2,722, doi:10.1029/2001wr000243, accessed September 30, 2013, at http://dx.doi.org/10.1029/2001WR000243.

Furey, P.R., and Gupta, V.K., 2003, Tests of two physically based filters for base flow separation: Water Resources Research, v. 39, no. 10, doi:10.1029/2002WR001621, accessed March 16, 2017, at http://dx.doi.org/10.1029/2002WR001621.

Genereux, D.P., Hemond, H.F., and Mulholland, P.J., 1993, Use of radon-222 and calcium as tracers in a three-end-member mixing model for streamflow generation on the West Fork of Walker Branch Watershed: Journal of Hydrology, v. 142, nos. 1–4, p. 167–211, doi:10.1016/0022-1694(93)90010-7, accessed March 15, 2017, at http://dx.doi.org/10.1016/0022-1694(93)90010-7.

Gustard, A., Bullock, A., and Dixon, J.M., 1992, Low flow estimation in the United Kingdom: Institute of Hydrology Report No. 108, 88 p., accessed March 15, 2017, at http://nora.nerc.ac.uk/6050/1/IH_108.pdf.

Halford, K.J., and Mayer, G.C., 2000, Problems associated with estimating ground water discharge and recharge from stream-discharge records: Groundwater, v. 38, no. 3, p. 331–342, doi:10.1111/j.1745-6584.2000.tb00218.x, accessed February 10, 2014, at http://dx.doi.org/10.1111/j.1745-6584.2000.tb00218.x.

Hall, F.R., 1968, Base-flow recessions—A review: Water Resources Research, v. 4, no. 5, p. 973–983, doi:10.1029/WR004i005p00973, accessed May 19, 2014, at http://dx.doi.org/10.1029/WR004i005p00973.

Hamel, Perrine, Daly, Edoardo, and Fletcher, T.D., 2013, Source-control stormwater management for mitigating the impacts of urbanisation on baseflow: A review: Journal of Hydrology, v. 485, p. 201–211, doi:10.1016/j.jhydrol.2013.01.001, accessed March 17, 2017, at http://dx.doi.org/10.1016/j.jhydrol.2013.01.001.

Henriksen, J.A., Heasley, John, Kennen, J.G., and Nieswand, Steven, 2006, Users' manual for the Hydroecological Integrity Assessment Process software (including the New Jersey Assessment Tools): U.S. Geological Survey Open-File Report 2006–1093, 80 p., http://pubs.er.usgs.gov/publication/ofr20061093.

Hewlett, J.D., and Hibbert, A.R., 1967, Factors affecting the response of small watersheds to precipitation in humid areas, *in* Sopper, W.E., and Lull, H.W., eds., Forest Hydrology: New York, Pergamon Press, p. 275–290.

Hooper, R.P., Christophersen, Nils, and Peters, N.E., 1990, Modelling streamwater chemistry as a mixture of soilwater end-members—An application to the Panola Mountain catchment, Georgia, U.S.A.: Journal of Hydrology, v. 116, nos. 1–4, p. 321–343, doi:10.1016/0022-1694(90)90131-G, accessed September 30, 2013, at http://dx.doi.org/10.1016/0022-1694(90)90131-G.

Hooper, R.P., and Shoemaker, C.A., 1986, A comparison of chemical and isotopic hydrograph separation: Water Resources Research, v. 22, no. 10, p. 1,444–1,454, doi:10.1029/WR022i010p01444, accessed June 9, 2010, at http://onlinelibrary.wiley.com/doi/10.1029/WR022i010p01444/full.

Institute of Hydrology, 1980, Low Flow Studies: Institute of Hydrology Report No. 1, 42 p., accessed March 15, 2017, at http://nora.nerc.ac.uk/9093/1/Low_Flow_01.pdf.

Klaus, J., and McDonnell, J.J., 2013, Hydrograph separation using stable isotopes: Review and evaluation: Journal of Hydrology, v. 505, p. 47–64, doi:10.1016/j.jhydrol.2013.09.006, accessed March 15, 2017, at http://dx.doi.org/10.1016/j.jhydrol.2013.09.006.

Kronholm, S.C., and Capel, P.D., 2015, A comparison of high-resolution specific conductance-based end-member mixing analysis and a graphical method for baseflow separation of four streams in hydrologically challenging agricultural watersheds: Hydrological Processes, v. 29, no. 11, p. 2,521–2,533, doi:10.1002/hyp.10378, accessed August 25, 2016, at http://dx.doi.org/10.1002/hyp.10378.

Li, L., Maier, H.R., Lambert, M.F., Simmons, C.T., and Partington, D., 2013, Framework for assessing and improving the performance of recursive digital filters for baseflow estimation with application to the Lyne and Hollick filter: Environmental Modelling & Software, v. 41, no. 0, p. 163–175, accessed March 7, 2014, at http://www.sciencedirect.com/science/article/pii/S1364815212002800.

Lindsey, B.D., Phillips, S.W., Donnelly, C.A., Speiran, G.K., Plummer, L.N., Böhlke, J.-K., Focazio, M.J., Burton, W.C., and Busenberg, Eurybiades, 2003, Residence times and nitrate transport in ground water discharging to streams in the Chesapeake Bay Watershed: U.S. Geological Survey Water-Resources Investigations Report 2003–4035, 201 p., accessed March 15, 2017, at https://pubs.er.usgs.gov/publication/wri034035.

Linsley, R.K., Jr., Kohler, M.A., and Paulhus, J.L.H., 1982, Hydrology for Engineers (3d. ed.): New York, McGraw-Hill, 508 p.

McDonnell, J.J., 1990, A rationale for old water discharge through macropores in a steep, humid catchment: Water Resources Research, v. 26, no. 11, p. 2,821–2,832, doi:10.1029/WR026i011p02821, accessed March 15, 2017, at http://onlinelibrary.wiley.com/doi/10.1029/WR026i011p02821/full.

McNutt, Marcia, 2014, The drought you can't see: Science, v. 345, no. 6204, p. 1,543, doi:10.1126/science.1260795, accessed September 7, 2016, at http://science.sciencemag.org/content/345/6204/1543.

Miller, M.P., Buto, S.G., Susong, D.D., and Rumsey, C.A., 2016, The importance of base flow in sustaining surface water flow in the Upper Colorado River Basin: Water Resources Research, v. 52, no. 5, p. 3,547–3,562, doi:10.1002/2015WR017963, accessed August 25, 2016, at http://onlinelibrary.wiley.com/doi/10.1002/2015WR017963/abstract.

Miller, M.P., Johnson, H.M., Susong, D.D., and Wolock, D.M., 2015, A new approach for continuous estimation of baseflow using discrete water quality data: Method description and comparison with baseflow estimates from two existing approaches: Journal of Hydrology, v. 522, p. 203–210, doi:10.1016/j.jhydrol.2014.12.039, accessed June 15, 2015, at http://dx.doi.org/10.1016/j.jhydrol.2014.12.039.

Miller, M.P., Susong, D.D., Shope, C.L., Heilweil, V.M., and Stolp, B.J., 2014, Continuous estimation of baseflow in snowmelt-dominated streams and rivers in the Upper Colorado River Basin: A chemical hydrograph separation approach: Water Resources Research, v. 50, no. 8, p. 6,986–6,999, doi:10.1002/2013WR014939, accessed June 15, 2015, at http://dx.doi.org/10.1002/2013WR014939.

Mutzner, Raphaël, Bertuzzo, Enrico, Tarolli, Paolo, Weijs, S.V., Nicotina, Ludovico, Ceola, Serena, Tomasic, Nevena, Rodriguez-Iturbe, Ignacio, Parlange, M.B., and Rinaldo, Andrea, 2013, Geomorphic signatures on Brutsaert base flow recession analysis: Water Resources Research, v. 49, no. 9, p. 5,462–5,472, doi:10.1002/wrcr.20417, accessed March 16, 2017, at http://dx.doi.org/10.1002/wrcr.20417.

Nathan, R.J., and McMahon, T.A., 1990, Evaluation of automated techniques for base flow and recession analysis: Water Resources Research, v. 26, no. 7, p. 1,465–1,473, doi:10.1029/WR026i007p01465, accessed March 16, 2017, at http://dx.doi.org/10.1029/WR026i007p01465.

Pellerin, B.A., Wollheim, W.M., Feng, Xiahong, and Vörösmarty, C.J., 2007, The application of electrical conductivity as a tracer for hydrograph separation in urban catchments: Hydrological Processes, v. 22, no. 12, p. 1,810–1,818, doi:10.1002/hyp.6786, accessed March 16, 2017, at http://dx.doi.org/10.1002/hyp.6786.

Phillips, S.W., ed., 2007, Synthesis of U.S. Geological Survey science for the Chesapeake Bay Ecosystem and implications for environment management: U.S. Geological Survey Circular 1316, 63 p., accessed March 16, 2017, at http://pubs.usgs.gov/circ/circ1316/.

Phillips, S.W., Focazio, M.J., and Bachman, L.J., 1999, Discharge, nitrate load, and residence time of ground water in the Chesapeake Bay Watershed: U.S. Geological Survey Fact Sheet FS–150–99, 6 p., accessed March 16, 2017, at https://pubs.usgs.gov/fs/fs15099/.

Phillips, S.W., and Lindsey, B.D., 2003, The influence of ground water on nitrogen delivery to the Chesapeake Bay: U.S. Geological Survey Fact Sheet FS–091–03, 6 p., accessed March 16, 2017, at https://pubs.usgs.gov/fs/2003/fs091-03/.

Poff, N.L., Richter, B.D., Arthington, A.H., Bunn, S.E., Naiman, R.J., Kendy, Eloise, Acreman, Mike, Apse, Colin, Bledsoe, B.P., Freeman, M.C., Henriksen, James, Jacobson, R.B., Kennen, J.G., Merritt, D.M., O'Keeffe, J.H., Olden, J.D., Rogers, Kevin, Tharme, R.E., and Warner, Andrew, 2010, The ecological limits of hydrologic alteration (ELOHA): a new framework for developing regional environmental flow standards: Freshwater Biology, v. 55, no. 1, p. 147–170, doi:10.1111/j.1365-2427.2009.02204.x, accessed March 16, 2017, at http://dx.doi.org/10.1111/j.1365-2427.2009.02204.x.

Price, Katie, 2011, Effects of watershed topography, soils, land use, and climate on baseflow hydrology in humid regions: A review: Progress in Physical Geography, v. 35, no. 4, p. 465–492, doi:10.1177/0309133311402714, accessed March 16, 2017, at https://doi.org/10.1177/0309133311402714.

Raffensperger, J.P., Baker, A.C., Blomquist, J.D., and Hopple, J.A., 2017, Hydrograph-separation results for 225 streams in the Chesapeake Bay watershed derived by using PART, HYSEP (Fixed, Local minimum, Slide), BFI, and a Recursive Digital Filter with streamflow data ranging from 1913 through 2016: U.S. Geological Survey data release, https://doi.org/10.5066/F757194G.

Rimmer, Alon, and Hartmann, Andreas, 2014, Optimal hydrograph separation filter to evaluate transport routines of hydrological models: Journal of Hydrology, v. 514, p. 249–257, doi:10.1016/j.jhydrol.2014.04.033, accessed May 19, 2014, at http://www.sciencedirect.com/science/article/pii/S0022169414003072.

Risser, D.W., Gburek, W.J., and Folmar, G.J., 2005, Comparison of methods for estimating ground-water recharge and base flow at a small watershed underlain by fractured bedrock in the eastern United States: U.S. Geological Survey Scientific Investigations Report 2005–5038, 31 p., accessed March 16, 2017, at https://pubs.usgs.gov/sir/2005/5038/pdf/sir2005-5038.pdf.

Robson, Alice, and Neal, Colin, 1990, Hydrograph separation using chemical techniques: An application to catchments in Mid-Wales: Journal of Hydrology, v. 116, nos. 1–4, p. 345–363, doi:10.1016/0022-1694(90)90132-H, accessed September 30, 2013, at http://dx.doi.org/10.1016/0022-1694(90)90132-H.

Rutledge, A.T., 1998, Computer programs for describing the recession of ground-water discharge and for estimating mean ground-water recharge and discharge from streamflow records—update: U.S. Geological Survey Water-Resources Investigations Report 98–4148, 43 p., accessed March 16, 2017, at https://pubs.usgs.gov/wri/wri984148/.

Sanford, W.E., Nelms, D.L., Pope, J.P., and Selnick, D.L., 2012, Quantifying components of the hydrologic cycle in Virginia using chemical hydrograph separation and multiple regression analysis: U.S. Geological Survey Scientific Investigations Report 2011–5198, 152 p., accessed September 4, 2013, at http://pubs.usgs.gov/sir/2011/5198/.

Sanford, W.E., and Pope, J.P., 2013, Quantifying groundwater's role in delaying improvements to Chesapeake Bay water quality: Environmental Science & Technology, v. 47, no. 23, p. 13330-13338, doi:10.1021/es401334k, accessed March 16, 2017, at http://dx.doi.org/10.1021/es401334k.

Sklash, M.G., and Farvolden, R.N., 1979, The role of groundwater in storm runoff: Journal of Hydrology, v. 43, nos. 1–4, p. 45–65, accessed March 16, 2017, at http://dx.doi.org/10.1016/0022-1694(79)90164-1.

Sklash, M.G., Farvolden, R.N., and Fritz, P., 1976, A conceptual model of watershed response to rainfall, developed through the use of oxygen-18 as a natural tracer: Canadian Journal of Earth Sciences, v. 13, no. 2, p. 271–283, doi:10.1139/e76-029, accessed November 1, 2016, at http://dx.doi.org/10.1139/e76-029.

Sloto, R.A., and Crouse, M.Y., 1996, HYSEP: a computer program for streamflow hydrograph separation and analysis: U.S. Geological Survey Water-Resources Investigations Report 96–4040, 46 p., accessed March 16, 2017, at https://pubs.usgs.gov/wri/1996/4040/report.pdf.

Stewart, Mark, Cimino, Joseph, and Ross, Mark, 2007, Calibration of base flow separation methods with streamflow conductivity: Ground Water, v. 45, no. 1, p. 17–27, doi:10.1111/j.1745-6584.2006.00263.x, accessed March 16, 2017, at http://dx.doi.org/10.1111/j.1745-6584.2006.00263.x.

Sujono, Joko, Shikasho, Shiomi, and Hiramatsu, Kazuaki, 2004, A comparison of techniques for hydrograph recession analysis: Hydrological Processes, v. 18, no. 3, p. 403–413, doi:10.1002/hyp.1247, accessed March 7, 2014, at http://dx.doi.org/10.1002/hyp.1247.

Tallaksen, L.M., 1995, A review of baseflow recession analysis: Journal of Hydrology, v. 165, nos. 1–4, p. 349–370, accessed March 16, 2017, at http://dx.doi.org/10.1016/0022-1694(94)02540-R.

Vasconcelos, V.V., Martins, P.P., Jr., and Hadad, R.M., 2013, Estimation of flow components by recursive filters: case study Paracatu River Basin (SF-7), Brazil: Geologia USP, Série Científica, v. 13, no. 1, p. 3–24, accessed March 16, 2017, at http://www.revistas.usp.br/guspsc/article/viewFile/54079/58009.

Wahl, K.L., and Wahl, T.L., 1988, Effects of regional ground water declines on streamflows in the Oklahoma Panhandle, *in* Symposium on Water-Use Data for Water Resources Management: Tucson, Arizona, American Water Resources Association, p. 239–249.

Wahl, K.L., and Wahl, T.L., 1995, Determining the flow of Comal Springs at New Braunfels, Texas, in Texas Water ‘95: San Antonio, Texas, August 16–17, 1995, American Society of Civil Engineers, p. 77–86.

Winter, T.C., 2007, The role of ground water in generating streamflow in headwater areas and in maintaining base flow: Journal of the American Water Resources Association, v. 43, no. 1, p. 15–25, doi:10.1111/j.1752-1688.2007.00003.x, accessed March 16, 2017, at http://dx.doi.org/10.1111/j.1752-1688.2007.00003.x.

Zhang, Ruigang, Li, Qiang, Chow, Thien Lien, Li, Sheng, and Danielescu, Serban, 2013, Baseflow separation in a small watershed in New Brunswick, Canada, using a recursive digital filter calibrated with the conductivity mass balance method: Hydrological Processes, v. 27, no. 18, p. 2,659–2,665, doi:10.1002/hyp.9417, accessed March 16, 2017, at http://dx.doi.org/10.1002/hyp.9417.

Prepared by USGS West Trenton Publishing Service Center.
Edited by Valerie M. Gaine.
Graphics and layout by Timothy W. Auer.
Cover illustration by Jeff P. Raffensperger.

For additional information, contact:
Director, MD-DE-DC Water Science Center
U.S. Geological Survey
5522 Research Park Drive
Baltimore, MD 21228

or visit our Web site at:
https://md.water.usgs.gov

Printed on recycled paper

ISSN 2328-031X (print)
ISSN 2328-0328 (online)
https://doi.org/10.3133/sir20175034

ISBN 978-1-4113-4135-7
9 781411 341357

Raffensperger and others—**Optimal Hydrograph Separation Using a Recursive Digital Filter Constrained by Chemical Mass Balance**—Scientific Investigations Report 2017–5034